THE UNIVERSITY OF CHICAGO

THE ROLE OF HOMEOBOX TRANSCRIPTION COFACTORS IN PROSTATE DEVELOPMENT AND TUMOR GROWTH

A DISSERTATION SUBMITTED TO
THE FACULTY OF THE DIVISION OF THE BIOLOGICAL SCIENCES
AND THE PRITZKER SCHOOL OF MEDICINE
IN CANDIDACY FOR THE DEGREE OF
DOCTOR OF PHILOSOPHY

COMMITTEE ON CANCER BIOLOGY

BY

HANNAH JANE BRECHKA

CHICAGO, ILLINOIS

AUGUST 2017

To my mother, Susan Essex-Brechka. You are with me every day.

TABLE OF CONTENTS

LIST OF FIGURES

LIST OF TABLES

ACKNOWLEDGEMENTS

There are many people, without whom, this thesis would not be possible. First, I would like to thank my mentor of five years, Dr. Donald Vander Griend, PhD. Don has been a tireless supporter and crusader for me the entire time that I have worked with him. And I really do feel that I have worked with him, and not simply worked for him. He always encouraged me to think more highly of my skills, and myself, even when I was having difficulties thinking highly of myself. He also risked a lot by taking me on, a green graduate student who didn't know much about the prostate. However, I also took a risk with him. I came into graduate school fully intending to work on breast cancer, and I was very close to joining a breast cancer lab. I really liked Don as a teacher and decided to do my last rotation with him. And boy, am I glad that I did. I ended up picking my lab based on his mentorship and I have never regretted that decision. By working in his lab, I was able to learn about my love of developmental biology that I never knew I had. I was also able to spread my wings, both scientifically and personally. Don has helped me become a better scientist, a better writer, a better self-promoter, and a better teacher. He leads by example and by constantly encouraging his students to always do their best. Thank you, Don.

I would also like to acknowledge my second, and unofficial mentor, Dr. Russell Szmulewitz, MD. Thank you for your honesty and support, even though you didn't have to, you still made me feel that you fully invested in my life and my research. You provided a constant reminder to me that the work we do is important for actual human patients. You also provided some much needed levity every chance you got. Being a cancer researcher can be disheartening and depressing, but it's nothing to treating patients who are at the end of their life, like you do

every day. You bring humor and silliness to our lab, while also being one of the most logical and innovative scientific minds I know. Thank you.

To my wonderful committee members, I thank you and acknowledge all of your support over the years. Dr. Kay Macleod PhD has been the head of the Committee on Cancer biology for about half of my time at the University of Chicago, but she has been a mentor and supportive rock for me long before that. Kay has always supported me and expected nothing but the best from me. I very much appreciate all of the opportunities that she afforded me, from inviting me to attend the Cancer Biology Training Consortium to asking me to organize our recruitment. Her office is always open for her students and I am grateful for her support. I would like to acknowledge Dr. James LaBelle, MD, PhD for being a constant ray of sunshine and support in my committee meetings. Ever since I TA-ed for James my second year, he has been a cheerleader for me. I have appreciated his practical logic and excellent questions, even though the prostate is very far from his area of expertise. He enabled me to see my project from an intelligent outsider's perspective, and I am so grateful for that. Dr. Gail Prins, PhD was a magnificent addition to my thesis committee. Even though she had to travel from UIC every time I had a committee meeting, she was there every meeting. I have so enjoyed getting to know Gail. She has been such a positive role model for me of a highly successful scientist, and I have really enjoyed having such lively conversations about science as though I was her peer. She never made me feel like a student, and her expectation of the best scholarship from me has made me a better scientist. Dr. Vicky Prince, PhD, has been hugely influential on my time here as a graduate student. She has provided the best advice and scientific critiques, and she has also afforded me some of the biggest opportunities for growth. Vicky has enabled me to have experiences like talking to the University of Chicago Board of Trustees, help teach a developmental biology class,

and to write about science outside of the laboratory. While she has always supported my professional development goals, I also very much enjoy her company, and hope that she and Reina do superbly at their next competition. Thank you, Vicky, for your never-ending confidence in me.

I would also like to acknowledge the excellent lab members that I have had the privilege of working with in the Vander Griend/Szmulewitz labs over the last five years. To past members, Jack Kach, PhD and Steve Kregel, PhD, you boys will always feel like my goofy older brothers. Thank you for being a wonderful box-mate, Jack. Your logical advice will always stay with me. Steve, I might not have joined the Vander Griend lab if you hadn't made me feel so welcome. Thank you for being my friend. To my current lab members: you are all exceptional. Thank you for helping me and befriending me and for being the coolest bunch of scientists this side of the Mississippi. Marc, I'll visit you in France and will not make you come to England. Thank you for always knowing what to do when a sequencing problem arose (or any problem, for that matter). Phill, thank you for being the rock of the lab and making sure that everything works smoothly. We'd be a disaster without you. Tiha, thank you for your leadership and friendship. If theses had author lists, Calvin VanOpstall would be second author. Thank you for your scientific and friendship contributions. To Lari de Wet, the social butterfly of our lab, you have so much potential, and I know that you'll grow into a marvelous scientist. Thank you for making this lab feel like a family. To my very lovely friend and co-graduate student, Erin McAuley: thank you for being an expert on everything, be it IHC protocols or the best nail polish brands. You are a life-long friend and I am so glad that I hoodwinked you into joining the lab. To Raj, thank you for your intellectual curiosity and all of your help with the work I present in this thesis. You'll be wonderful doctor. Ryan Brown, I have watched you grow from a boy to a man, and I am so

proud to have you on our team. To Anthony, the lab Dad, thank you for your friendship. You are the person everyone, including me, goes to for advice and you handle that leadership with grace. When you're running some super successful lab/company/non-profit one day, I will be the first to say, "I knew him when..." You're going to change the world for the better, my friend.

I wish to acknowledge the support of the University Of Chicago Section Of Urology led by Dr. Arieh Shalhav, MD. Also, the Department of Surgery Research has been instrumental in my research success, in particular Ruth Crawford and Dr. Karl Matlin, PhD. I would also like to acknowledge the support of the University of Chicago Comprehensive Cancer Center (UCCCC) led by Dr. Michelle Le Beau. I would also thank Dr. Yi Cai for the superb technical assistance on the project. I'd also wish to thank the expert technical assistance of the Human Tissue Resource Center core facility led by Dr. Mark Lingen, and the assistance of Mary Jo Fekete. We also thank the Immunohistochemistry Core Facility run by Terri Li.

To my graduate school friends, your support and commiseration has meant the world to me. Thank you to Anna Dembo and Erin McAuley, Ryan Jay Ohr and Scott Biering, to Andrew Kirkley and Andrew Belcher, to Payal Tiwari and Ali Yesilkanal, to Ashley Sample (my thesis buddy) and to Jacquie Handley-Cora. Thank you also to the significant others that I have met and become friends with because of you all (Leidy, Brittany, Hallie, Daniel and Ryan). Thank you for all of the dinners and potlucks and drinks and weddings and travels and coffee dates together. Getting to know all of you has made my life richer and a lot more fun. Thank you in particular to Anna Dembo, my best friend in Chicago, my bridesmaid, my travel companion and my darling friend. You are like a sister to me and I could never have made it through this nonsense of a graduate degree without you.

To my friends from Skidmore, thank you for always sticking with me and mostly for encouraging me to go out and get my PhD in the first place. Thank you Bryn Schockmel, Abbie Hamlin, Kelsey Weiss, Yahia Imam, Ben Shanks and a particular thank you to Carly Shanks, PhD. Thank you for being my first and best science friend, Carly. I wouldn't be here without those hours looking at algae under microscopes with you. I would also like to acknowledge my undergraduate mentors, David and Cathy Domozych, PhD. The Domozych's trained me how to be a scientist, how to work hard and trust my instincts, and encouraged me to pursue my dreams. Corny as it is, I would not be at the University of Chicago, let alone getting a PhD without your support. Thank you both.

I would also like to thank my wonderful family. Dad, you have always nurtured my love for science. You are the one who took me out on my first nature walks, where I made comprehensive lists of the flora and fauna of Oak Lane when I was four years old. You brought me to science camp. You bought me my first microscope. You told me I could be whatever I wanted to be and you've helped me achieve more than I thought possible. Thank you for your constant love, and constant support. I hope I have made you proud, and I hope that you know that every atom of whom I am is because of you. Thank you.

To my beloved Auntie, thank you for always loving me and teaching me about what it means to love your family completely. You are always cheering for me, whether it was a sand castle or my undergraduate research project. Thank you for you caring nature. I would not be here without you. To my favorite sister in the whole wide world, Mollie. Thank you for teaching me how to be patient and caring. You are so unique and I love you so very much. I have always looked up to your creativity and kindness, and I thank you for being my role model and the best

sister anyone could ask for. To my other sister, Maureen Brady. We may not actually be related to each other, but your friendship of 25 years has meant the world to me. You are my best friend and the first person I want to call when something wonderful or sad or funny happens. Thank you for your love and encouragement. To the rest of the Brechka clan, thank you for always loving and supporting me, no matter how far away we are from each other. I love you all so very much.

To my husband, Patrick Fitzsimons Brechka. Thank you for taking my last name. Thank you for making me so very happy. Your partnership is all I have ever wanted, and I cherish every day we spend together. Your ability to help me though the darkest and grumpiest and bitterest lows of my graduate career has made it possible for me to write this thesis. You are my constant. My true partner. Thank you for feeding me and comforting me and providing me the emotional support to complete this crazy PhD journey. Thank you for laughing with me, and thank you for marrying me. We have a big adventure ahead of us, and there is no one I would rather adventure with than you.

Finally, I would like to acknowledge my mother, Susan Essex-Brechka. I am approaching the year 2020 when I will have been alive longer without you than with you. Even though breast cancer took you away, I feel like I have grown closer to you and loved you more deeply as I've gotten older. I imagine the kinds of advice and conversations that we would have had if we had gotten to become friends, like I see my peers becoming friends with their mothers. Your kindness and warmth still bring me solace and guide my life. I will make better decisions because of what you taught me. I will be kind because you showed me what joy could be found in kindness. I will work hard because you worked so hard to make a better life for me. I will do

what is best for myself and for my family because you empowered me to. You only got to be with me for fifteen years, but I will have you with me all of my life. Thank you for making me who I am; I hope that you are proud of me.

ABBREVIATIONS

ADT (Androgen Deprivation Therapy)

AMH (Anti- Müllerian Hormone)

AR (Androgen Receptor)

BP (base pairs)

CDM (Caudal Müllerian Duct)

ChIP (Chromatin Immunoprecipation)

CMDM (Caudal Müllerian Duct Mesenchyme)

CRC (Colorectal Cancer);

CRPC (Castration-Resistant Prostate Cancer)

DEG (Differentially Expressed Genes)

FPKM (Fragments Per Kilobase Mapped)

GFP (Green Fluorescent Protein)

GO (Gene Ontology)

H&E (Hematoxylin and eosin)

HDAC (Histone Deacetylase)

HDACi (Histone Deacetylase Inhibitors)

hESCs (human Embryonic Stem Cells)

Hoxb13 (Homeobox B13)

IPA (Ingenuity Pathway Analysis)

LOF (Loss of Function)

MEIS (Murine Ectopic Integration Site);

MEIS1 (Myeloid Ecotropic Integration Site 1)

MEIS2 (Myeloid Ecotropic Integration Site 2)

NCI (National Cancer Institute);

NKX3.1 (NK3 Homeobox 1)

PCS (Principal Components Analysis)

PIN (Prostatic Intraepithelial Neoplasia)

PrCa (Prostate Cancer)

PrEC (Prostate Epithelial Cell)

PSA (Prostate-Specific Antigen)

PSA (Prostate-Specific Antigen)

Q-RT-PCR (Quantitative Reverse Transcription PCR)

qPCR (Quantitative PCR)

RT-PCR (Reverse Transcription PCR)

SVEC (Seminal Vesicle Epithelial Cell)

TALE (Three Amino Acid Loop Extension)

TSS (Transcription Start Site)

UCCCC (University of Chicago Comprehensive Cancer Center)

UGS (Urogenital Sinus)

UGSM (Urogenital Sinus Mesenchyme)

CHAPTER I

INTRODUCTION

BACKGROUND AND SIGNIFICANCE

Unanswered Questions in the Prostate Cancer Field

Prostate cancer is the most common non-cutaneous cancer and the second leading cause of cancer related mortalities among American men [1]. While doctors have made advances in the early detection and treatment of prostate cancer in the past few decades since Dr. Huggins first treated men with hormonal therapy [2, 3], there are still outstanding questions in the field. The first of which is how can we differentiate between aggressive and indolent prostate cancer? Prostate cancer is unusual as compared to cancer of other organ sites in that there are a large number of patients who present with a very slow-growing form of prostate cancer that is unlikely to cause mortality, while some patients' prostate cancer is very aggressive and progresses to fatal metastases very quickly [4, 5]. Pathologists have a guideline called the Gleason Score in order to determine the biological malignancy of prostate cancer, whereby the morphologic appearance correlates strongly to the aggressiveness of the cancer [4, 6]. By examining the histology of two biopsy cores, a pattern number from 1 to 5 is assigned based on how similar or different the cells appear from healthy prostate glands. The closer to normal, the lower the number. The two pattern numbers are added together to determine the Gleason Score of the patient, with a score of 6 commonly the lowest to be considered a tumor. The higher the score, the more likely a patient is to be shuttled into aggressive therapy quickly [4-6].

The main clinical intervention for prostate cancer includes some combination of androgen deprivation and surgical removal of the cancerous gland, along with possible radiation and chemotherapy [7, 8]. None of these interventions are without considerable risk and side effects, but some prostate-specific treatment side effects include androgen deprivation and prostatectomies. Androgen deprivation therapy is essentially chemical castration, leading to systemic morbidities including hot flashes, sexual dysfunction, skeletal fragility, anemia, metabolic alterations, and psychological or cognitive effects[9]. The anatomic location of the prostate means that prostatectomy surgery risks include sexual dysfunction and incontinence, in addition to the risks involved in any major surgery[10-12]. None of these clinical interventions should be taken lightly.

Thanks to the Gleason Score, doctors are excellent at identifying men who require aggressive therapies immediately, and they are also able to identify men who have very slow growing cancers, however there are 'Men in the Middle' who fall in between those two categories. They are often shuttled into aggressive treatments, as there is a mentality to err towards overtreatment of cancer, particularly prostate cancer [13]. Doctors need better tools to identify which men have prostate cancer that will progress to lethal disease and which men could be spared the life-altering side effects of treatment.

Another question unanswered in the PrCa field is why prostate cancer is so much more common than other male urological cancers. It is estimated that in 2017, upwards of 160,000 men will be diagnosed with PrCa while there have been less than 50 recorded cases of seminal vesicle cancer ever [14]. Both of these structures have similar functions of contributing to male ejaculate and require androgen receptor signaling for normal development and function [15-17].

So what is different about the two tissues that lead to such drastic differences in cancer incidence? As described above, androgen deprivation is the main clinical intervention used when treating prostate cancer. As the AR pathway is developmentally critical, we hypothesized that other developmental pathways may also play a key role in oncogenesis and tumor progression. This implies that there are unique differences between prostate and seminal vesicle tissues, which strongly predispose prostate tissue to neoplasia and cancer. These differences could be accounted for by their specific developmental differences and their distinct embryologic origins, as well as exposure to infectious and inflammatory agents, distinct secreted factors produced by their gland of origin, or differences in the kinetics of tissue turnover [18, 19].

Our lab recently identified differentially regulated gene networks between the prostate and seminal vesicle, and has used these data to determine prognostic cancer gene-centered biomodules specific to the prostate [20]. One such signaling module to emerge was the MEIS/HOX axis. This work indicates that prostate cancer patients with high levels of *MEIS1* or *MEIS2* expression survive longer than men with lower expression (**Figure 1.1**) [20]. In order to determine the molecular basis of this phenomenon, an understanding of MEIS and HOX expression and function in prostate cancer and prostate development is necessary.

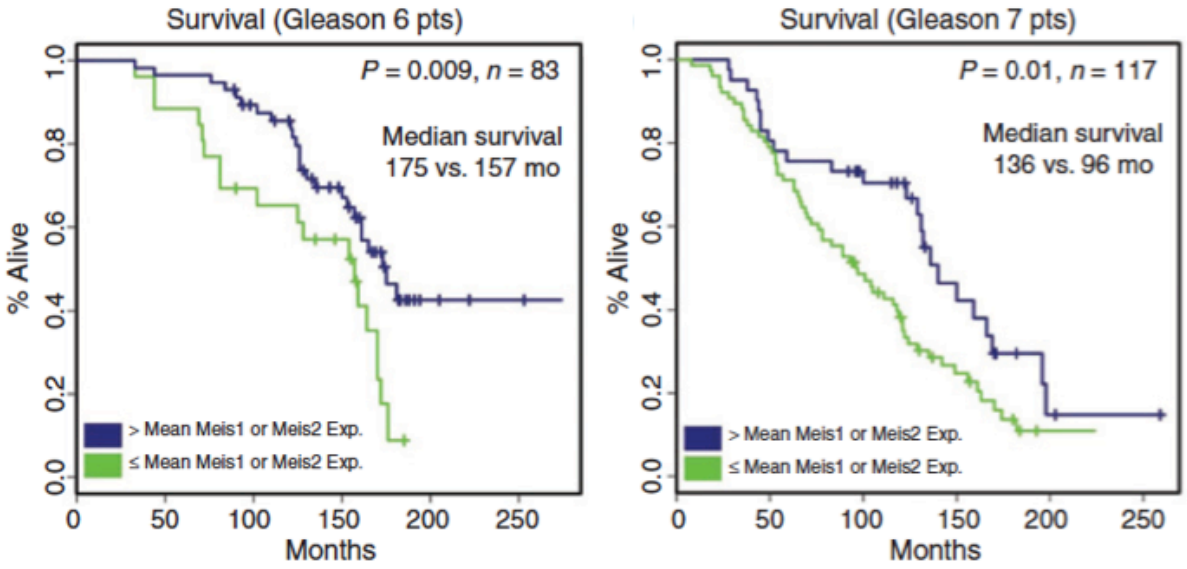

Figure 1.1 Lower MEIS Expression Correlates with Shorter Patient Survival. Figure adapted from previously published work from our lab[20]. Left. Gene expression profile of 83 Gleason 6 tumors biopsy specimens (GSE16560) for their changes in Meis1 and Meis2 using Kaplan–Meier techniques. Decreased expression of either Meis1 or Meis2 (below the mean Meis levels, green lines) significantly decreased patient survival compared with controls (at or above mean Meis levels, blue lines) and showed an 18-month survival difference (P = 0.009). Right. Gene expression profile of 117 men with Gleason 7 tumors biopsy specimens (GSE16560) analyzed using Kaplan–Meier techniques. Decreased expression of either Meis1 or Meis2 (below the mean Meis levels, green lines) significantly decreased patient survival compared with controls (at or above mean Meis levels, blue lines) and showed a 40-month difference in median survival (P = 0.01).

The recent and exciting identification of germline *HOXB13 (G84E)* mutations within a subset of familial prostate cancers by Isaacs and Cooney in 2012 highlights a novel set of genes and transcriptional signaling pathways to understand prostate tumor etiology and develop new treatment modalities to combat prostate tumor initiation and progression [21]. In particular, the location of the G84E mutation in the MEIS-interacting domain of *HOXB13* is particularly intriguing. Prior to this discovery, much was already known regarding the expression and function of Homeobox genes, both *HOX* genes and their crucial co-factors, in development and cancer. However, there remain significant gaps in our current understanding of Homeobox biology in prostate development and disease.

The Role of *HOX* Genes in Organismal Development

HOX proteins are highly evolutionarily conserved, homeodomain-containing transcription factors best known for their roles in body axis patterning and tissue differentiation of developing embryos [22, 23]. Furthermore, recent studies have shown HOX proteins not only have a role development and organogenesis, but they also contribute to the control of several other processes into adulthood such as cell proliferation, cell cycle, apoptosis, cell differentiation, and cell migration [22, 24, 25]. In humans, the 39 HOX proteins are divided into four *HOX* gene clusters: A, B, C, and D located on chromosomes 7p15, 17q21.2, 12q13, and 2q31 respectively [26]. Each cluster is comprised of a subset of paralogous genes 1-13 whose 3' to 5' organization and expression both follow a pattern of spatial and temporal co-linearity with development, although not every paralog is present in each cluster. The 3' *HOX* genes are most highly expressed in the anterior body regions that arise early in development, while the 5' *HOX* genes encode more posterior regions that form later in development. The term, "HOX Code,"

refers to the phenomenon where tissue specificity is determined by nested and partially overlapping expression of several *HOX* genes in a given region. The most 5' *HOX* gene expressed in a given tissue, however, has dominance in determining a specific tissues' identity compared to the more 3' *HOX* gene that may be co-expressed [27]. For example, while 36 of the 39 *HOX* genes are expressed at a detectable level by qRT-PCR in a gross sample of human prostate tissue, it is the 5' *HOX* genes like *HOXA13* and *HOXB13* that are most highly expressed and most significantly confer prostatic identity [28]. Several excellent and in-depth reviews have been published on the general role of *HOX* genes in development and cancer [22, 25, 29-31].

HOX **expression in Male reproductive System**

The male reproductive tract is derived from two main developmental structures: the Wolffian (mesonephric) duct, which gives rise to the testis, epididymis, vas deferens, and seminal vesicle; and the urogenital sinus (UGS), which gives rise to the prostate, bulbourethral (Cowper's) gland, bladder, and urethra [32]. Given that the reproductive tract is one of the most posterior systems in the body, expression of primarily posterior *HOX* genes like those in paralog groups 9-13 is most commonly observed (**Figure 1.2 A and B**) [23, 27, 33]. However, several 3' *HOX* genes are also expressed in the testis and are thought to have critical roles in spermatogenesis rather than in testis function (**Figure 1.2 A**) [33].

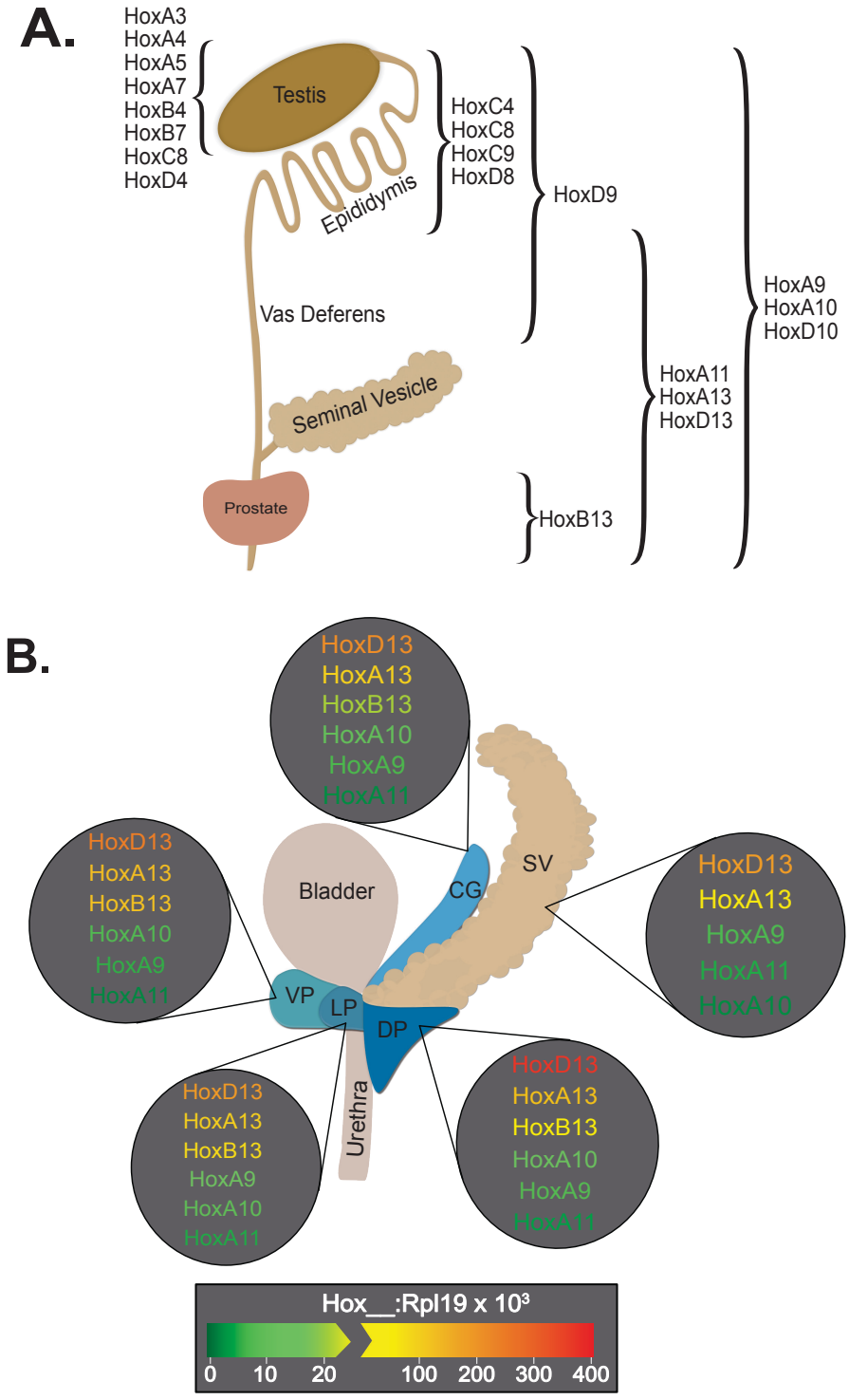

Figure 1.2: Expression Patterns of HOX Genes in the Rodent Male Reproductive System.

Figure 1.2 Continued: Expression Patterns of HOX Genes in the Rodent Male Reproductive System. A) Depiction of the spatially-restricted pattern of HOX expression in rodent reproductive structures throughout development. Data is compiled from multiple references [15, 23, 27, 34-40]. **B)** Representation of lobe specific, posterior HOX gene expression in the adult rat prostate and seminal vesicle, determined by real time RT-PCR in Huang et al. 2007 [23]. The seminal vesicle (SV), coagulating gland (CG), ventral prostate (VP), lateral prostate (LP), and dorsal prostate (DP) each have a unique signature of posterior HOX gene expression levels that likely aids in conferring identity. Notably, HOXB13 shows the largest variation in expression between lobes of the prostate and is restricted to urogenital sinus (UGS) derived structures; thus it is absent in the SV. It should also be noted that for studies done in mice, Podlasek et al. demonstrated a different relative expression pattern of HOXA10, HOXA13, and HOXD13 between lobes of the prostate compared to the rat [34, 35]. In their studies, they found that the lowest prostatic expression of HOXA10 was in the CG, rather than VP [34]. Additionally, highest expression of HOXD13 was in the SV rather than DP, and followed in order of decreasing expression by the VP, CG, and DP [15]. HOXA13 followed a similar pattern as HOXD13, although the CG does not seem to have been analyzed for HOXA13 expression [35]. The drawing of the rodent prostate is adapted from Abate-Shen et al. 2000 [41].

Many of the *Hox* paralogs have redundant and overlapping functions rendering the identification of specific roles for each gene complicated; however, some insight has been gained by observing phenotypes of various *Hox* gene knockout rodents. For example, while homozygous loss of *Hoxa13* (*Hoxa13*$^{-/-}$) is considered embryonic lethal due to the perceived role of *Hoxa13* in umbilical artery maintenance, examination of *Hoxa13*$^{-/-}$ fetuses shows severe hypoplasia of the urogenital sinus and arrested or delayed rostral-to-caudal progression of Müllerian ducts [42]. Additionally, *Hoxd13* deficient mice (*Hoxd13*$^{-/-}$) reveal diminished folding in the seminal vesicle stromal sheath, reduced ductal branching and size of the dorsal and ventral prostate lobes, and agenesis of the bulbourethral gland [15]. Furthermore, compound homozygous mutant (double *Hoxa13*$^{-/-}$ and *Hoxd13*$^{-/-}$) fetuses have undetectable development of the genital tubercle, nor any distinct hindgut and urogenital sinus, among other deformities [42]. In contrast, mice expressing *Hoxb13* with a loss-of-function mutation in the homeodomain show no gross morphological defects, but rather have prostate ventral lobe-specific defects in histology and secretory function [43]. Histologically, ventral lobe epithelium from *Hoxb13* mutant mice are composed of simple cuboidal rather than the tall columnar luminal cells that make up healthy prostate epithelium, and are also devoid of the ventral-specific secretory proteins p12 and p25 [43]. For a thorough review of reproductive system phenotypes observed with various 5' *Hox* gene knockouts, please refer to "Homeobox genes and the male reproductive system" by Rao and Wilkinson [44].

In addition to the spatial and temporal patterns of *Hox* gene expression there is also clear species specificity to the pattern. This is especially well demonstrated when noting the *Hox* patterns of the prostate in developing mice, rats, and adult humans; however, it should be noted that there is very little data regarding *HOX* expression in the developing embryonic human

prostate. While at a glance, many of the same *HOX* genes are expressed in all three of these species, the timing, location, and amount of expression can all vary. In murine prostates, Bushman et al. found that *Hoxa10* expression peaked at embryonic day 19 (E19) and decreased rapidly after birth to near undetectable levels by post-natal day 5 (P5) [34]. They also showed that *Hoxa13* and *Hoxd13* expression both peaked around E15 and steadily diminished from there into adulthood; spatially, both *Hoxa13* and *Hoxd13* had epididymal expression which peaked in the seminal vesicle [35]. This observation of *Hoxa13* and *Hoxd13* expression appears to contrast to the work of Prins et al. within the rat prostate demonstrating a postnatal increase in expression that is maintained into adulthood for all three of the previously mentioned genes [23]. They also demonstrated that *Hoxa13* and *Hoxd13* peaked in expression within the dorsal prostate rather than seminal vesicle, and also had a clear anterior boundary at the epididymis [23]. Furthermore, in the rat prostate, Prins et al. demonstrated *Hoxd13* to be the highest expressing *Hox* gene in each lobe, followed closely by *Hoxa13* and *Hoxb13*, and lastly *Hoxa9*, *Hoxa10*, and *Hoxa11* each with approximately 10-fold less RNA expression compared to the *Hox13* levels [23]. In a study evaluating *HOX* gene expression in a variety of normal adult human organs including prostate, *HOXA9, HOXA11, HOXA13, HOXB13*, and *HOXD9* were all identified as the highest expressing *HOX* genes with *HOXA10* and notably *HOXD13* each at a 10-fold lower expression level in the prostate compared to *HOXA13* and *HOXB13* [28]. In summary, as expected the 5' *HOX* genes (*Hoxa-d13*) clearly appear to be critical for prostate and GU development, but the timing and location across species is distinct and should be taken into consideration when using animal model systems for HOX biology.

The function of HOXB13 in the Developing and Adult Prostate

HOXB13 is unique in the prostate because it is highly expressed into adulthood in multiple species, and yet it is the most differentially-expressed HOX protein when comparing between lobes of the rodent prostate, suggesting that it may have more important functions in determining prostatic identity and maintaining organ homeostasis in an adult [23, 45]. Within the normal adult prostate, *HOXB13* is localized exclusively in prostate luminal epithelial cells [43, 46]. In rodent models, *Hoxb13* is most highly expressed in the ventral prostate lobe, has been shown to drive differentiation of prostate luminal epithelial cells, and is also required for the normal secretory function of the ventral prostate [23, 43, 45].

An important and somewhat controversial body of data pertains to the relationship between HOXB13 and the Androgen Receptor (AR). This pertains to both the regulation of *HOXB13* by AR and cooperation with AR signaling. *HOXB13* expression in the prostate is thought to be androgen-independent, as demonstrated by Bieberich et al. whereby the steady state mRNA level of *HOXB13* in the murine prostate was undiminished 8 days after host castration [46]. However, Prins et al. observed increased *Hoxb13* expression in the rat prostatic ventral lobe upon administration of testosterone, and expression was decreased in the dorsal and lateral lobes upon castration [23]. This apparent discrepancy could be accounted for by changes in prostatic cellularity in the context of hormone administration or depletion, since castration results in a significant reduction of *HOXB13*-positive luminal epithelial cells. In addition to regulation of *HOXB13* by androgen signaling, it has been shown that HOXB13 can act as a bivalent regulator of AR chromatin binding and function as either a growth-promoter or growth-suppressor in prostate cancer cells depending on the cellular context [47]. For example, in

androgen-sensitive prostate cancer cell lines such as LNCaP, increased HOXB13 activity can decrease levels of Cyclin D1 and lead to growth inhibition through reduction of pRb phosphorylation and stabilization of the pRB-E2F complex [24, 25]. Conversely, in castration-resistant prostate tumors, HOXB13 overexpression can inhibit p21 and thus act as an oncogene through subsequently promoting E2F activation and cell cycle progression [25]. A final noteworthy observation of HOXB13 localization is that, in human radical prostatectomy samples, the nuclear/cytoplasmic ratios of HOXB13 are drastically reduced in prostatic intraepithelial neoplasia (PIN) and prostate cancer when compared to normal glands, indicating much higher cytoplasmic retention and thus lower amounts of functional HOXB13 in the nucleus of tumor cells [24]. This suggests a potential mechanism of abrogating the growth-suppressive function of HOXB13 by cytosolic retention. Collectively, these observations highlight numerous important and interesting roles of HOXB13 in the prostate, but also underscore the need for additional mechanistic and functional studies to elucidate the molecular function of HOXB13 within the normal prostate and during prostate tumor initiation.

The Current Paradigm for Prostate Development from the Urogenital Sinus

Prostate cancer and benign prostatic hyperplasia (BPH) impact a significant cohort of men as they age. A fundamental understanding of prostate development and tissue homeostasis has the high potential to reveal mechanisms for prostate disease initiation and identify novel therapeutic approaches for disease prevention and treatment. In particular, it is essential to elucidate the contributions of cell types and key transcription factors involved in prostate

development and cellular turnover, as many of these cell types and genes play key roles in disease initiation and progression.

It is well established that the prostate gland is derived from embryonic urogenital sinus (UGS), since UGS epithelial cells morphologically bud, branch, and canalize to form the prostate [48]. In addition to forming the prostate, however, UGS epithelial cells also develop into urethral glands, which are functionally distinct from HoxB13-positive mature prostate epithelial acini [18]. The human prostate is composed of multiple zones arranged symmetrically and includes the transition, central and peripheral zones [49]. The peripheral zone is where most prostate cancer arises and the central zone wraps around the ejaculatory duct emerging from the seminal vesicle. The transition zone surrounds the urethra, which brings this zone into close proximity to periurethral glands. Urethral glands emerge along the urethra but are functionally and morphologically distinct from the surrounding prostate glands [50]. Paradoxically, while the prostate and urethral glands are derived from the same epithelial precursor cells, urethral gland epithelial cells rarely derive hyperplasia or cancer. This disparity highlights potential understudied mechanisms in prostate vs. urethral gland epithelial development that make prostate epithelial cells more susceptible to disease initiation.

The current paradigm of prostate development provides a general explanation for how the UGS can give rise to multiple distinct regions and glands [48, 51]. The cranial-caudal axis of the UGS allows for geographically distinct epithelial-mesenchymal interactions along the tissue. The differentiation and morphologic differences are controlled by temporal expression of distinct growth factors emerging from the mesenchyme. This primitive map allows for regional identity of the adult glands in general, but there are gaps in knowledge about what factors are necessary for distinguishing urethral glands from prostatic glands.

HOX Protein Binding Partners

It has been a long-established paradox that HOX proteins achieve exquisite *in vivo* gene specificity to program development using simple "AT-rich" gene recognition motifs; such motifs are much too common across the genome to allow HOX proteins working alone to attain such gene specificity (expertly reviewed in Mann et al.) [52]. To accomplish such specificity, HOX proteins rely on multiple co-factors to bind and specify transcriptional activity. The TALE (three amino acid loop extension) proteins are the predominant subtype of Homeobox proteins that partner with HOX proteins and specify gene targeting and activity. This family of proteins includes the MEIS, PBX, PKNOX and TGIF Homeobox proteins [53]. While they contain the homologous DNA binding domain canonically found in Homeobox genes, there are three unique characteristics of the TALE family. First, a three amino acid insertion in their homeodomains allows for cooperative binding to other transcription cofactors [54]. It is this ability to create complexes that provide increased binding affinity of Homeobox complexes to the DNA. Importantly, not every TALE protein group can bind to every other Homeobox gene, increasing specificity of DNA binding depending on the combination of factors present in a complex [54]. Second, the regions flanking the homeodomains of TALE proteins are highly conserved across species [55]. Third and finally, unlike their spatiotemporally-restricted HOX relatives, TALE factors are more widely expressed across an organism.

While many TALE factors have been implicated in cancers, the recent discovery of the *HOXB13* mutations in hereditary prostate cancer to confer a risk for prostate cancer discussed above has sparked an interest in the MEIS proteins in particular [21]. Many of the mutations within the *HOXB13* gene fall within the MEIS binding domain (**Figure 1.3**).

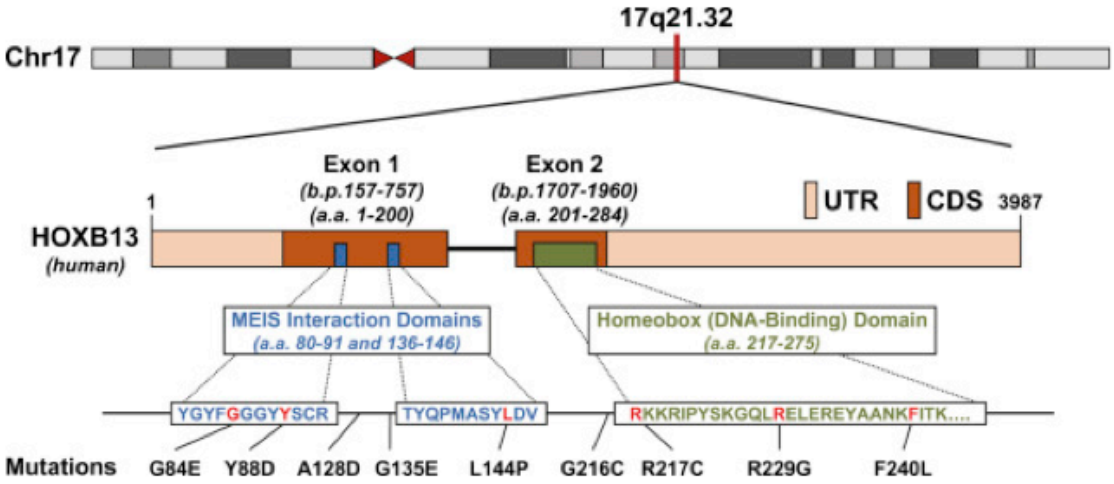

Figure 1.3: Genomic Location, Domains, and Known Mutations of Human HOXB13. Since the original report of somatic *HOXB13(G84E)* mutations in a subset of familial cancer, more hereditary mutations conferring increased risk of prostate cancer have been identified [21]. The *HOXB13* gene is located on human Chromosome 17q21.32 at the 5' end of the 17q21-22 HOXB cluster, and consists of two exons and three known functional domains (accession number NC_000017/11 and ProtID Q92826). The HOXB13 transcript is 3987 base-pairs (b.p.) long, and Exons 1 and 2 are positioned at 157-757b.p. and 1707-1960b.p, respectively. The regions in beige indicates the untranslated regions (UTR), while the regions in brown indicate coding regions (CDR). The HOXB13 protein is 284 amino acids in length and contains two MEIS-interacting domains (amino acids 80-91 and 136-146) and a single DNA-binding homebox domain (amino acids 217-275). The two MEIS-interaction domains were functionally defined by Williams et al. [56, 57], and the homeodomain was functionally defined in Zeltser et al. [58]. Clusters of mutations can be seen within or nearby the two MEIS-interacting domains and the homeodomain.

Even though it is now clear, as will be discussed in depth further on in this chapter, that *HOXB13* mutations are strongly associated with increased prostate cancer risk, there are significant gaps of knowledge regarding the mechanism of action of *HOXB13* mutations, and how co-factor modulations impact prostate cancer initiation.

The *MEIS* (murine ecotropic integration site) gene was implicated in cancer based upon the discovery that the *MEIS1* gene was the most common location for an ecotropic murine leukemia virus to integrate [59]. When the virus integrated, higher *MEIS1* expression was noted as the mice developed leukemia, and this was the first indication of *MEIS* as oncogenes in liquid tumors [59]. MEIS proteins function as DNA-binding cofactors with the HOX and PBX families such that the cooperative binding increases DNA binding specificity [52, 60-62]. Our current understanding of MEIS-HOX interactions is that, upon DNA binding of the two, DNA-bound MEIS/HOX complexes recruit collaborator proteins to compile a multimeric protein complex at specific gene promoters [52]. It should be noted, however, that TALE proteins have both HOX-dependent and HOX-independent functions and their role in development and disease likely extends beyond regulation of HOX protein DNA specificity [52, 62].

Deregulation of MEIS Proteins in Cancer

While little is known about the MEIS and PBX proteins in the context of prostate cancer, current understanding of functions in other cancer types may provide directions for future work. MEIS proteins have complicated and context-dependent roles in cancer initiation and progression. They are down-regulated in some cancer types, but overexpressed in others, making it unclear if *MEIS* genes are bona fide oncogenes or tumor suppressors genes. This phenomenon

of fluidity between tumor suppression and oncogenesis is not unheard of; in fact, *HOX* genes display a very similar pattern, as discussed above [31].

The most well studied context for the role of MEIS, PBX and HOX proteins in cancer is leukemia, and specifically AML (Acute Myeloid Leukemia) and MLL (Mixed Lineage Leukemia). MEIS1 is required for normal adult bone marrow hematopoiesis, with deletion of *MEIS1* leading to stem cell exhaustion and an inability to self-renew [63]. MEIS1 alone is not sufficient to transform hematopoietic cells however, as MEIS1 requires the cooperation of HOXA9 to accelerate HOX-induced leukemia [64]. There is a common theme across many publications investigating MEIS in leukemia; MEIS proteins can mitigate differentiation while also increasing proliferation, a deadly and oncogenic combination. *MEIS1* and *HOXA9* are direct targets of the MLL fusion gene [65] and MEIS1, in addition to the redundant contributions of PBX2 and PBX3, appears to be the rate-limiting step in the cell cycle progression of MLL leukemia stem cells [66]. In fact, it was shown recently that PBX3 is crucial to help stabilize MEIS1 proteins, and that the dimerization of PBX3 and MEIS1 is required for HOX-induced leukemia [67]. In myeloid leukemias, the full length MEIS1-A is able to stop differentiation through G-SCF and promotes proliferation [68].

The connection between MEIS1 and the cell cycle, as well as maintenance of a more primitive stem cell state across multiple cell types are likely mechanisms of action that lead to its deregulation in a range of pathological contexts. For example, MEIS1 slows adult and neonatal proliferation in cardiomyocytes by modulating the progression of the cell cycle [69]. There are also multiple papers indicating a role for MEIS in Restless Leg Syndrome, and more information on MEIS' role in this disease can be found in a 2014 review by Garcia-Borreguero et al. [70].

Neuroblastoma displays *MEIS1* up-regulation in many cell lines and tumors [71]. Neuroblastoma is also the context where many novel, and potentially functionally distinct, MEIS isoforms have been investigated [72]. In neuroblastoma SJNB-8 cells, the exogenous expression of MEIS-E, an isoform lacking a DNA binding domain, induces changes in cell growth proliferation apoptosis, cytoskeleton, long-distance gene regulation, morphogenesis, protein transport, and differentiation markers [72, 73]. This analysis, however, did not indicate the direction of change for many of these processes [73]. MEIS2 is critical for neuroblastoma cell survival and proliferation by asserting control over M-phase of the cell cycle, again illustrating a cell cycle control function for MEIS in cancer cells [74]. Lung adenocarcinomas, in particular those with LKB1 mutations, also show up-regulation of MEIS2, though investigation of the mechanism of action has not been elucidated [75]. Thus, in numerous tumor sites, MEIS1 and MEIS2, and potential splice-variants of each, appear to function as promoters of cell cycle progression, and in some instances to maintain cancer cells in a less-differentiated state.

While the majority of cancer-related research into the MEIS and PBX transcription factors has been focused on their overexpression in leukemia, there are many pathological contexts where MEIS proteins appear to function as tumor suppressors. In fact, MEIS proteins can act as a tumor suppressor or oncogene even within a specific organ site of carcinogenesis; however, their roles are restricted to specific molecular subtypes. For example, in the majority of AML cases *MEIS1* and *HOXA9* act as oncogenes, while within a particular subtype of patients *MEIS1* and *HOXA9* expression are significantly decreased compared to other AML subtypes where such transcripts are over-represented [76]. Patients with the AML-ETO fusion protein show low *MEIS1* and *HOXA9* mRNA as compared to other AML patients where high *MEIS1* expression are typical. *MEIS1* down regulation in the AML-ETO patient population is due to

methylation at its promoter [76] indicating a role for epigenetic modification in regulating levels of MEIS expression. Additionally, lung adenocarcinomas with LKB1 mutations display over-expression of MEIS whereas in NSCLC (non-small cell lung cancer) patients, MEIS1 over-expression inhibits cell growth and *MEIS1* knock down using siRNA-targeting increases proliferation [77]. In this NSCLC context, DNA synthesis is increased when *MEIS1* decreased [77]. Colorectal adenomas displayed a seven-fold decrease in *MEIS* transcripts, in particular a homeodomain-truncated splice-variant *MEIS1-D* [78, 79]. Thus, in numerous tumor types, *MEIS* expression appears to be actively inhibited, either via down-regulation or expression of dominant-negative splice variants.

MEIS and PBX Proteins in Prostate Cancer

MEIS and PBX proteins have been vastly understudied in the context of prostate cancer, and there are numerous avenues of future investigation with clear clinical impact. MEIS1 has been shown to act as an androgen receptor suppressor, where ectopic expression slows LNCaP prostate cancer cell growth [80]. MEIS1 can physically interact with the androgen receptor, the most critical driver of prostate cancer and the main target of clinical intervention [20, 80, 81]. Moreover, work published by our group demonstrates that higher expression of *MEIS1* and *MEIS2* provide a survival benefit to men with intermediate and low-grade prostate cancer [20]. In the normal prostate, MEIS expression is highest in basal epithelial cells and stromal cells, with a detectable but significantly lower expression in luminal epithelial cells. Tumors with below average *MEIS1* and *MEIS2* expression convey a significant decrease in patient survival, suggesting a functional role for decreased MEIS expression and the initiation and progression of

poor-prognosis prostate tumors [20]. Similarly, tumor expression of PBX3 was associated with improved prostate cancer specific survival compared to patients expressing low levels; this study statistically demonstrated that PBX3 expression could be used to potentially predict outcome and enhance tumor staging [82]. However, significant additional work is required to more comprehensively understand the function of MEIS and other TALE proteins in prostate cancer, especially in the context of HOXB13 mutations.

The Germline *HOXB13-G84E* Mutation and Prostate Cancer

The identification of the germline *HOXB13(G84E)* mutation by Ewing et al. within a subset of familial prostate cancers in 2012 brought HOXB13, the genes regulated by HOXB13, and HOX-protein co-factors, into the spotlight of prostate cancer research [21]. This discovery highlighted a novel transcriptional regulation pathway that has a key role in prostate development and tumor etiology [21]. Patients with the mutation, which substitutes a glutamic acid for glycine at the second position of codon 84, have significantly higher odds for developing prostate cancer than men without the mutation [21]. The G84E mutation occurs within the MEIS interaction domain of *HOXB13*, emphasizing the importance of MEIS-HOX protein interactions in prostate cancer (**Figure 1.3**). Since the initial study, several additional studies have validated the G84E mutation as associated with increased prostate cancer risk (**Table 1.1**).

Table 1.1 *HOXB13(G84E)* Mutations in Prostate Cancer

Table 1 HoxB13(G84E) mutations in prostate cancer.

Author	PMID	Study year	Patient population	Age of PrCa Onset G84E Carrier[h]	Study type[i]	Genotyping assay	Sample #		Cancer cases		Non-cancer controls		OR (95% CI)	*P*-value
							Cancer	Non-cancer	Mutation	Non-mutation	Mutation	Non-mutation		
Akbari	22781434	2012	Multiple ethnicities, multiple countries	59.4	HB	Sanger sequencing	1853	2225	10	1843	2	2223	5.8 (1.3—26.5)	0.01
Albitar F	25874003	2015	USA, Caucasian	NR	HB	Sanger sequencing	232	110	2	230	1	109	0.95 (0.09—10.6)	0.97
Beebe-Dimmer[a]	26108461	2015	Mayo Clinic Biobank, Primarily Caucasian	NR	HB	Taq-Man	42	7218	19	23	1343	5875	1.99 (1.37—2.90)	<0.0001
Breyer	22714738	2012	Multiple countries, multiple ethnicities	53.4	HB	Taq-Man	928	930	20	908	2	928	7.9 (1.8—34.5)	0.0062
Chen	23393222	2013	Multiple countries, multiple ethnicities	NR	HB	iPLEX MassARRAY	20	3887	7	13	701	3186	RR = 2.45 (1.48—4.07)	0.01
Ewing*	22236224	2012	USA, Caucasian	52.6	HB	Taq-Man	5083	2662	72	5011	4	2658	20.1 (3.5—803.3)	8.50E-07
Gudmundsson[a]	23104005	2012	Chicago-SPORE, Caucasian	58.3	HB	Illumina SNP Chips	1988	1260	11	1971	5	1255	1.40 (0.49—4.04)	5.30E-01
Gudmundsson[b]	23104005	2012	Iceland, Caucasian	66.2	HB	Illumina SNP Chips	4537	54444	13	4524	44	54400	3.55 (1.91—6.60)	1.00E-04
Gudmundsson[c]	23104005	2012	Netherlands, Caucasian	63.9	HB/PB	Illumina SNP Chips	1520	1916	23	1497	4	1912	7.34 (2.53—21.3)	3.90E-10
Gudmundsson[d]	23104005	2012	Spain, Caucasian	NR	HB	Illumina SNP Chips	717	1692	1	716	0	1692	7.09 (0.29—174.2)	2.30E-01
Gudmundsson[e]	23104005	2012	United Kingdom, Caucasian	61.7	HB	Illumina SNP Chips	561	1825	6	505	1	1824	21.67 (2.60—180.4)	4.40E-03
Gudmundsson[f]	23104005	2012	Romanian, Caucasian	69.4	HB	Illumina SNP Chips	722	857	1	721	1	856	1.19 (0.07—19.0)	9.31E-01
Karlsson[a]	22841674	2014	Swedish, Caucasian	NR	PB	iPLEX MassARRAY	2805	1709	130	2675	24	1685	3.4 (2.2—5.4)	6.40E-10
Karlsson[b]	22841674	2014	Swedish, Stockholm-1 group, Caucasian	NR	HB	iPLEX MassARRAY	2098	2880	91	2007	37	2843	3.5 (2.4—5.2)	2.00E-11
Kluzniak	23334858	2013	Polish, caucasian	67.3	PB	Taq-Man	3515	2604	20	3495	3	2601	4.96 (1.47—16.7)	0.0097
Kote-Jarai	25595936	2015	United Kingdom, Caucasian	NR	HB	Taq-Man	8652	5252	134	8518	28	5224	2.94 (1.95—4.42)	<0.0001
Laitinen	23292082	2013	Finnish, Caucasian	<=55	HB/PB	Multiple methods	4571	923	160	4411	28	895	1.15 (0.77—1.74)	0.47
MacInnis	23457453	2013	Australian, caucasian	52.7	PB	Taq-Man	1384	N/A	19	1365	N/A	N/A	Incidence: 16.4 (2.5—107.2)	N/A
Storebjerg	26779768	2016	Danish	61.7	HB	Sanger sequencing	995	1622	25	970	8	1614	5.12 (0.26—13.38)	1.30E-05
Stott-Miller	23129385	2013	USA, Caucasian	NR	PB	Taq-Man	1457	1442	18	1439	5	1437	3.6 (1.3—9.7)	0.01
Witte	23396964	2013	Multiple countries, multiple ethnicities	NR	FB/HB	Taq-Man	1645	1019	20	1625	3	1016	4.17 (1.24—14.1)	0.02
Xu	23064873	2013	Multiple countries, caucasian	62.8	FB	iPLEX MassARRAY	326	117	154	172	36	81	2.01 (1.29—3.16)	0.002

a, b, c, d, e, f: Data from multiple populations present within a single study.
h: Not reported.
i: FB = Family Based; HB = Hospital Based; PB = Population Based.

It is important to note that the majority of these studies were conducted on Caucasian men of European ancestry, with only 5 of these 22 studies included multiple ethnicities in the study group. In a study conducted by the International Consortium for Prostate Cancer Genetics (ICPCG), they observed a geographical frequency gradient of the G84E mutation across the European continent, with a higher mutation frequency in Nordic countries [83]. While multiple studies have corroborated that the G84E mutation is associated with increased prostate cancer risk, the data on the association of G84E with other clinically relevant variables has been mixed. Regarding age of diagnosis, the G84E mutation has been shown to be significantly associated with younger age of diagnosis in the majority of studies [21, 84-89], with other studies reporting no difference in age of diagnosis [90]. A similar pattern has emerged regarding a positive family history of prostate cancer, with all studies reporting a significantly higher odds of the G84E mutation being present in patients with a positive family history or hereditary prostate cancer. In the context of G84E and a potential role in the initiation of more aggressive prostate tumors, Storjberg et al. determined that patients carrying the G84E mutation had a significantly higher PSA at diagnosis, higher Gleason score, and a higher likelihood of positive surgical margins at time of radical prostatectomy than non-carriers, implying that the G84E mutation maybe associated with more aggressive prostate cancers [91]. However, further analyses are necessary to determine whether mutation of *HOXB13* is associated with poor-prognosis prostate tumors. In summary, the presence of G84E mutation clearly impacts prostate cancer initiation, but data thus far has not strongly implicated the presence of the mutation in contributing to cancer progression and metastasis.

Other Germline *HOXB13* Mutations Associated with Prostate Cancer

Since the discovery of the G84E mutation, there has been greater focus on identifying other novel germline mutations of *HOXB13* associated with increased prostate cancer risk. This is of particular importance for non-Caucasian populations, as the risk of prostate cancer associated with the G84E mutation has the highest frequency in European/ Caucasian populations. Indeed, new mutations of *HOXB13* conferring increased prostate cancer risk have begun to be identified in non-Northern European populations. Notably, Lin et al. identified the novel G135E mutation to be associated with increased prostate cancer risk in a population of Chinese men, and did not identify the presence of the G84E mutation [92]. Similarly, Maia et al. identified the A128D and F240L mutations in a population of Portuguese men to be associated with prostate cancer risk [93]. Ewing et al. reported the identification of several rare missense variants of *HOXB13* (Y88D, L144P, G216C, R217C, and R229G, **Figure 1.2 and Table 1.2**) during their initial study of G84E. Not all of these more recently discovered mutations are located in the MEIS-interacting domain, but the most common and mutation with the highest odds ratio of prostate cancer risk is the G84E mutation. Of these rare mutations, the R229G and G216C were identified in men with some African ancestry [21]. Given the paucity of data, however, on non-G84E mutations of *HOXB13*, and the lack of study of prostate cancer risk mutations in non-Caucasian populations, continued efforts to identify novel risk mutations of *HOXB13* are necessary. Future studies are needed to understand how the other mutations confer the increased risk, and whether the mutations function similarly or differently from one another.

Table 1.2 Germline and Somatic *HOXB13* Mutations in Cancer

Table 2 Germline and somatic HoxB13 mutations in cancer.

Author	PMID	Study year	Cancer primary	Patient population	Study type[f]	Primary mutation	Germline or somatic	Cancer cases		Non-cancer controls		Genotyping assay	OR (95% CI)	*P* value
								Mutations	Non-mutations	Mutations	Non-mutations			
Akbari MR[a]	23099437	2012	Breast	Canadian Caucasian	HB	G84E	Germline	2	1802	1	924	Taq-Man	1.0 (0.09–11.3)	0.98
Akbari MR[b]	23099437	2012	Breast	Polish Caucasian	HB	G84E	Germline	5	2228	3	1834	Taq-Man	1.37 (0.33–5.75)	0.67
Akbari MR	23541221	2013	Colorectal	Canadian, Australian	PB	G84E	Germline	13	2682	8	4585	Taq-Man	2.8 (1.2–6.7)	0.02
Beebe-Dimmer[b]	26108461	2015	Bladder	Primary Caucasian	HB	G84E	Germline	3	23	205	5875	Taq-Man	1.99 (0.84–3.86)	0.06
Beebe-Dimmer[c]	26108461	2015	Leukemia	Primary Caucasian	HB	G84E	Germline	3	23	86	5875	Taq-Man	3.17 (1.35–6.03)	0.01
Beebe-Dimmer[d]	26108461	2015	Sarcoma	Primary Caucasian	HB	G84E	Germline	1	23	123	5875	Taq-Man	1.48 (0.23–3.80)	0.4
Beebe-Dimmer[e]	26108461	2015	Testis	Primary Caucasian	HB	G84E	Germline	1	24	49	5888	Taq-Man	2.31 (0.36–5.86)	0.18
Laitinen[a]	23292082	2013	Breast	Finnish, Caucasian	HB/PB	G84E	Germline	16	970	16	1433	Multiple methods	1.48 (0.74–2.97)	0.27
Laitinen[b]	23292082	2013	Colorectal	Finnish, Caucasian	HB/PB	G84E	Germline	7	435	0	459	Multiple methods	15.83 (0.90–277.95)	0.06
Lin	22718278	2013	Prostate	Chinese	PB	G135E	Germline	3	639	0	1491	iPLEX MassARRAY	16.33 (0.84–316.54)	0.065
Maia	26176944	2015	Prostate	Portuguese	FB	A128D/ F248L	Germline	3	459	0	132	AB 3500 Genetic Analyzer	2.02 (0.10–39.3)	0.64
Ewing	22236224	2012	Prostate	USA, Caucasian	HB	Y88D	Unknown[g]	N/A	N/A	N/A	N/A	Taq-Man	N/A	N/A
Ewing	22236224	2012	Prostate	USA, Caucasian	HB	L144P	Unknown[h]	N/A	N/A	N/A	N/A	Taq-Man	N/A	N/A
Ewing	22236224	2012	Prostate	USA, Caucasian	HB	G216C	Germline	1	90	N/A	N/A	Taq-Man	N/A	N/A
Ewing	22236224	2012	Prostate	USA, Caucasian	HB	R229G	Germline	1	90	N/A	N/A	Taq-Man	N/A	N/A
Xu	23064873	2013	Prostate	Multiple countries, caucasian	FB	R217C	Germline	2	6420	0	1902	iPLEX MassARRAY	1.48 (0.07–30.9)	0.8

a, b, c, d, e: Data from multiple populations present within a single study.
f: FB = Family Based; HB = Hospital Based; PB = Population Based.
g: Unknown, mutation found in LAPC4 Cell Line.
h: Unknown, mutation found in LNCaP Cell Line.

Germline *HOXB13-G84E* in Non-Prostate Tumors

Given the strong relationship between the *HOXB13(G84E)* mutation and prostate cancer risk, as well as the importance of *HOXB13* in development and cancer, several studies have examined the role of *HOXB13* mutations in increasing the risk of other tumor types (**Table 1.2**). Results between the association of G84E and non-prostate cancer risk have been mixed. Notably, Akbari et al. and Beebe-Dimmer et al. showed that the G84E mutation was associated with a significantly increased risk of colorectal carcinoma and leukemia, respectively [94, 95]. However, Latinen et al. showed no significant association between the G84E mutation and colorectal cancer risk, although their results did approach significance [89]. The G84E mutation has also been investigated in cancer of the breast, bladder, testis, and in sarcoma, but results have not shown a significant association between the mutation and increased cancer risk among those cancers studied [94]. However, it should be noted that a few of these studies approached near significance, and additional studies containing a larger sample size has the potential, in some instances, to establish a significant correlation between the G84E mutation and non-prostate cancer risk.

Deregulation of *HOXB13* in Non-Prostate Tumors

Despite its emerging role in prostate cancer, deregulation of *HOXB13* expression has been implicated in a variety of human cancers, functioning either as a tumor-promoting factor in some tumor types, or a tumor-repressing factor in others (**Table 1.2**). Surprisingly, aberrant expression of *HOXB13* has been documented in a variety of non-posterior axis cancers, including thyroid, breast, metastatic melanoma, and oral squamous cell (**Table 1.2**). In many instances,

however, the functional significance of such expression has yet to be determined. In endometrial, ovarian, melanoma, and breast tumors, increased *HOXB13* expression appears to promote tumor progression [96-98]. In endometrial tumors, Yamashita et al. demonstrated *HOXB13* expression in tumor tissues and demonstrated that HOXB13 over-expression led to increased cellular invasion *in vitro* [96]. In ovarian cancer, Miao et al. demonstrated that over-expression of *HOXB13* in ovarian cancer cells resulted in increased cell proliferation and survival [97]. In melanoma, Maeda et al. showed that the expression levels of *HOXB13* were significantly higher in patients with metastatic melanoma compared to patients with a non-metastatic primary melanoma [99]. In breast cancer, *HOXB13* expression is predictive of a poor clinical outcome in tamoxifen-treated breast cancers, indicating that increased *HOXB13* could have a prognostic role in breast cancer [100]. Furthermore, ectopic expression of HOXB13 in MCF10A breast epithelial cells enhances motility and invasion *in vitro*, and *HOXB13* expression is increased in both pre-invasive and invasive primary breast cancer [100].

While the majority of the current literature demonstrates that *HOXB13* is generally over-expressed and tumor promoting in most cancers, several studies support a role for *HOXB13* as a tumor suppressor within other cancer contexts. Jung et al. and Kanai et al. showed that *HOXB13* expression is decreased in primary colorectal adenocarcinoma, and that over-expression of HOXB13 inhibits cell proliferation in colorectal cancer cell lines [100, 101]. Furthermore, Cantile et al. showed a progressive decrease in HOXB13 nuclear expression in the transition from non-neoplastic thyroid to adenoma to different histologic types of thyroid cancer [102]. In bladder cancer, Marra et al. found that the loss of nuclear HOXB13 is implicated in shorter disease free survival in non-muscle invasive bladder cancer and decreased nuclear HOXB13 correlates with muscle invasion [103]. Thus, it is clear that aberrant expression of HOXB13

plays a key role in the progression of many different cancer types, including both non-genitourinary and genitourinary cancers. Moreover, the context-dependent tumor promoting or repressing functions of HOXB13 further underscore key organ-specific roles of HOXB13 in cancer. Hence, it is the HOXB13-associated binding partners that provide specificity to DNA binding and subsequent gene targets who are the key mediators of HOX-associated tumor initiation and progression. Additional investigation into the function of HOXB13 and its binding partners across various tumors types is thus warranted.

CHAPTER II

CONTRIBUTION OF CAUDAL MÜLLERIAN DUCT MESENCHYME TO PROSTATE DEVELOPMENT

Introduction

A fundamental understanding of prostate development and tissue homeostasis has the high potential to reveal mechanisms for prostate disease initiation and identify novel therapeutic approaches for disease prevention and treatment. Our current understanding of prostate lineage specification stems from the use of developmental model systems that rely upon the embryonic pre-prostatic urogenital sinus mesenchyme to induce the formation of mature prostate epithelial cells. It is unclear, however, how the urogenital sinus epithelium can derive both adult urethral glands and prostate epithelia. Furthermore, the vast disparity in disease initiation between these two glands highlights key developmental factors that predispose prostate epithelia to hyperplasia and cancer.

In this study we demonstrate that the caudal Müllerian duct mesenchyme (CMDM) is able to drive prostate epithelial differentiation and is a key determinant driving cell lineage specification between urethral glands and prostate epithelia. The CMDM is canonically associated with female urogenital development as the expression of anti-Müllerian hormone (AMH) in male sertoli cells causes the irreversible regression of the Müllerian Ducts in males [104, 105]. However, the role of the Müllerian duct precursor tissue, the CMDM, has not been investigated in the context of the prostate. Utilizing both human embryonic stem cells and mouse embryonic tissues, we document that formation of AR, PSA, NKX3.1, and HOXB1313-positive prostate epithelial cells can be induced upon recombination with caudal Müllerian duct

mesenchyme. These results help to explain key developmental differences between prostate and urethral gland differentiation, and provide support to investigate how factors secreted by the caudal Müllerian duct may be involved in prostate disease prevention and treatment.

Materials and Methods

Human subjects

All human tissues were acquired under an expedited protocol approved by the University of Chicago Institutional Review Board (IRB). Tissue samples were managed by the University of Chicago Human Tissue Resource Center core facility.

Mice

Animal studies were carried out in strict accordance with the recommendations in the Guide for the Care and Use of Laboratory Animals of the National Institutes of Health and procedures were approved by the University of Chicago Institutional Animal Care and Use Committee. All mouse surgery was performed under Ketamine/Xylazine anesthesia, and all efforts were made to minimize animal suffering. Wild type C57BL/6 mice were obtained from the Jackson Laboratory. Timed-pregnant C57BL/6 mice, six-week-old male nude mice, and timed-pregnant Sprague Dawley rats were obtained from Harlan Laboratories (Indianapolis, IN).

Cell Culture

The human embryonic stem cell (hESC) line WA01(H1) was acquired from WiCell (Madison, WI) and cultured using the feeder-independent protocol using mTeSR1 media (Stem

Cell Technologies; Vancouver, B.C.). The human ES cells were used within ten passages of thawing, and were dissociated using mTeSR1 media with an Accutase (Millipore; Billerica, MA) digestion.

Tissue Recombination

Tissue recombination and renal grafting were performed using previously reported techniques and all recombination experiments were conducted in triplicate with appropriate controls [106]. In this study, the mesenchymal cells were derived from euthanized female newborn rats. The caudal Müllerian duct (MD), including the primordium of cervix and upper vagina, was separated from the UGS. The tissues were digested separately using 1% trypsin (BD Biosciences; San Joes, CA) in Ca^{2+} and Mg^{2+}-free HBSS (Gibco) and placed in a refrigerator at 4°C for 75 minutes. After neutralizing the trypsin with 10% FBS in DMEM/F12 medium (Gibco; Grand Island, NY), the mesenchymal sleeves were carefully teased from the epithelial tube. The caudal Müllerian duct mesenchyme (MDM) and urogenital sinus mesenchyme (UGSM) were transferred into DMEM/F12 medium + 10% FBS + 1% Pen/Strep + 1% NEAA plus 1nM R1881 (Sigma; St. Louis, MO) and incubated at 37°C with 5% CO_2 overnight. After removing the culture medium, the mesenchyme was digested with 0.2% collagenase in DMEM/F12 medium and placed the tube in 37°C on a shaker for 1 hour. The digested tissues were vigorously vortexed to yield a homogenous single cell suspension and collagen-neutralized using DMEM/F12 medium + 10% FBS. The dissociated mesenchymal cells were washed with HBSS, and suspended in DMEM/F12. Cell numbers were counted using a Cellometer (Nexelom Bioscience; Lawrence, MA).

To harvest urethral epithelium, 10-week old adult C57BL/6 male mice were used as donors as they are post-pubescent and thus beyond tissue morphogenesis and within homeostatic tissue maintenance. The urethra was isolated and the muscle layer was manually teased off. The epithelial sheath was transferred into DMEM/F12 medium and digested into a single cell suspension using 0.2% collagenase as described above.

To induce human prostate glands, caudal MDM cells or UGSM cells were mixed with hES cells at a 1:2.5 ratio of hES/mesenchymal cells. The cell mixtures were re-suspended with 75% Matrigel (BD Biosciences) and injected into the sub-renal capsule of adult male nude mice. As controls, caudal MDM cells, UGSM cells, and hES cells were grafted alone into adult male nude mouse hosts. After 10 weeks, glandular tissues were harvested and analyzed. To induce mouse prostate glands, either caudal MDM cells or UGSM cells were mixed with adult mouse urethral epithelial cells at a 1:2.5 ratio of epithelial/mesenchymal cells and implanted as described above.

Tissue collection, preparation, and prostate microdissection

After euthanasia, the urogenital tract was dissected from the surrounding tissues, removed en bloc including the urethra, all prostate lobes, two seminal vesicles, and bladder, and photographed. To dissect prostatic lobes, the mouse prostate was dissociated using 0.2% collagenase (type IV, Sigma) for 15 minutes. The tissue was gently teased using needles under a dissection microscope (Leica MZ16F stereomicroscope) and photographed. The tissues were embedded in 2% agar gel with optimal orientation and then embedded in paraffin and serially sectioned. Tissue samples were processed by the University of Chicago Human Tissue Resource

Core facility. Briefly, tissue samples were formalin-fixed for 24 hours and embedded in paraffin immediately after necropsy. Sections (5 μm thick) were adhered to positively charged slides.

Histology and Immunostaining

H&E staining was performed using a SAKURA Tissue-Tek Prima Autostainer. For immunohistochemistry staining, formalin-fixed, paraffin-embedded (FFPE) slides were deparaffinized in xylene, and hydrated using graded ethanol washes. Tissues were treated with antigen retrieval buffer (S1699 from DAKO; Glostrup, Denmark) in a steamer for 20 minutes. Anti-p63 (D2K8X rabbit monoclonal, Cell Signaling Technology; Danvers, MA) and anti-AR (N-20 rabbit polyclonal, Santa Cruz Biotechnology; Santa Cruz, CA) were applied for 1 hour at room temperature in a humidity chamber. Following TBS wash, the antigen-antibody binding was detected with Envision+system (K4001, DAKO; Carpinteria, CA) and DAB+Chromogen (DAKO, K3468). Tissue sections were briefly immersed in hematoxylin for counterstaining and were cover-slipped. For immunofluorescence staining, after deparaffinization and rehydration, tissues were treated with heat-induced antigen retrieval using Tris-EDTA Buffer (10mM Tris Base, 1mM EDTA Solution, pH 9.0) in a pressure cooker for 3 min. After 30 min of blocking in 10% normal goat serum PBS, slides were incubated with primary antibodies followed by secondary Alexa Fluor goat anti-rabbit IgG or/and anti-mouse IgG (Cell Signaling). Following PBS wash, the tissues were counterstained with DAPI and were cover-slipped.

Antibodies used for immunostaining were AR (Santa Cruz Biotechnologies, N20, rabbit polyclonal, 1:400), p63 (Santa Cruz Biotechnologies, 4A4, mouse monoclonal, 1:100), NKX3.1 (Biocare, rabbit polyclonal, 1:50), Hoxb13 (Santa Cruz Biotechnologies, H-80, rabbit polyclonal, 1:100), chromogranin A (Santa Cruz Biotechnologies, LK2H10, mouse monoclonal, 1:100),

PSA (Santa Cruz Biotechnologies, C-19, goat polyclonal, 1:100). DAPI (Invitrogen, 1:1000) was used to counterstain the nucleus. Secondary staining reagents included Alexa Fluor goat anti-rabbit IgG (Cell Signaling Technologies), Alexa Fluor goat anti-mouse IgG (Cell Signaling Technologies), or Alexa Fluor donkey anti-goat IgG (Invitrogen).

Colorimetric images were captured using a Panoramic Scan Whole Slide Scanner (Cambridge Research and Instrumentation; Hopkinton, MA) and images captured using the Panoramic Viewer software version 1.14.50 (3DHistech; Budapest, Hungary). For immunofluorescence staining slides, images were captured using an Olympus FV1000 laser scanning confocal microscope.

Results

Transcription Factors NKX3.1 and HoxB13 Differentiate between Prostate and Urethral Epithelia

To elucidate the differences between the prostate and urethral glands, we analyzed the expression of transcriptional factors associated with epithelial (ΔNp63), genitourinary (Androgen Receptor), or prostatic lineage (Nkx3.1 and Hoxb13) using both human and mouse tissues (**Figure 2.1 A and C**). ΔNp63 is a basal-restricted transcription factor that is necessary for prostate development and maintenance of basal epithelial cells in bi-layered epithelia, which include both the urethral and prostate glands [107, 108]. Androgen Receptor (AR) is a central steroid transcription factor with a well-documented and important role in prostate genitourinary development, prostate homeostasis, and prostate cancer [18, 109]. Urethral glands also contain

nuclear AR and are therefore responsive to testosterone [110]. NKX3.1 is an androgen-induced homeobox transcriptional factor that regulates organogenesis and epithelial differentiation of the prostate [111-113]. Nkx3.1 is expressed early in the male urogenital epithelium, and its presence indicates induction of prostatic epithelial identity [18, 114]. Genetic lineage tracing has demonstrated that Nkx3.1+ cells can reconstitute all three lobes of the rodent prostate in renal capsule experiments [115]. Hoxb13 is another homeobox transcriptional factor that is critical in prostate development and adult organ function and mutations in Hoxb13 are associated with a subset of familial prostate tumors [21, 43, 84, 116]. Hoxb13 is commonly used as a persistent marker of terminally differentiated prostatic luminal epithelium. During fetal development, the urogenital sinus contributes to the development of the bladder, urethra, and prostate. Urethral epithelial cells branch off to form the urethral glands, and are located along the urethra. However, at the proximal region of the urethra, some epithelial ducts grow beyond the urethral wall and repeatedly branch to form prostate acini [104, 117].

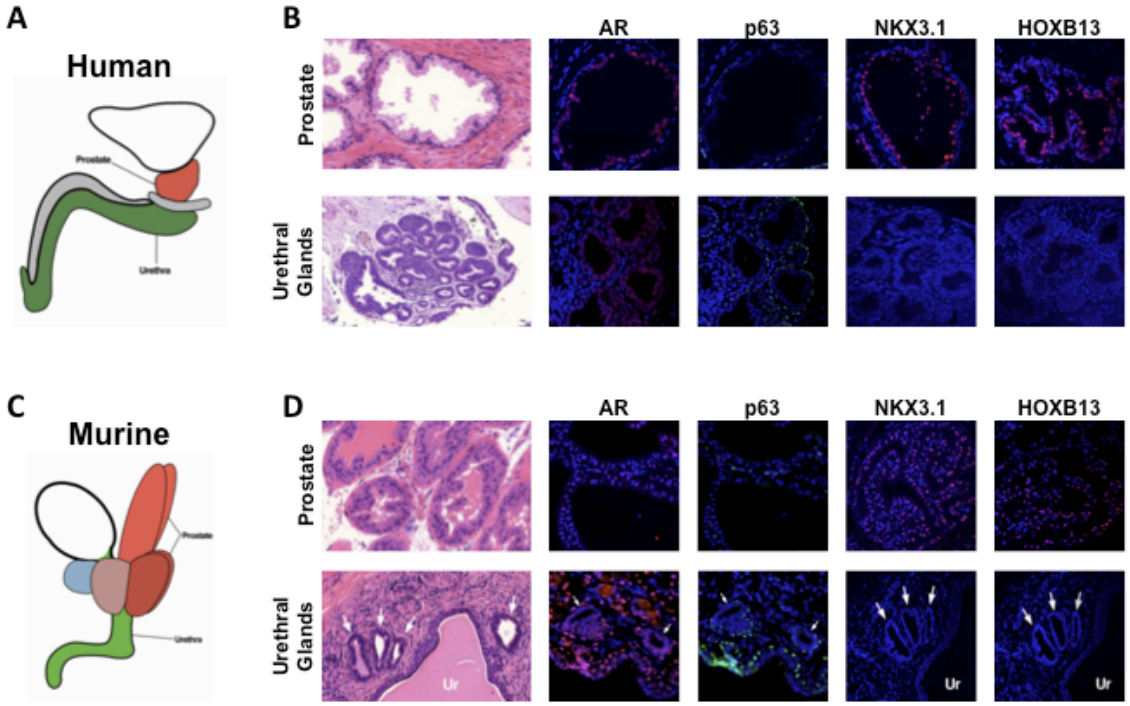

Figure 2.1: **NKX3.1 and Hoxb13 Expression in Prostate but not Urethral Gland Epithelia. A and C.** Schematic depicting the anatomy of the human prostate (red), urethra (green), and bladder (white). **B.** Hematoxylin and eosin (H&E) staining and Immunofluorescence (IF) staining of Androgen Receptor (AR), DNp63 (p63), NKX3.1, and Hoxb13 in human prostate and urethral glands. **D.** H&E staining and IF staining of AR, p63, NKX3.1, and Hoxb13 in the murine urethral and prostate glands. UR indicates urothelium. NKX3.1 and HoxB13 are seen in the human and murine prostate but not in the neighboring urethral gland epithelia. Arrows indicate urethral glands located by the urethra.

As expected, both human and mouse prostate epithelium and urethral gland epithelium contain ΔNp63-positive basal cells and AR-positive luminal cells (**Figure 2.1 B and D**) [118]. Human and mouse prostate luminal cells express NKX3.1 and Hoxb13, however urethral gland epithelial cells lack both NKX3.1 and Hoxb13 expression (**Figure 2.1 B and D**). Given the common derivation of both prostate and urethral epithelial cells from the UGS, we sought to investigate how these divergent epithelial structures formed, and the role of the stroma in determining their cell fate.

To determine at what point during development the UGS epithelium gives rise to distinct urethral and prostate epithelia, we followed the expression of ΔNp63, HOXB13, and Nkx3.1 during mouse prostate development (**Figure 2.2 A**). First, we analyzed protein expression of the mouse UGS at embryonic day (E) 11.5, when the urorectal septum separates the UGS anteriorly from the hindgut posteriorly (**Figure 2.2 A and Figure 2.3 A**) [50]. HOXB13 is sparsely seen in epithelial cells of the UGS, but uniformly expressed in the hindgut epithelium (**Figure 2.2 B**). As expected, the majority of UGS epithelial cells express ΔNp63 (**Figure 2.2 B**), as it has been previously shown to be required for differentiation of the urogenital tract and inhibits differentiation toward the intestinal epithelium [119, 120]. In contrast, hindgut epithelial cells lack p63 expression (**Figure 2.2 B**). At E14.5, ΔNp63 was expressed in the whole UGS epithelium, while Hoxb13 expression is observed in a small area of upper UGS (**Figure 2.3 B**). At E17.5, Hoxb13 expression is undetectable in all UGS epithelial cells, while there is robust expression in the epithelial cells of the colon (**Figure 2.2 C**). By postnatal day 5 (P5), Hoxb13 is detected in the prostate, but absent in the urothelium, urethral glands and the urethral portion of the prostatic ducts (**Figure 2.3 C**).

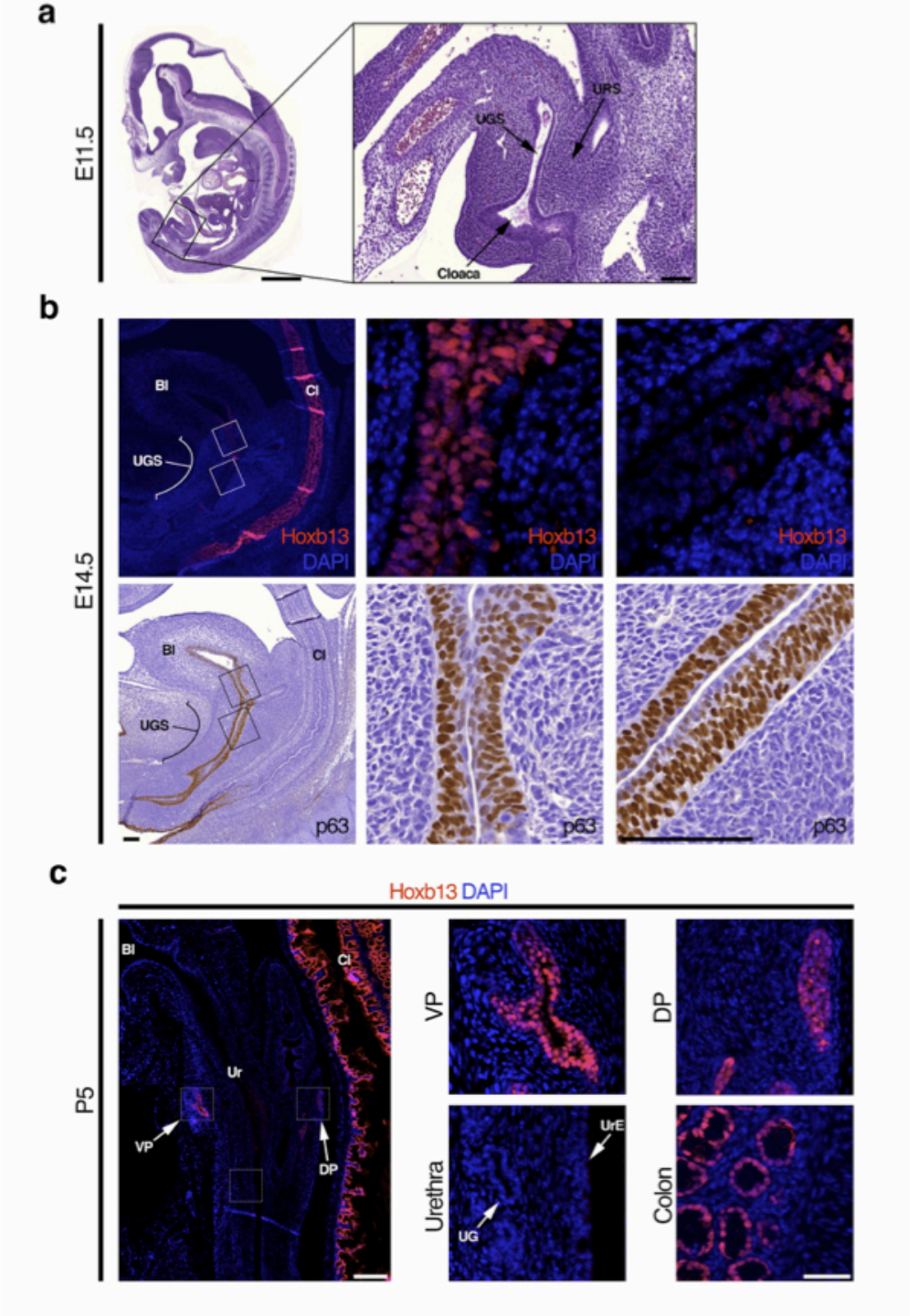

Figure 2.2: Cell fate transition during development of the UGS. A. H&E staining of sagittal-sectioned E11.5 mouse embryo. URS, urorectal septum. **B.** IF staining of Hoxb13 and immunohistochemistry staining of p63 in E14.5 mouse embryo. Bl, bladder. Cl, colon. **C.** IF staining for Hoxb13 in post-natal day 5 prostate, ventral prostate, dorsal prostate, urethra, and colon.

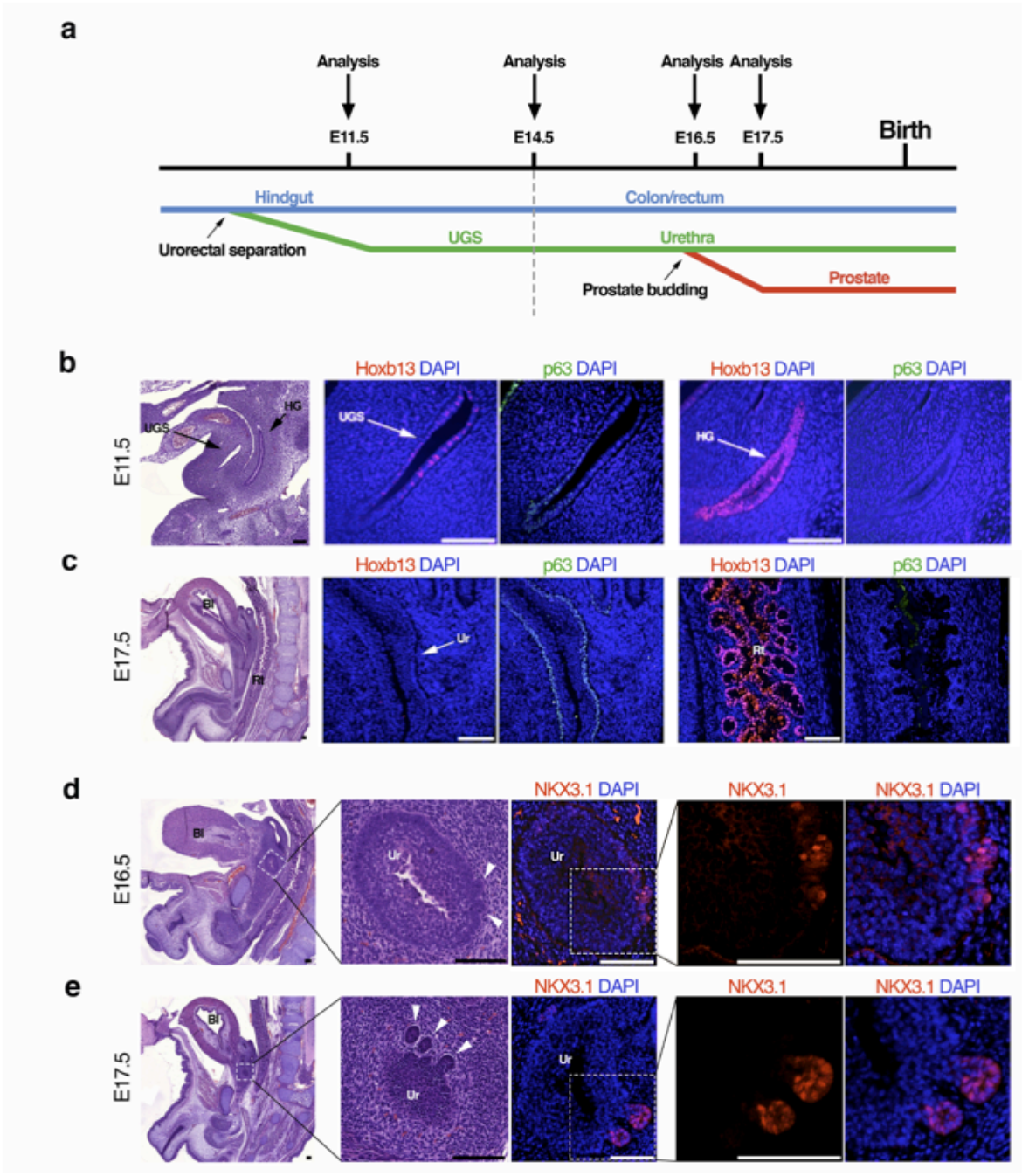

Figure 2.3: Sequential Analyses of Prostate and Urethral Gland Development from the Hindgut to UGS to the prostate. A. Schematic depicting development of the UGS and time points when analyses of transcription factors were performed. **B.** H&E staining and IF staining of Hoxb13 and p63 in the urogenital sinus (UGS) and hindgut (HG) of E11.5 mouse embryo. **C.** H&E staining and IF staining of Hoxb13 and p63 in the urethra (Ur), rectum (Rt), and bladder (Bl) of E17.5 mouse embryo. Arrows indicate regions of interest. **D and E.** H&E staining and IF staining of NKX3.1 in the urethra of E16.5 and E17.5 mouse embryos documenting prostatic budding. Arrowheads mark prostatic buds. Scale bars represent 100 μm.

Previous studies documented that NKX3.1 mRNA is first detected in the UGS epithelium at E15.5 [121]. However, we did not observe NKX3.1 protein expression in serial sections of mouse UGS tissues at E15.5 (**Figure 2.4 A**). The earliest prostatic buds are seen at E16.5 and coincide with detectable NKX3.1 protein expression (**Figure 2.3 D**). Notably, NKX3.1 is only detectable in epithelial buds, while the UGS epithelium lacked NKX3.1 expression (**Figure 2.3 D**). At E17.5, prostatic buds are more prevalent, and NKX3.1 expression remains in prostate epithelial ducts while remaining absent in the UGS epithelium (**Figure 2.3 E**). As the urethral shape gradually matures, the prostate ducts extend and grow outside the urethral wall and are clearly demarcated by NKX3.1 expression (**Figure 2.4 B**). The appearance and maintained expression of NKX3.1 and Hoxb13 in prostate epithelial buds, and distinct lack of expression in urethral glands, suggests that there are key differences in the stromal microenvironment that promote transcription factor expression and prostate lineage specification.

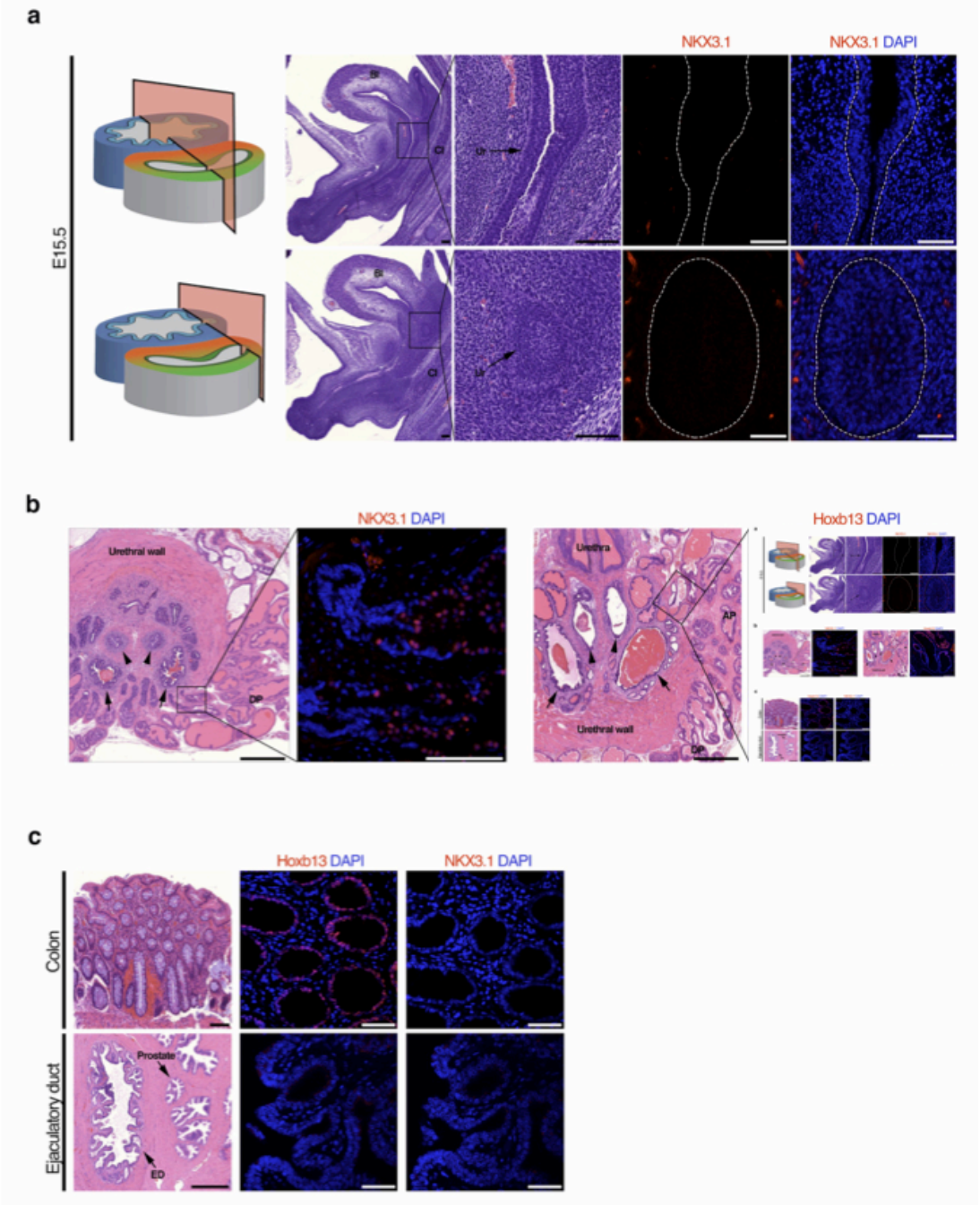

Figure 2.4: De novo expression of NXK3.1 and re-expression of HOXB13 in the prostate. A. Diagram shows serial sagittal section positions in E15.5 mouse embryo. H&E staining and IF staining of NKX3.1 in serial sagittal-sectioned E15.5 mouse embryo. Dash lines encircle the urogenital sinus epithelium. Ur, urethra. **B.** H&E staining and IF staining of NKX3.1 and Hoxb13 in the junction of urethra and prostate. AP, anterior prostate. DP, dorsal prostate. Arrows, seminal vesicle ducts. Arrowheads, ejaculatory ducts. Scale bars, 500 μm (H&E staining), 100 μm (IF staining). **C.** H&E staining and IF staining of NKX3.1 and HOXB1313 in the human colon and ejaculatory ducts. Scale bars, 100 μm (HE staining), 50 μm (IF staining).

Caudal Müllerian Duct Mesenchyme is Sufficient to Specify Prostatic Epithelial Cell Fate

The common origin of prostate and urethral epithelial cells implies that different stromal cues dictate the lineage of each gland during development. During embryogenesis, the Wolffian duct (WD) and the Müllerian duct (MD) converge in the region where the prostatic buds initiate [50]. In human males, the ejaculatory ducts are derived from the Wolffian duct and pass through the prostate, and lack expression of either Hoxb13 or NKX3.1 (**Figure 2.4 C**), supporting that the Wolffian duct mesenchyme does not induce prostatic cell lineage specification. We have previously hypothesized that the caudal Müllerian duct mesenchyme (MDM) participates in prostate development [104]. This is based upon the observation that, although the MD regresses in the male due to the presence of anti-Müllerian hormone, the middle portion of the MD undergoes regression via epithelial-mesenchymal transition. Thus, a portion of MDM may persist and induce prostate development. Further supporting the role of MDM in prostate development is the expression pattern of AR in MDM and therefore the potential to secrete paracrine growth factors in response to host androgens (**Figure 2.5**).

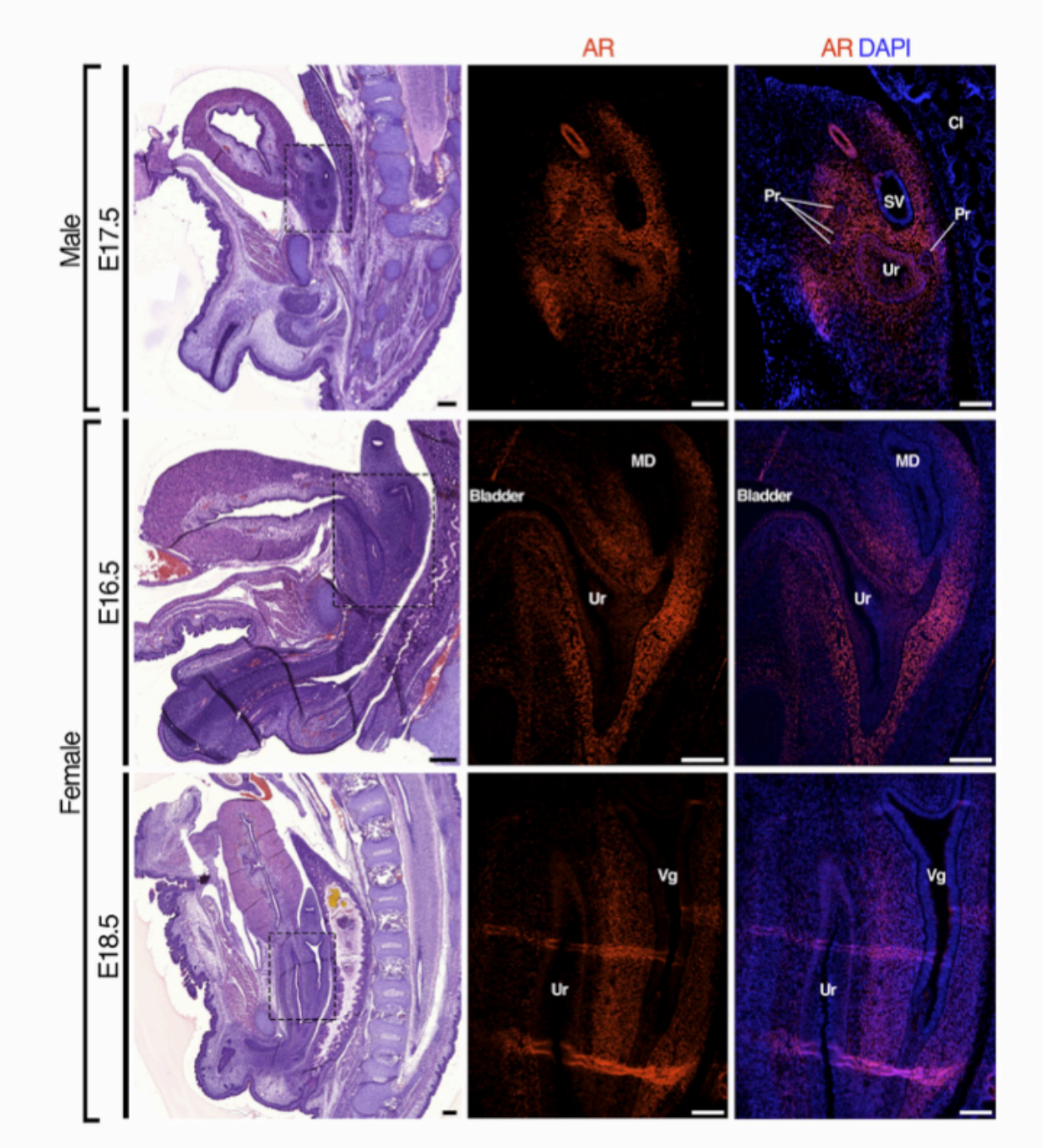

Figure 2.5: AR expression in the mouse caudal MDM and UGSM. H&E staining and IF staining of AR in sagittal section. E17.5 male embryos, as well as E16.5 and E18.5 female embryos are represented here. SV, seminal vesicle. Pr, prostate. MD, Müllerian duct. Vg, vagina. Scale bars, 200 μm.

To test the ability of MDM to promote prostate epithelial development, we utilized a tissue recombination approach whereby human embryonic stem (hES) cells are induced by embryonic rodent stroma to form human prostate glands [106, 122]. The caudal MDM includes the cervix and upper vagina and was derived from female rat neonates (**Figure 2.6 A**). The UGSM was used as a control stroma, and was harvested from the urethra of female rat neonates; male UGSM was not used due to the potential contamination of adjoining caudal MD. We reconstituted hES cells with either caudal MDM cells or UGSM cells from female rat neonates; these recombinants were implanted under the renal capsule of adult male nude mice (**Figure 2.6 A**). After a growth period of 12 weeks, both caudal MDM- and UGSM-induced glands had a continuous p63-positive basal cell layer (**Figure 2.6 B**).

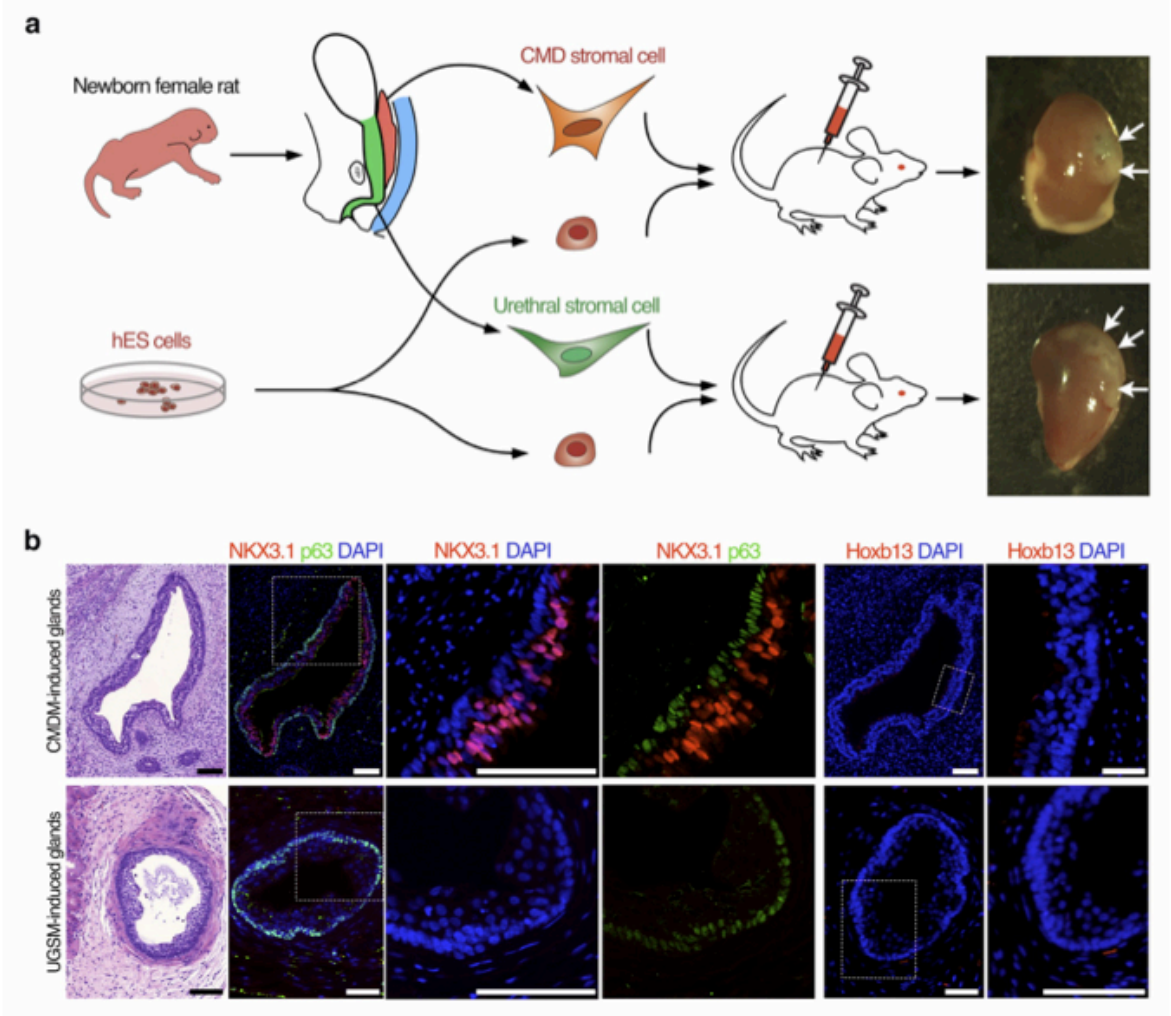

Figure 2.6: Caudal Müllerian Duct Mesenchyme Induces Partial Prostatic Cell Fate in Glands Derived from Human ES cells. A. Diagram shows tissue recombination approach using hES cells. Human ES cells were mixed with either caudal Müllerian duct stromal cells or urethral stromal cells from newborn female rats. Arrows mark tissue recombinants underneath the mouse renal capsule. **B.** H&E staining and IF staining of NKX3.1, Hoxb13 and p63 in the hES cell-derived glands induced by rat caudal MDM cells or rat UGSM cells. These data demonstrate induction of NKX3.1-positive epithelia indicative of prostate, but such tissue lacks Hoxb13 expression indicating incomplete prostatic fate determination. Scale bars represent 100um.

Control hES cells implanted alone formed teratomas as expected, and mesenchyme implanted without hES cells did not yield any tissue for analyses after 12 weeks. Both caudal-MDM and UGSM-induced glands expressed AR and human-restricted PSA, demonstrating human origin of tissues and a lack of contaminating mouse epithelium (**Figure 2.7 A and B**). As further confirmation of the formation of multiple cell lineages, hESC-derived glands contained chromogranin A-expressing neuroendocrine cells (**Figure 2.7 C**). Significantly, the luminal cells within caudal-MDM-induced glands expressed NKX3.1, while UGSM-induced glands lacked NKX3.1 expression (**Figure 2.6 B**). Neither CMDM nor UGSM-induced epithelia, however, expressed detectable Hoxb13 protein (**Figure 2.6 B**). These data support our hypothesis that the caudal Müllerian duct is sufficient to induce prostate epithelial cell lineage specification as documented by the expression of human-specific PSA and NKX3.1.

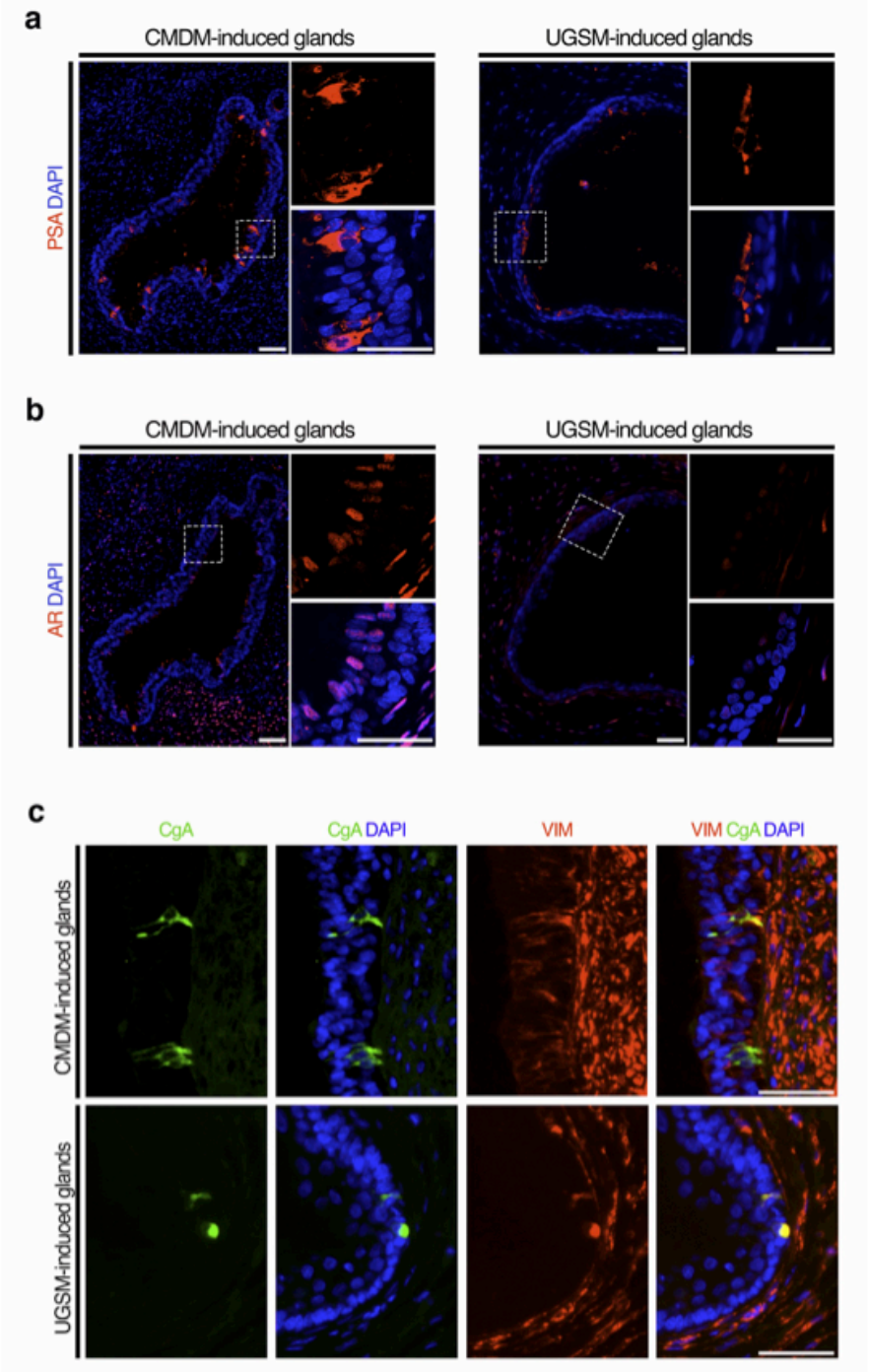

Figure 2.7: Expression of PSA, AR and chromogranin A in hES cell-derived tissue recombinant glands. A. IF staining of PSA in CMDM-induced and UGSM-induced glands. Scale bars, 200um, 50um (enlarged pictures). **B.** IF staining of AR in CMDM-induced and UGSM-induced glands. Scale bars, 200um, 50um (enlarged pictures). **C.** IF staining of Chromogranin A (CgA) and vimentin (VIM) in CMDM-induced and UGSM-induced glands. Scale bar, 50um.

Maintenance of Hoxb13 Expression by Caudal Müllerian Duct but not Urogenital Sinus Mesenchyme

When hES cells were used for human prostate epithelium induction, glandular structures induced by caudal MDM or UGSM lacked Hoxb13 expression (**Figure 2.6 B**). We hypothesized that this was due to the use of pluripotent hES cells to form human prostate epithelium, which are more primitive than hindgut epithelium from which prostatic epithelium is derived and therefore may not have been conditioned properly to be able to express HoxB13. It is possible that the expression of HoxB13 is not initiated by but maintained by the mechanism that separates prostatic from urethral epithelia. To test this, we harvested urethral epithelium from adult mice and reconstituted them with either caudal MDM cells or UGSM cells from female rat neonates (**Figure 2.8 A**). Indeed, luminal cells within glands induced by caudal-MDM express both NKX3.1 and Hoxb13, while glands induced by UGSM lack expression of both transcriptional factors (**Figure 2.8 B**). These data demonstrate that Hoxb13 expression in the prostatic epithelium is maintained after differentiation into hindgut epithelium, and implies that UGSM suppresses Hoxb13 in urethral gland epithelia while the caudal MDM maintains Hoxb13 expression (**Figure 2.8 B**). Taken together, these data demonstrate that the caudal MDM is able to specify the formation of prostate epithelial cells. During this process, the caudal MDM induces the expression of NKX3.1, and maintains the expression of Hoxb13 to contribute to the delineation of prostate epithelium from urethral epithelium (**Figure 2.9**). These data strongly implicate a key role for the caudal Müllerian duct in specifying prostate lineage from urethral gland lineage.

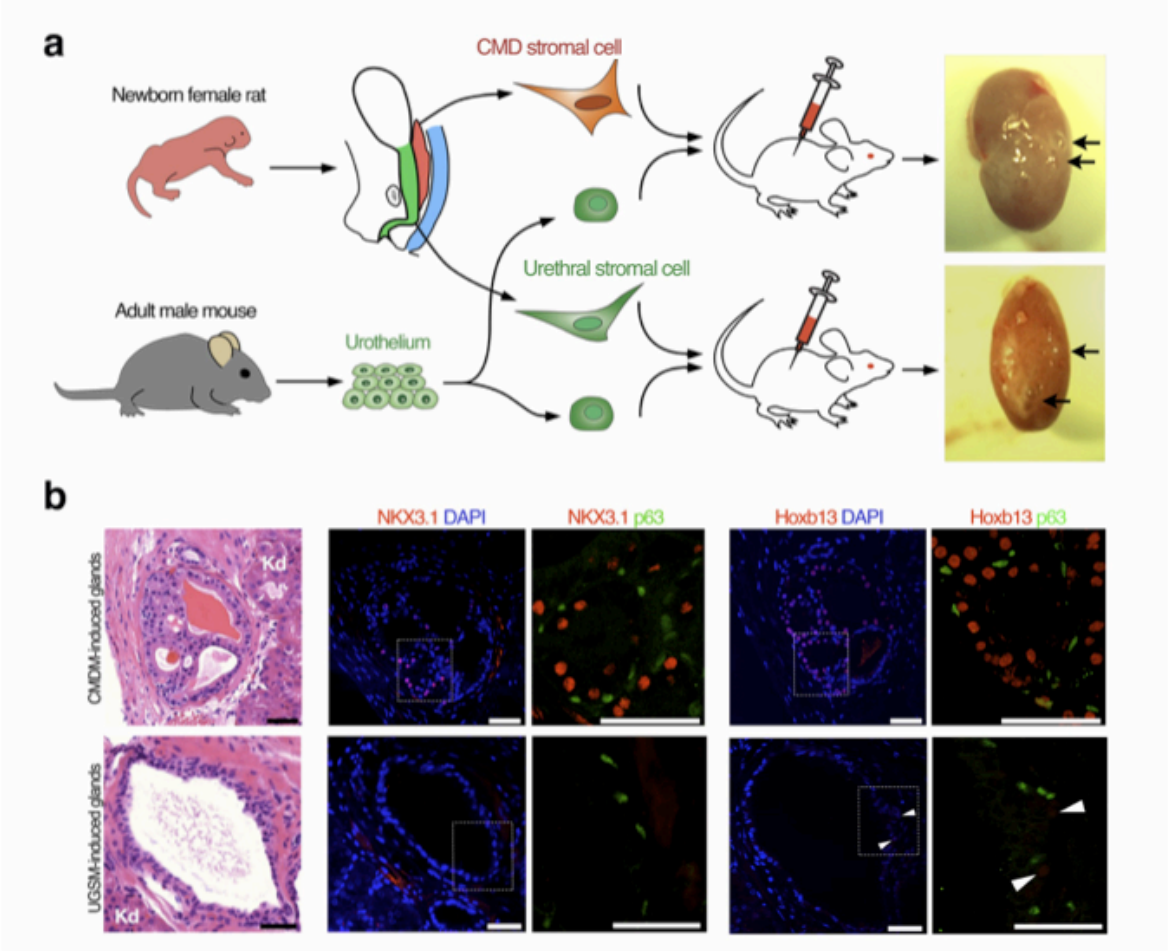

Figure 2.8: Caudal Müllerian Duct Mesenchyme Induces Prostate Cell Fate in Urothelial Cell-Derived Glands. A. Diagram shows tissue recombination using adult mouse urothelial cells. Arrows mark the tissue recombinants underneath the mouse renal capsule. Urothelial cell epithelia from adult male mice was recombined with either caudal Müllerian duct stromal cells or urethral stromal cells from newborn female rats. **B.** H&E staining and IF staining of NKX3.1, Hoxb13 and p63 in the urothelium-derived glands induced by rat caudal MDM cells or rat UGSM cells. Kd, kidney. Arrowheads mark sporadic expression of Hoxb13. These data demonstrate that recombination of adult urothelium and caudal Müllerian duct generates prostatic epithelium that is positive for both NKX3.1 and Hoxb13. Scale bars, 50 μm.

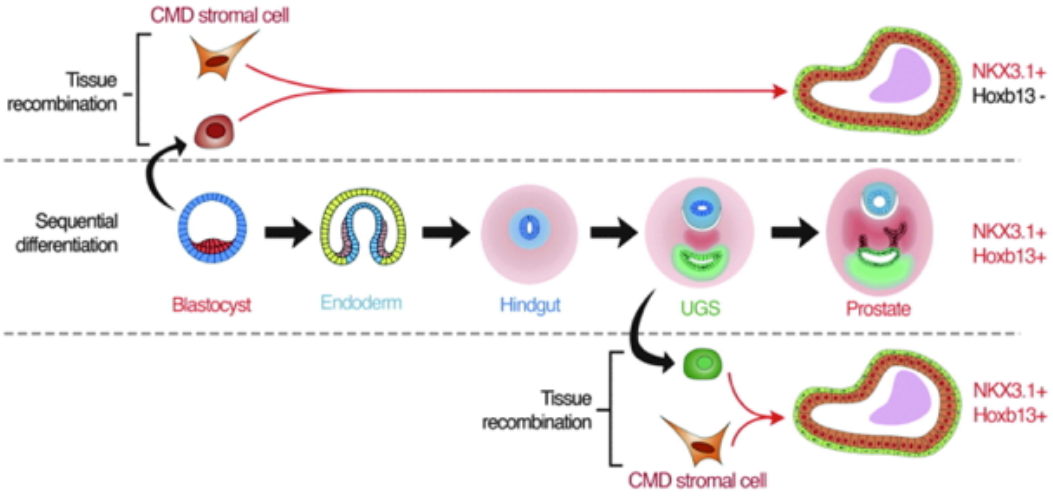

Figure 2.9: Diagram of Prostatic Cell Fate and Role of Caudal Müllerian Duct Mesenchyme. Diagram shows the differences among the sequential differentiation and tissue recombinations using either pluripotent embryonic stem cells or urothelial cells as the originating epithelial cell precursor.

Discussion

In this study we provide evidence that the caudal Müllerian duct mesenchyme is able to induce prostate epithelia and is likely a key determinant in delineating prostate vs. urethral gland cell fate. This is in contrast to the conventional belief that the prostate is induced solely by the urogenital sinus mesenchyme. A limitation of our study is that the use of adult urethra epithelial cells may be a poor substitute for the embryonic urogenital sinus epithelial cells, or adult prostate stem cells, that give rise to the prostatic epithelium. Future studies should be aimed at understanding the relationship between CMDM and UGSM into adult prostate homeostasis and their impact on prostate epithelium and responses to androgen deprivation.

In the developing male urogenital tract, it has long been presumed that AMH inhibits the Müllerian duct epithelial cells to develop the female reproductive organs. However, the fate of the Müllerian duct mesenchyme is unclear. Our data support a model whereby androgens induce the caudal MDM to develop into prostate, thereby highlighting a sexual dimorphic differentiation of the CMDM. Müllerian duct-derived glands have been found in males of lower vertebrates such as amphibians [123, 124] and play roles in improving fertility by increasing sperm velocity and providing nutrients [125]. Thus, our findings suggest that factors derived from the caudal MDM-derived stroma could serve as efficacious targets for cancer prevention and initiation. The identification of such targets using comparative approaches and additional functional studies is an obvious area for future research.

CHAPTER III

MEIS PROTEINS ARE NOVEL TUMOR SUPPRESSORS OF PROSTATE CANCER

Introduction

Prostate cancer (PrCa) is the most commonly diagnosed cancer in men with hundreds of thousands diagnosed each year [126]. While PrCa can progress slowly, leaving the patient relatively asymptomatic for years, some patients present with aggressive metastatic PrCa and a subsequently poor prognosis [126, 127]. Despite advances in the treatment of PrCa, it can be difficult to distinguish which men will fall into the indolent or aggressive groups [128], particularly patients with intermediate Gleason scores. Our lab recently has identified differentially regulated gene networks between the prostate and seminal vesicle, and has used these data to determine prognostic cancer gene-centered biomodules specific to the prostate [20]. One such signaling module to emerge was the MEIS (Myeloid Ecotropic Integration Site) and HOX gene axis [20].

In a retrospective analysis of outcomes from a large cohort of watchful waiting patients with mid-range Gleason scores ("Men in the Middle") high MEIS expression correlated with significantly longer overall survival (**Figure 1.1**) [20]. Additionally, recent work indicates that MEIS1 may act as a negative regulator for the androgen receptor [129], suggesting that MEIS proteins may act as tumor suppressors in the context of PrCa. Thus, the long-term goal of our lab, is to understand how MEIS proteins function in the context of prostate cancer initiation in order to identify novel molecular biomarkers to understand how disease progression.

MEIS proteins belong to the TALE (three amino-acid loop extension) protein family [53] and are critical for multiple components of normal human development and adult maintenance

including hematopoiesis [63, 130, 131], vascular patterning [132], limb patterning [133], and anterior-posterior axis determination in combination with Homeobox (HOX) genes [56, 134, 135]. HOX transcription factors play a key role in the anterior-posterior axis formation in mammals, but require co-factors to help specify DNA binding locations[52] and stabilize their interactions with the genome [136]. MEIS proteins have been shown to bind to HOX proteins specifically at the Meinox domain [53, 55, 56, 134]. The other main functional domain on MEIS proteins is the homeodomain [53] which binds to DNA and provides specificity to HOX-DNA binding [60, 137, 138].

MEIS1 and *MEIS2* are separate but highly homologous genes, however each one has multiple splice variants that tend to fall into a few categories; some have extended C-terminals and some have an abrogated homeodomain which prevents DNA binding [72]. Developmental studies indicate differential functions and distribution of MEIS isoforms, specifically distinct functions for the isoforms with abrogated homeodomains in Xenopus neural crest migration [139] as well as specific roles in gene promoter activity [140]. The expression pattern of MEIS in the adult healthy or cancerous prostate is unknown.

Deregulation of HOX proteins has been implicated in many types of cancer [31], including prostate [141]. Overexpression of HOXB13 was found to have growth suppressive effects on PrCa cells [81, 142], and has been suggested to be a negative regulator of the PrCa oncogene androgen receptor [81]. Recently, one of the first hereditary mutations found to incur an increased risk of PrCa was identified in the MEIS-binding domain of HOXB13 [21]. The most frequent mutation was a G84E mutation, however there were several mutations in the same domain. More men with PrCa carrying the G84E mutation were also diagnosed with early onset PrCa as compared patients with wild type HOXB13 [21, 143]. However, the functional role of

this mutation has not been investigated. Overexpression of wild type HOXB13 has also been shown to promote invasion and migration of PrCa cells [144]. MEIS proteins have critical roles in normal proliferation and cell-fate determination in development so it is logical that their roles could be exploited in cancer. Altered expression of MEIS has also been implicated in a variety of cancers including leukemia [65], colorectal cancer [79], neuroblastoma [72], and NSCLC[77]. MEIS proteins seem to have a complicated and context-dependent role in cancer progression, as they are down regulated in colorectal cancer [79], but sometimes overexpressed in hematopoietic cancers [53, 145], making it unclear if MEIS are oncogenes or tumor suppressors in a given organ type of cancer until you explore that tissue specifically. Distinct isoforms of MEIS have been documented to have distinct cancer-related functions, specifically the homeodomain-less form was found to be down regulated in colorectal cancer [79] and neuroblastoma cell lines [72]. Finally, it was recently suggested that it is possible for MEIS1 to be a negative regulator of the androgen receptor [129], the most predominant oncogene in PrCa [2, 126] however the impact of MEIS2 was not investigated.

Thus, while there is evidence of MEIS proteins playing a role in multiple cancers, the range of alterations and functional differences suggest a predominantly context specific role for the MEIS proteins, reflective of their flexibility and cofactor-dependent specificity in normal development. In this work, we hypothesize that MEIS proteins function as tumor suppressors in advanced prostate cancer. Our laboratory's work was the first to implicate the importance of MEIS proteins in prostate cancer. My work provides the levels and distribution of MEIS isoforms in the normal and cancerous prostate, ultimately helping the burgeoning field of MEIS/HOX investigation move ahead, as well as providing new areas of investigation for both the developmental and cancer biology fields.

Materials and Methods

Cell lines and Materials

R1881 was purchased from Sigma-Aldrich (St. Louis, MO) and was stored at -20 in ethanol. All human prostate cancer cell lines were grown as previously described [146]. All cultures were routinely screened for the absence of mycoplasma contamination using the ATCC Universal Mycoplasma Detection Kit (Manassas, VA). PC-3 and VCAP cell lines were purchased from ATCC, and Dr. John Issacs at The Johns Hopkins University generously provided the DU145, LNCaP, LAPC4, CWR22Rv1, CWR-R1, and 957EhTERT cell lines and have all been previously characterized [147-150]. Cell growth was measured using 0.2 μm filtered Trypan Blue (HyClone, Logan, UT) exclusion assay with cells counted on a hemacytometer (Hausser Scientific; Horsham, PA).

Lentiviral MEIS1, MEIS2D and control vectors (pReciever LV105) were purchased from GeneCopia (Rockville, MD). Lentiviral vectors were cloned to add a Flag tag (DYKDDDDK) and to create multiple isoforms. High titer lentivirus was made by cotransfecting with ViraPower Lentiviral packaging mix (Invitrogen; Grand Island, NY) and Lenti-X Concentrator (Clontech; Mountain View, CA) according to manufacturer's instructions.

Non-malignant epithelial cultures were established from fresh human prostate tissue obtained from surgical specimens as described previously [147, 151]. The tissues were acquired under an expedited protocol approved by the University of Chicago Institutional Review Board (IRB). The University of Chicago Anatomic Pathology laboratory processed tissue samples. Patients' consents were waived, as the tissues were de-identified. Biopsy punches (4 mm) of non-tumor tissue were taken from prostate tissue removed during radical prostatectomies. Half of

the punch was fixed and analyzed by a pathologist to confirm that lack of tumor. Dissociation of the remainder of the punch and subsequent outgrowth of cell cultures was performed as described previously [152, 153]. These methods allowed us to establish patient matched prostate epithelial (PrEC) and stromal (PrSC) cell cultures. PrEC cultures were grown in Keratinocyte Serum-Free Defined media supplemented with growth factors (standard K-SFM, Invitrogen Life technologies) and PrSC cultures were grown in standard RMPI with 10% fetal bovine serum. Primary epithelial cells can be cultured up to eight passages before noteworthy cell senescence [154]. For our experiments, all cultures were analyzed on or earlier than their fourth passage.

Western Blotting and Immunostaining

Whole-cell lysates of 100,000 or more cells were used per lane. Western blotting was performed as previously reported (REF). In brief, cells were rinsed with cold PBS and scraped into RIPA buffer supplemented with protease inhibitors, sonicated twice and added 4X sample buffer (BioRad) supplemented with 10% Beta-mercaptoethanol (Sigma-Aldrich, St. Louis MO). Protein concentrations determined by the Pierce BCA protein assay kit (Thermo Fisher Scientific) and 30 ug of protein was loaded and electrophoresed on a 10% SDS-polyacrylamide gel. Transfer to nitrocellulose membrane (LI COR, Odyssey, Lincoln, NE) was performed overnight at 4°C after which the membrane was blocked for at least one hour at room temperature in 5% skim milk. Primary antibodies used include: anti-Flag (Cell Signaling Technology; Danvers, MA), anti-MEIS2 (Middle Region, ARP34683_P050, Aviva Systems Biology, San Diego, CA), anti-MEIS1 (Ab19867, Abcam, Cambridge, MA), anti-Beta Actin, (Clone AC-15, Sigma-Aldrich, St. Louis, MO). The secondary antibodies goat anti-mouse IRDye

800 CW or donkey anti-rabbit IRDye 680 from LI-COR Biosciences were used. An infrared Odyssey scanner (LI-COR) captured protein signal.

Quantitative Real Time PCR (Q-RT-PCR) and PCR Array Analyses

RNA was purified using the Qiagen RNeasy Mini Kit with the optional DNAse digestion kit (Qiagen, Valencia, CA) and quality tested using an Agilent Bioanalyzer 2100 (Agilent Technologies, Santa Clara, CA). For standard Q-RT-PCR, extracted RNA was converted to cDNA by reverse transcription using SuperScript III Reverse Transcriptase (Invitrogen). Levels of *MEIS1*, *MEIS2*, *MEIS3*, *HOXB13* and *GAPDH* transcript were quantified using Power SYBR Green Master Mix (Invitrogen) using custom primers that captured all isoforms for *MEIS1* F 5'-TGG CTG TTC CAG CAT CTA ACA CAC-3' R 5'-ACT GGT CTA TCA TGG GCT GCA C-3' *MEIS2* F 5'-ATC TCG CTG ACC ATA ACC CT-3' R 5'-CCG GAT CAT CAT CGT CAC CT-3' *MEIS3* F 5'-TCT ATG GAC ACC CGC TCT TC-3' R 5'-CTC AGA GCG AAC CTG CTT G-3' *HOXB13* F 5'-GCA GCA TTT GCA GAC TCC AG-3' R 5'-GCC TCT TGT CCT TGG TGA TG-3'

Standard curves were used to assess primer efficiency and average change in threshold cycle (ΔCT) values was determined for each of the samples relative to endogenous GAPDH levels and compared to vehicle control (ΔΔCT). Experiments were performed in triplicate to determine mean standard error, and student's t-tests performed with normalization to control to obtain p-values.

In Vivo Tumor Formation

All animal studies were carried out in strict accordance with the recommendations in the Guide for the Care and Use of Laboratory Animals of the National Institutes of Health. The

protocol was approved by the University of Chicago Institutional Animal Care and Use Committee (IACUC, protocol numbers 72066 and 72231). All surgery was performed under Ketamine/Xylazine anesthesia, and all efforts were made to minimize suffering. *In vivo* tumor formation of derived lines from LAPC-4, LNCaP and CWR-22Rv1 cells were conducted via a sub-cutaneous inoculation of one million for LNCaP or 250,000 cells for CWR22Rv1 and LAPC4 in 4–6 week old male athymic nude mice (Harlan; Indianapolis, IN) using a 75% Matrigel (Corning, Bedford, MA) and 25% HBSS solution (BD Biosciences). To measure tumor take in a uniform androgen environment, host mice were surgically castrated at least one week prior to cell inoculation and implanted with a 2.4 mm testosterone pellet subcutaneous. Mice were allowed to recover and testosterone levels to equilibrate for 7 days before tumor injections.

Flow Cytometry

Cell lines were pulsed with BrdU (BioLegend, San Diego, CA) for 3 hours. Cells were then trypsinized and fixed with ice cold 70% ethanol. Cells were incubated on ice in 0.1 N HCl/0.7% Triton X solution for 10 min, then washed 2X with PBS. Then cells were heated at 100° C for 10 mins in 0.5 mL dH2O with 16 uL 0.1N HCl. After placing cells on ice, they were washed 2X with IFA/0.5% Tween 20.

FITC-conjugated anti-BrdU antibody (BioLegend, San Diego, CA) was incubated with cells at 1:20 for 30 mins and after 1 wash, boiled RNase A was added and cells were incubated in 37° water bath for 15 mins. 10 μL propidium iodide (BioLegend, San Diego, CA) was added and cells were incubated overnight at 4°. Flow Cytometry data was collected in biological triplicates on a BD LSRII (BD Biosciences, San Jose CA). Cell cycle analysis was performed on FlowJo software.

RNA Sequencing Library Preparation

RNA was purified using the Qiagen RNeasy Mini Kit with the optional DNAse digestion kit (Qiagen, Valencia, CA) and quality tested using an Agilent Bioanalyzer 2100 (Agilent Technologies, Santa Clara, CA). Only RNA with a RIN score of 7 or higher was used for library preparation. The KAPA Stranded mRNA-Seq Kit (KapaBiosystems, Wilmington, MA) was used for library preparation of 2.5 μg of intact, total RNA for 50 basepair, single end sequencing. Illumina TruSeq adapters were used to multiplex 6 samples per lane, with two lanes of sequencing. Samples were prepped and sequenced in biological triplicates. Average fragment lengths with adapters fell within 283-302 bps and had 10 amplification cycles. In order to properly multiplex, the Kapa Library Quantification Kit (KapaBiosystems, Wilmington, MA) was used with no ROX on a Mastercycler ep *realplex* Smart Cycler machine.

Bioinformatics Analysis

Sequencing was performed by the Functional Genomics Core Facility at the University of Chicago on the Illumina HiSeq4000. Quality control and alignment were performed using the Kallisto program on the AltAnalyze application created by Cincinnati Children's Medical Hospital at the University of Cincinnati [155-157]. DEG's were identified as significant with a fold change above 1.5 and when they passed the Benjamini-Hochberg significance procedure for a FDR α 0.05. The Stand Up to Cancer Next-Generation RNA sequencing data was accessed through cBioPortal and all patient information was de-identified before analysis [158, 159]. TCGA Research Network methylation data from the Illumina Infinium HumanMethylation 450K BeadChip array [160] was mined for targeted gene queries. Methylation of *MEIS1* or *MEIS2* from TCGA were analyzed by the Wanderer web tool [161] with a Wilcoxon adjusted p-value < adj. pval threshold 0.001. GO analysis was performed with the PANTHER Overrepresentation

Test release #20170413, on the GO Ontology database released 2017-05-25. The reference list used was Homo sapiens, all genes in database. Bonferroni correction for multiple testing was used, with a Bonferroni count of 8492. Genes with a fold change greater than 1.5 and an adjusted p-value of <0.05 were considered differentially expressed and were investigated via IPA (Ingenuity Systems Inc., Redwood City, CA). Outcomes from Next Generation RNA-sequencing were uploaded to Qiagen's IPA system for core analysis and overlaid with the Ingenuity pathway knowledge base.

Results

MEIS1 and MEIS2 Expression is Lower in Healthy Prostate Epithelial Cells than Adjacent Stromal Cells and Low to Non-detectable in in vitro Models of Prostate Cancer

Our lab recently identified differentially regulated gene networks between the prostate and seminal vesicle, and has used these data to determine prognostic cancer gene-centered biomodules specific to the prostate [20]. One such signaling module to emerge were MEIS proteins, and our previous work indicated that prostate cancer patients with high levels of *MEIS1* or *MEIS2* expression survive longer than men with lower expression [20]. In order to determine the molecular basis of this phenomenon, an understanding of MEIS expression across current model systems of prostate cancer was necessary. If current prostate cancer tissue culture models display similar patterns to the Swedish Watchful Waiting cohort studied in Chen et al. 2012 [20], they could be manipulated to understand the biology of MEIS proteins in prostate cancer.

Using qPCR primers that amplify all translational isoforms of each gene, we found that the PrCa cell lines LNCaP, CWR22Rv1, and LAPC4 have significantly less *MEIS1* and *MEIS2* expression than normal prostate epithelial cells ($p<0.05$, **Figure 3.1 A**); the expression of *MEIS3*

was consistent across all cell types. Expression of *MEIS1* and *MEIS2* was also decreased in the cell lines Du145 and PC3, but still detectable, unlike MEIS2 expression in the other cell lines (**Figure 3.1 A**). Western blot analysis of these PrCa cell lines displays low but detectable levels of MEIS1 and MEIS2 protein, as well as varying levels of HOXB13 (**Figure 3.1 C**).

As normal prostate epithelial cells (PrECs) are derived from a single individual and used within ten passages, we were interested in asking whether MEIS1 or 2 levels were similar across healthy prostate samples. There were no significant differences between the five PrEC samples for either MEIS1 or MEIS2 expression. However, in normal prostate stromal cells (PrSCs), there was significantly more MEIS1 and MEIS2 expression as compared to the paired PrECs (#1 and #2) ($p<0.05$, **Figure 3.1 B**). Western blot analysis of MEIS1 and MEIS2 protein expression of paired PrEC and PrSC's indicate a similar pattern to mRNA expression, where high levels of MEIS proteins are found in the stromal compartment, while there is lower but easily detectable MEIS levels in epithelial cells (**Figure 3.1 D**). Immunohistochemical detection of MEIS1/2 in normal prostate tissue documented strong nuclear staining of basal-epithelial cells with weak luminal-epithelial cell staining (**Figure 3.1 E left panel**). Furthermore, MEIS1/2 was expressed in stromal fibroblasts. In all prostate tumors, MEIS1/2 expression was undetectable (**Figure 3.1 E right panel**, Gleason Grade 4 tumor). Stromal and adjacent normal tissue retained MEIS1/2 expression. This significant loss of MEIS1/2 expression is quantified across increasing Gleason Grade tumors and lymph node metastasis as compared to healthy prostate tissue (**Figure 3.1 F**).

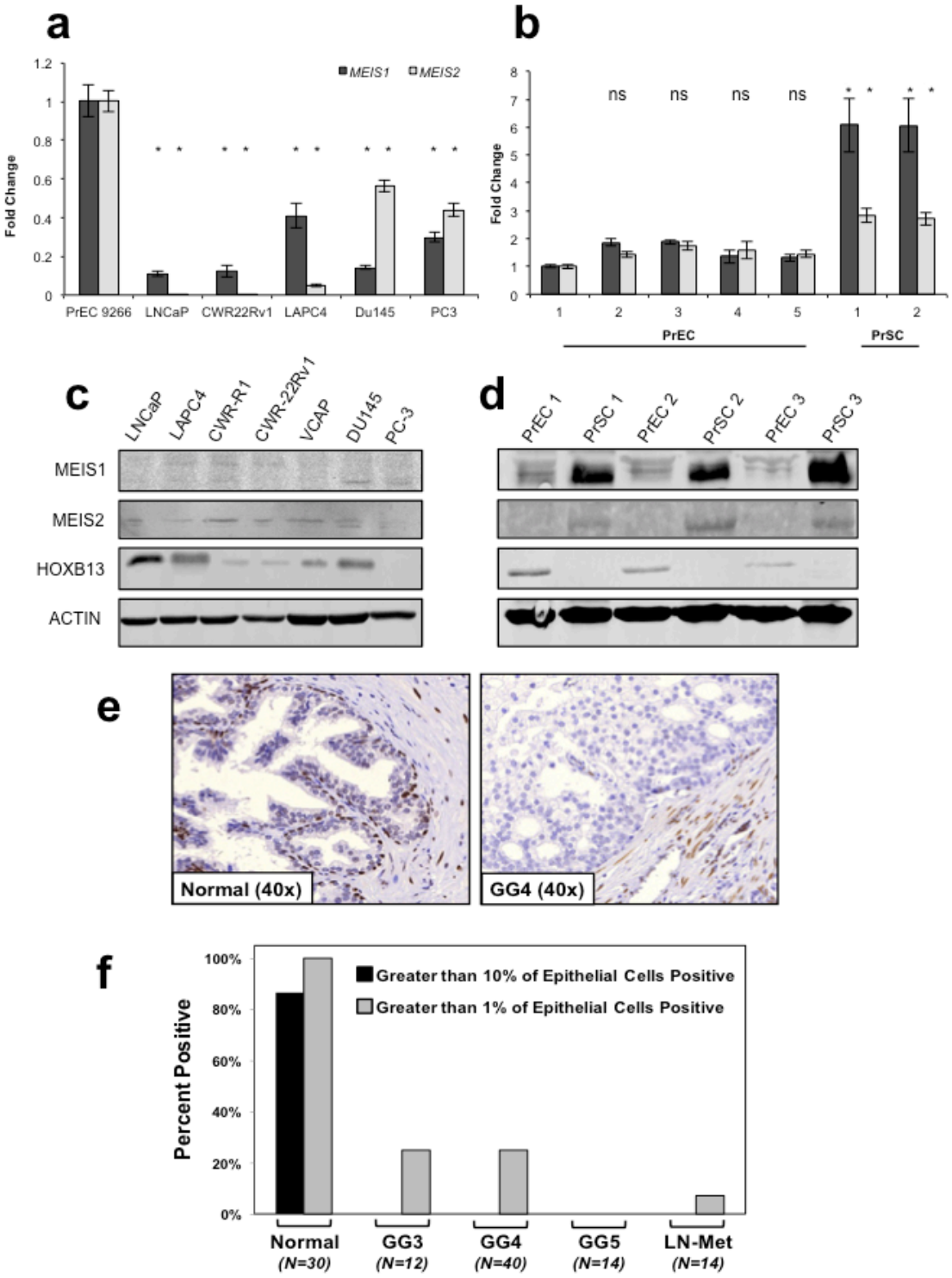

Figure 3.1: Loss of MEIS1 and 2 Expression in *in vitro* Prostate Models and Human Prostate Tumors. A. RT-PCR for *MEIS1* (dark grey) or *MEIS2* (light grey) on five of the most common prostate cancer cell line models (LNCaP, CWR22Rv1, LAPC4, Du145 and PC3) as compared to a PrEC line (* p-value < 0.05). Continued on next page.

Figure 3.1: Loss of MEIS1 and 2 Expression in *in vitro* Prostate Models and Human Prostate Tumors. Continued. B. RT-PCR for *MEIS1* (dark grey) or *MEIS2* (light grey) on five PrEC lines and two PrSC lines (* p-value < 0.05, ns not significant). Primers for MEIS1 and MEIS2 are pan-MEIS, able to quantify every isoform. **C and D.** Western Blot analysis of MEIS1 and MEIS2 protein expression in 30 μg of protein from prostate cancer cell lines (**C**) and PrEC/PrSC pairs (**D**). HOXB13 expression also measured across cell lines, actin used as loading control. **E.** Immunohistochemical detection of MEIS1/2 in normal prostate tissue with a pan-MEIS antibody that detects both MEIS1 and MEIS2. Example panels of tumor and normal IHC slides scored for analysis in panel (**F**). **F.** Summary of epithelial MEIS1/2 staining of prostate tissues. Bars represent the percentage of normal glands (Normal), tumors (GG3, GG4, GG5), or lymph-node metastases (LN-Met), which had more than 1% (grey bars) or 10% (black bars) of cells staining positive for MEIS1/2. This loss of epithelial MEIS1/2 expression from normal prostate tissue to tumor was highly statistically significant (p-value < 0.001). **E and F** are modified from previously published work from our lab [20].

MEIS1 and MEIS2 Expression is Lower in Human Prostate Tumors than Healthy Prostates

Publically available 450k Illumina array data obtained from The Cancer Genome Atlas (TCGA) Research Network were analyzed for expression of *MEIS1* or *MEIS2* levels in normal prostate tissue or tumor tissue (**Figure 3.2 A and B**). There was significantly lower expression of both *MEIS1* (**Figure 3.2 A**, Wilcoxon p-value = 7.459981e-18) and *MEIS2* (**Figure 3.2 B**, Wilcoxon p-value = 3.360055e-17) in prostate tumor tissue than healthy prostate tissue. Fragments per Kilobase (FPKB) values of MEIS1 and MEIS2 expression was assessed from the publically available Stand Up 2 Cancer Next Generation RNA sequencing of benign, tumor and metastases PrCa tissue [158, 159]. There was a stepwise decrease in expression of both MEIS1 and MEIS2 from benign to tumor to metastases (**Figure 3.2 C and D**). As we explored the Next Generation data, we realized that multiple isoforms of MEIS1 and especially MEIS2 are present in prostate tissue. Even 100 base pair (bp) sequencing can't quite capture every isoform, as the different isoforms are so homologous. In particular, we were interested in determining whether the isoform described as lacking a DNA-binding homeodomain was present in prostate tissue.

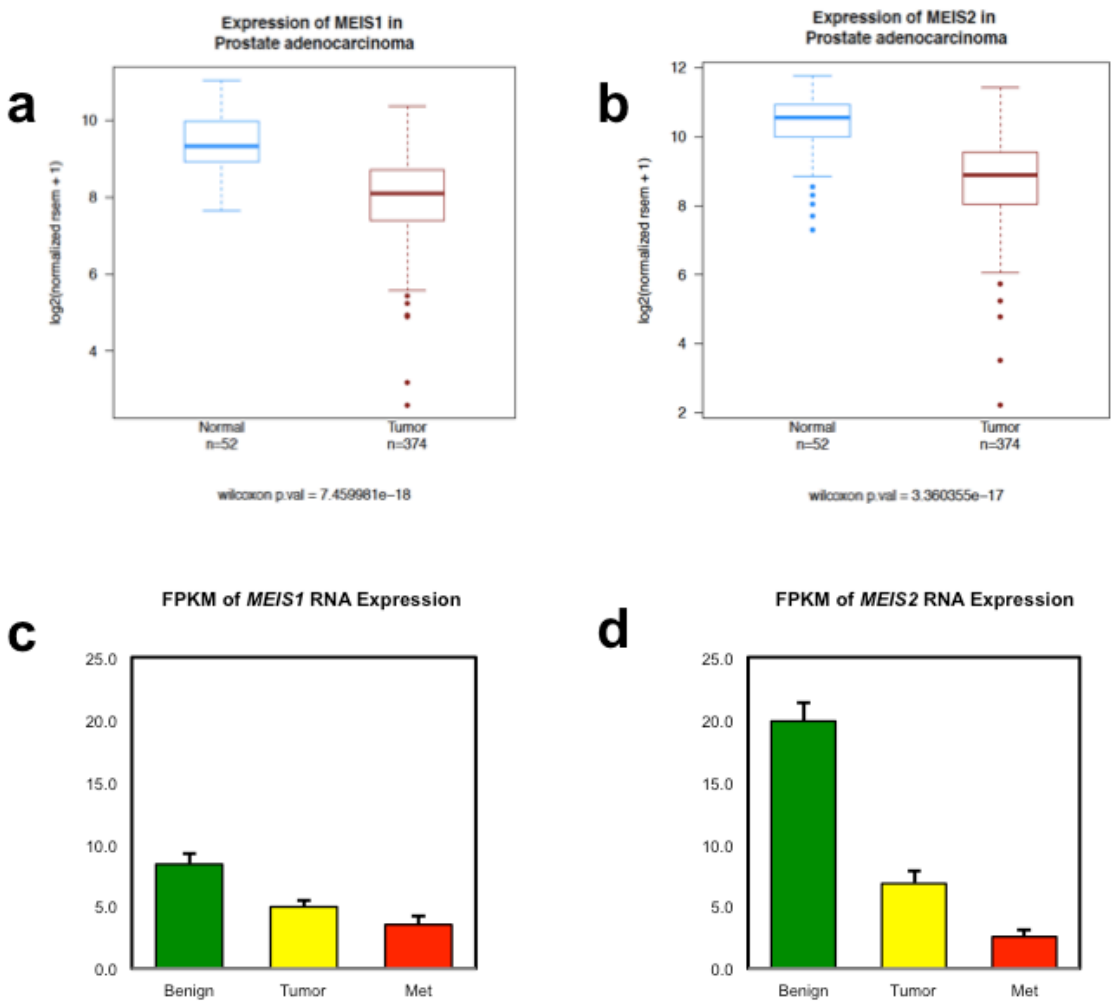

Figure 3.2: MEIS1 and MEIS2 Expression Lower in Human Prostate Cancer than Normal Prostate Tissue. A and B. Publically available prostate data from The Cancer Genome Atlas (TCGA) was analyzed for MEIS1 (**A**) or MEIS2 (**B**) expression comparing normal to tumor (TCGA, Wilcoxon p-values shown below graphs). For MEIS1 expression (**A**) and MEIS2 expression (**B**) the same 52 normal and 374 tumor samples were compared (Wilcoxon p-value = 7.459981e-18). **C and D.** Stepwise progressive loss of *MEIS1* (**C**) and *MEIS2* (**D**) as measure by FPKM from publically available next-generation RNA-Sequencing comparing benign (n=3), tumor (n=25), or metastasis (n=51) [158, 159].

Isoform Distribution of MEIS2 in Prostate Tissue and Models of Disease

The same PrEC and PrSC pairs analyzed in Figure 3.1 were assessed for expression of the homeodomains-less form of MEIS2, the MEIS2E variant (**Figure 3.3 A and C**). Special primers were designed to only amplify the MEIS2E variant, as that isoform is the only one to have an exon 8-10 junction (**Figure 3.3 C**), then the levels of MEIS2E were compared to total MEIS2 expression using the same pan-MEIS2 primers as Figure 3.1. For each cell line analyzed, MEIS2E levels were normalized to the pan-MEIS2 expression (**Figure 3.3 A**). MEIS2E levels were undetectable in all PrEC and PrSCs (**Figure 3.3 A**). MEIS2E levels were also undetectable in all PrCa cell lines tested, with the LNCaP and 957hTERT cells, immortalized PrEC's, lacking any expression of pan-MEIS2 (**Figure 3.3 B**). While MEIS1 (Uniprot #O00470) has at least one other documented isoform, the homeodomainless E variant is specific to MEIS2 (Uniprot # O14770). The schematic illustrating the most common translational isoforms of MEIS2 is found in Figure 3.3 C. The Meinox domain is the binding site for other TALE proteins as well as other Homeobox proteins, including the HOX genes [72, 162]. In **Table 3.1**, the presence or absence of each MEIS2 isoform was determined by TA-TOPO cloning of at least 100 colonies for each cell line. Notably, MEIS2E was absent in all cell lines, corroborating our qRT-PCR from **Figure 3.3 A and B**. When moving forward, we chose to use MEIS2 isoform A as a representative full length MEIS2 isoform to compare with the DNA-binding domain-less MEIS2E. Using these two isoforms, we can test whether the homeodomain is required for the phenotype of reintroducing MEIS's into cancer cells.

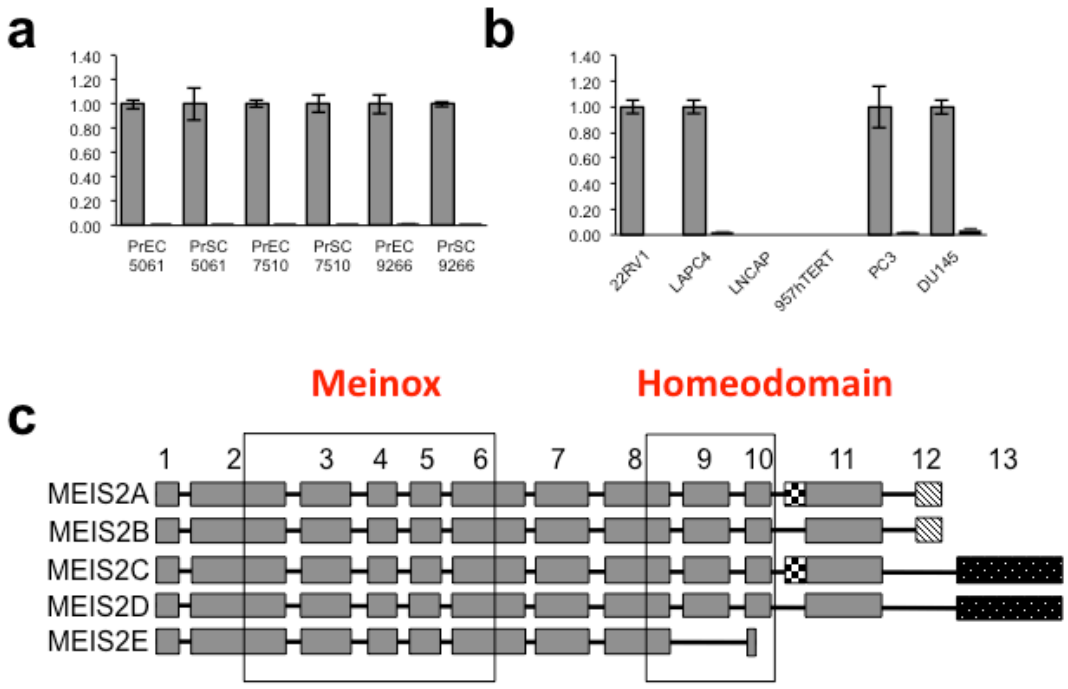

Figure 3.3: Isoform Distribution of MEIS2 in Prostate Tissue and Models of Disease. **A.** Total *MEIS2* (dark grey bars) and *MEIS2E*-specific (black bars) detection by qRT-PCR in three PrEC and PrSC pairs. Detection of E-specific isoform was determined through qPCR primers designed to amplify only *MEIS2E*. Each cell line was normalized to total *MEIS2* levels. **B.** Total *MEIS2* (dark grey bars) and *MEIS2E*-specific (black bars) detection by qRT-PCR in five PrCa cell lines and one immortalized PrEC line (957hTERT). Detection of E-specific isoform was determined through qPCR primers designed to amplify only *MEIS2E*. Each cell line was normalized to total *MEIS2* levels, with the exception of LNCaP and 957hTERT cell lines, which had no detectable *MEIS2* or *MEIS2E*. **C.** Schematic indicating the most common translational isoforms of MEIS2 (UniProt Identifier # O14770) modified from Versteeg et al. [72]. Boxes represent exons as numbered on top. The two main functional domains, Meinox and Homeodomain, are boxed off in black.

Table 3.1: Isoform Distribution of *MEIS2* in Models of Prostate Cancer. Table represents presence or absence of each *MEIS2* isoform A through E present in a variety of cell lines as identified by TOPO-TA cloning. A 5% cutoff was considered to indicate the presence of a particular isoform, whereas below that threshold the presence of the isoform is not definitive.

Table 3.1	MEIS2 Isoforms				
Cell Line	A	B	C	D	E
PREC 70	+	+	+	+	-
CWR-22Rv1	+	-	+	+	-
LNCaP	-	+	+	+	-
LAPC4	+	+	+	+	-

Epigenetic Modifications Alter MEIS Expression

In order to better understand how the MEIS genes are differently regulated between normal prostate and cancer, we used publically available TCGA Research Network methylation data from the Illumina Infinium HumanMethylation 450K BeadChip array [160]. Targeted gene queries for *MEIS1* or *MEIS2* were analyzed by the Wanderer web tool [161]. The Beta-values for prostate tumor and normal tissue at CpG's were compared for each gene, MEIS1 (**Figure 3.4 A top panel**) or MEIS2 (**Figure 3.4 A bottom panel**) flanking their transcription start site (TSS). MEIS1 tumor samples had 16 CpGs with significantly increased Beta-values within the 10 CpG's flanking the TSS on each side as compared to normal prostate tissue (Wilcoxon adjusted p-value < adj. pval threshold 0.001, **Figure 3.4 A top**). For *MEIS2*, tumors samples only had 5 CpG's in the 10+/- flanking the TSS were statistically different from normal prostate (Wilcoxon adjusted p-value < adj. pval threshold 0.001, **Figure 3.4 A bottom**). In both genes, at least two of the significantly increased methylated sites are located in CpG islands.

In order to understand how expression of *MEIS1* and *MEIS2* would change upon treatment with epigenetic modifying drugs, we mined publically available RNA-sequencing data of drug-treated LNCaP PrCa cells from Welsbie et al. [163] for FPKM of *MEIS1* and *MEIS2* (**Figure 3.4 B**). PrCa cells were treated with high or low concentrations of three non-selective Histone Deacetylase inhibitors: Panobinostat (LBH589), suberanilohydroxamic acid (SAHA), or Trichostatin A (TSA) [163]. For almost every treatment, except for the low SAHA, *MEIS2* FPKMs were higher than the threshold (**Figure 3.4 B**). While the same trend is seen for *MEIS1* FPKM, the effect appears to be much stronger for *MEIS2* than *MEIS1*. This observation can also be seen in the Western blot analysis (**Figure 3.4 C**) in response to the same HDACi Panobinostat as Welsbie et al. [163]. Both MEIS1 and MEIS2 protein levels increase in response to the

HDACi, with a more dramatic increase noted in MEIS2. Surprisingly, the hypomethylating agent Decitabine did not change protein expression of either MEIS1 or MEIS2 (**Figure 3.4 C**).

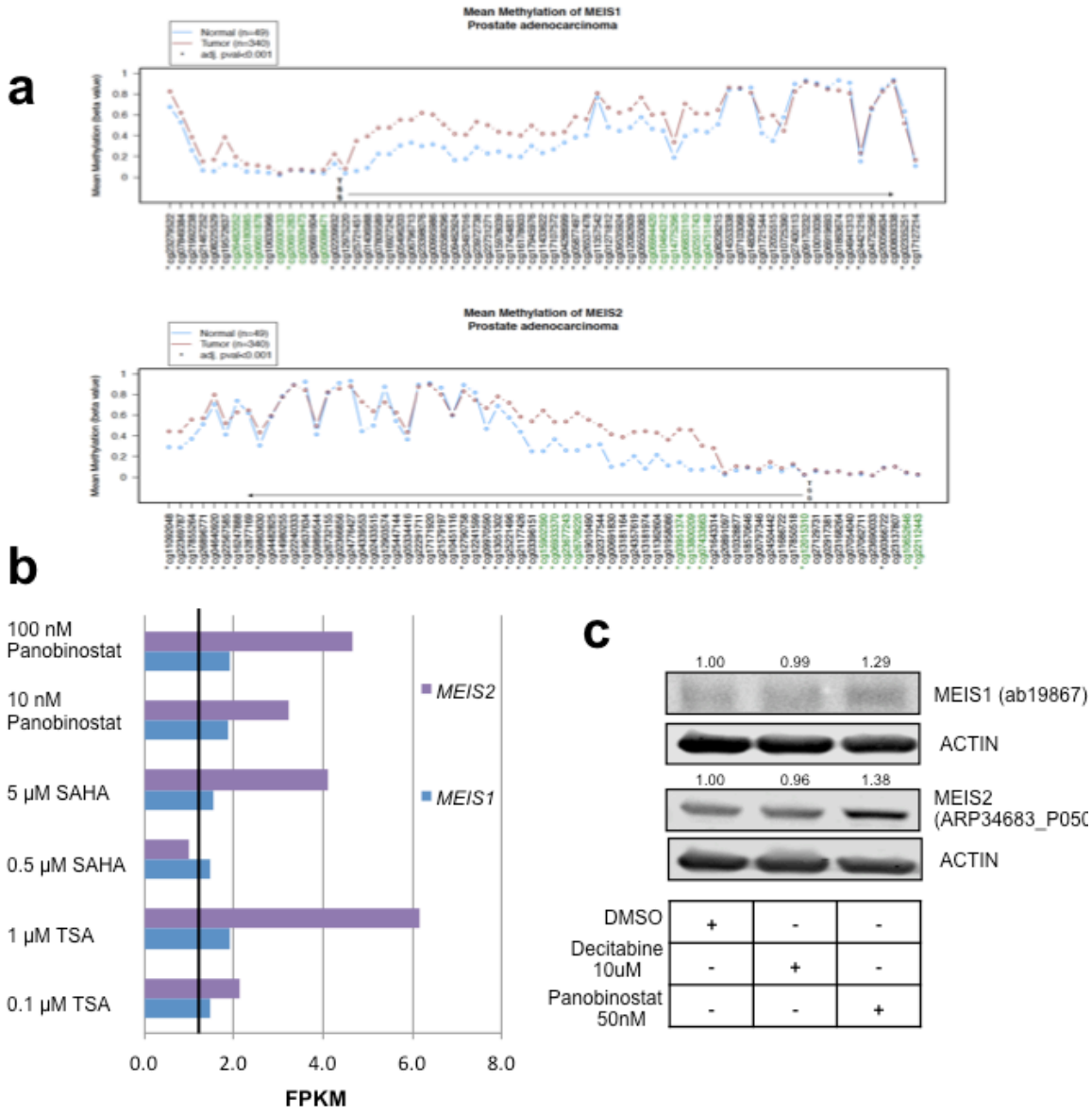

Figure 3.4: Epigenetic Modifications Alter MEIS Expression. A. Visualization of MEIS1 (top) or MEIS2 (bottom) methylation profiles from TGCA Research Network [164], Illumina 450K array [160]. Targeted gene queries were obtained via Wanderer software [161]. Profile plot displays average gene-specific methylation between normal (blue marks) versus tumor (red marks) human prostate tissue. CpG islands noted in green. Methylation marks displayed artificially evenly from the TSS. Vertical axis indicates beta values for each probe. CpGs showing statistical difference between normal and tumor are indicated with an asterisk (Wilcoxon adjusted p-value < adj. pval threshold 0.001). **B.** FPKM values from publically available RNA-sequencing of LNCaP cells treated with one of three epigenetic modifying drugs (Panobinostat, SAHA or TSA) at a high or low dose for each [163]. MEIS1 (purple) and MEIS2 (blue) FPKM expression shown. **C.** Western blot analysis of PrCa cell line CWR22Rv1 when treated with HDACi's. Densitometry relative to vehicle treatment indicated above each panel.

Reintroduction of Full Length MEIS Suppresses Prostate Cancer Growth *in vitro* and *in vivo*

In order to determine the biological mechanism behind the observations previously published [20] and described (**Figures 3.1 and 3.2**) that MEIS proteins may act as PrCa tumor suppressors, we reintroduced full length MEIS into PrCa cells. We chose to compare the following constructs: GFP control, a full length MEIS1, a FLAG-tagged full length MEIS2A and the FLAG-tagged DNA binding domain-less MEIS2E. Each construct was lentivirally infected into three parental PrCa cell lines, CWR22Rv1, LNCaP and LAPC4. As the CWR22Rv1 cells are the most aggressive PrCa cell line, we will move forward with results in one cell line. Confirmation of overexpression was determined by qRT-PCR ($p<0.05$, **Figure 3.5 A and B**) and Western blot analysis (**Figure 3.5 C**). While overexpression of *MEIS1* significantly increased the *MEIS2* transcripts, and vice versa, there is not an observable difference by protein. Lenti-viral re-expression either full-length LV-MEIS1 or LV-FLAG-MEIS2 was sufficient to decrease PrCa cell number over time as measured by Trypan Blue exclusion assay ($p<0.05$, **Figure 3.5 D**). This decrease in cell proliferation did not include an observable increase in cell death by Trypan Blue exclusion. Interestingly, re-expression of the MEIS2-E isoform lacking a DNA binding domain did not suppress proliferation, implying that DNA-binding was necessary for growth suppression (**Figure 3.5 D**).

In order to investigate whether the reduction in cell number was due to a slowing of the cell cycle, we analyzed BrdU incorporation and total DNA content via propidium idodide in the CWR2Rv1 overexpressor cell lines (**Figure 3.5 E**). LV-MEIS2E and LV-GFP were not statistically different, so LV-MEIS2E cells were used as control. LV-MEIS1 and LV-MEIS2A had fewer cells in the G2 cell cycle phase than the LV-MEIS2E cells ($p<0.05$).

When the four stable CWR22Rv1 cell lines were inoculated in a subcutaneous model of tumor formation in athymic nude mice, the full-length LV-MEIS1 and LV-FLAG-MEIS2A tumors were significantly smaller than the LV-GFP controls (**Figure 3.5 F and G**). Surprisingly, the LV-FLAG-MEIS2E tumors were also significantly smaller than the LV-GFP control tumors (**Figure 3.5 F and G**).

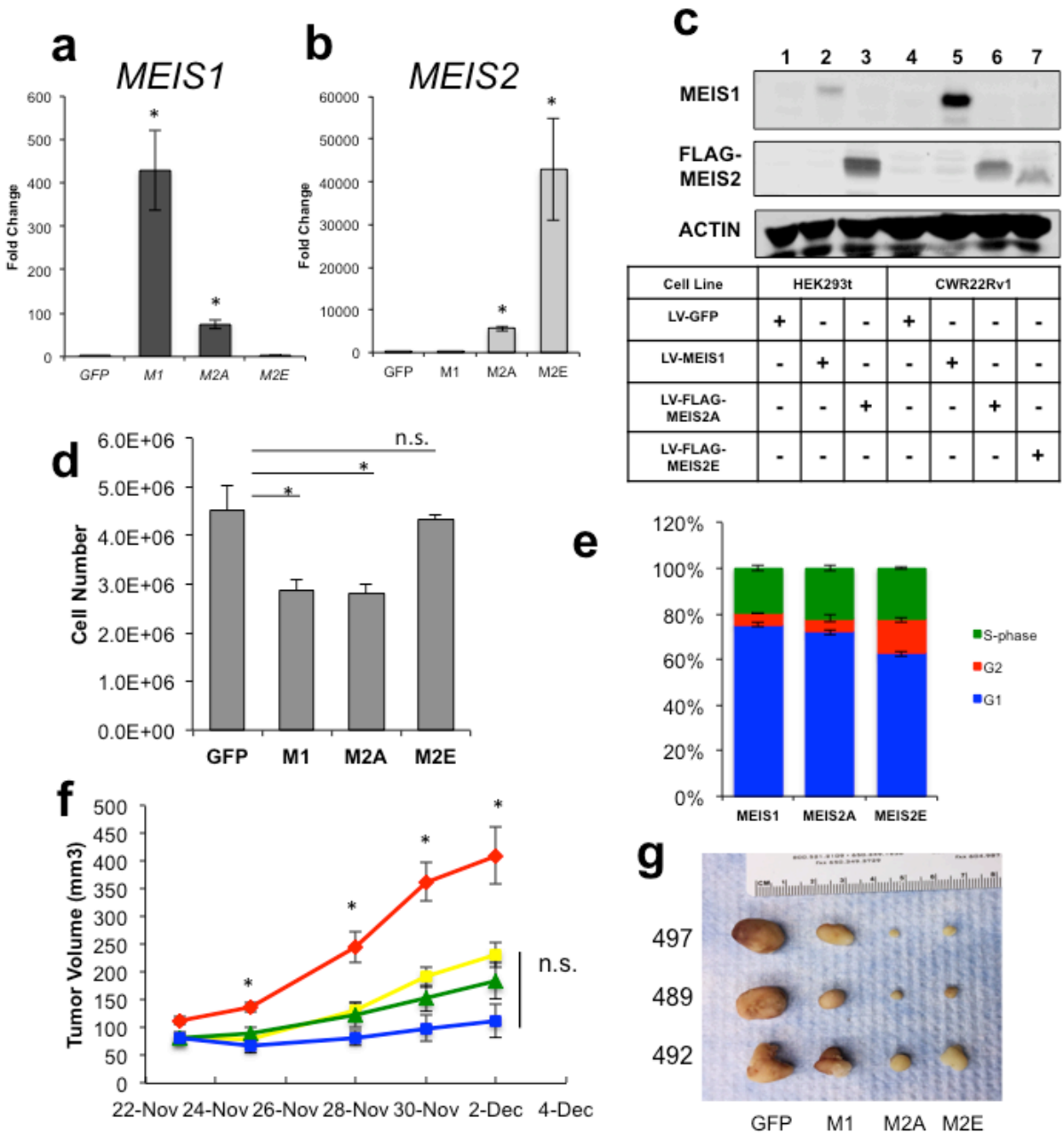

Figure 3.5: Reintroduction of Full Length MEIS Suppresses Prostate Cancer Growth *in vitro* and *in vivo*. **A.** qRT-PCR analysis of PrCa cell line CWR22Rv1 infected with LV-GFP, LV-MEIS1 (M1), LV-FLAG-MEIS2A (M2A), or LV-FLAG-MEIS2E (M2E) and amplified with primers specific to all MEIS1 isoforms (**A**) or all MEIS2 isoforms (**B**) (Student's T-test, *p<0.05). **C.** Western blot analysis of lentiviral overexpression. Lanes 1-3 contain HEK293t transfection expression of MEIS1 or FLAG-tagged MEIS2A, Lanes 4-7 contain the same construct in CWR22Rv1 cells, with the addition of homeodomainless LV-FLAG-MEIS2E in Lane 7. **D.** Cell number over time was assessed by Trypan Blue exclusion assay with CWR22Rv1 cells. Day 5 of three biological replicates shown, error graphed is SEM (p<0.05). **E.** Cell cycle analysis of CWR-22Rv1 cells after 3 hours BrdU incorporation. SEM shown (p<0.05).

Figure 3.5: Reintroduction of Full Length MEIS Suppresses Prostate Cancer Growth *in vitro* and *in vivo* continued. F. Subcutaneous tumor formation. CWR22Rv1 cells expressing LV-GFP (red), LV-MEIS1 (yellow), LV-MEIS2A (green), or LV-MEIS2E (blue) were injected subcutaneously into 4-6 week old athymic nude mice, and tumor volume was measured over time (n= 10 for each injection, 1-way ANOVA, pos-hoc Tukey-Kramer $p<0.05$) **G.** Example tumors from three mice (497, 489 and 492), harvested at time of sacrifice, then fixed.

Next Generation RNA Sequencing Identifies Pathways of MEIS-Mediated Growth Suppression

In order to identify what pathways are altered upon MEIS introduction, we sequenced the transcriptome of CWR-22Rv1 cell lines. We created libraries in biological triplicate for 50 bp, single end sequencing as we were interested in capturing downstream changes in mRNA expression from the addition of MEIS proteins. Libraries were created and multiplexed for each cell line (GFP, MEIS1, MEIS2A, MEIS2E) (**Table 3.2**). The cell line controls of both MEIS2E and GFP were included as we observed such different *in vivo* and *in vitro* phenotypes with the MEIS2E construct.

Table 3.2 RNA-Sequencing Flow Cell Summary

Flowcell Summary

Clusters (Raw)	Clusters(PF)	Yield (MBases)
965,976,480	746,546,353	37,327

Lane Summary

Lane	Sample	Barcode sequence	PF Clusters	% of the lane	% Perfect barcode	% One mismatch barcode	Yield (Mbases)	% PF Clusters	% >= Q30 bases	Mean Quality Score
7	DvG-pl1-HB1	CGATGT	80,148,669	21.2	97.6	2.5	4,007	100	96.8	39.3
7	DvG-pl1-HB2	TGACCA	31,341,938	8.3	96.9	3.1	1,567	100	96.7	39.3
7	DvG-pl1-HB3	ACAGTG	37,571,300	9.9	96.9	3.1	1,879	100	96.7	39.3
7	DvG-pl1-HB4	GCCAAT	49,299,085	13.0	96.4	3.6	2,465	100	96.7	39.3
7	DvG-pl1-HB5	GATCAG	125,410,083	33.1	96.8	3.2	6,271	100	96.7	39.3
7	DvG-pl1-HB6	CTTGTA	29,796,822	7.9	97.1	2.9	1,490	100	96.8	39.3
7	Undetermined	*unknown*	20,313,638	5.4	100.0	NaN	1,016	16.27	96.4	39.3
8	DvG-pl2-HB7	CGATGT	44,502,256	12.1	96.7	3.3	2,225	100	96.3	39.1
8	DvG-pl2-HB8	TGACCA	54,170,241	14.7	96.5	3.5	2,709	100	96.2	39.1
8	DvG-pl2-HB9	ACAGTG	36,783,344	10.0	96.5	3.5	1,839	100	96.2	39.1
8	DvG-pl2-HB10	GCCAAT	114,721,460	31.2	94.4	5.6	5,736	100	96.3	39.1
8	DvG-pl2-HB11	GATCAG	61,287,555	16.7	96.4	3.6	3,064	100	96.2	39.1
8	DvG-pl2-HB12	CTTGTA	34,090,952	9.3	97.0	3.0	1,705	100	96.3	39.1
8	Undetermined	*unknown*	22,539,167	6.1	100.0	NaN	1,127	16.4	95.9	39.1

Top Unknown Barcodes

Lane	Count	Sequence	Lane	Count	Sequence
7	2,313,703	AAAAAA	8	2,692,217	AAAAAA

Principal components analysis (PCA) was performed using the AltAnalyze software program after running a Kallisto alignment [155]. Each of the three biological replicates group together, as expected. The MEI2E and GFP triplicates also group together, supporting the hypothesis that these two cell lines would have more similar RNA expression profiles than when either of the full length MEIS constructs are expressed (**Figure 3.6 A**). From the AltAnalyze output files, we were able to identify significant differentially expressed genes (DEG's) between different groups. As we are interested in what genes contribute to the growth suppression phenotype seen in overexpression of both MEIS1 and MEIS2A, we began our analysis with shared DEG's. When comparing MEIS1 to GFP, there were 172 DEG's, and for MEIS2A versus GFP 122 DEG's that passed the following criteria: protein-coding transcripts, fold change above 1.5 and pass the Benjamini-Hochberg significance procedure for a FDR α 0.05. There are 88 genes that are shared between those two lists (**Figure 3.6 B**).

When those 88 genes were analyzed with the Gene Ontology (GO) PANTHER classifications system, 31 GO Biological Processes were identified as overrepresented via the PANTHER Overrespresentation Test ($p<0.05$, Bonferroni correction for multiple testing). We identified 15 processes with a fold enrichment above 2 (**Figure 3.6 C**). A common theme among these processes is development and differentiation, particularly in renal and genitourinary systems.

In order to understand with more depth and detail what pathways fall under the more general category of 'processes', we analyzed each set of DEG's (MEIS1 vs GFP or MEIS2A vs GFP) through Ingenuity Pathway Analyses (IPA). The activation z-score gives a general sense of whether that pathway identified is up or down regulated, but as there can be as many as 150 or

more genes per pathway, this is difficult to predict with certainty. The pathways were narrowed down by the following criteria: pathways must have a z-score, must not be biased, must have a z-score above 1 or below -1, and have more than 2 molecules included in the IPA pathway. What is clear is the common theme of cell growth, proliferation and movement present in the IPA pathways identified (**Figure 3.6 D and E**). There are some differences between the two genes. MEIS1 vs GFP DEG's show an enrichment of vasculogenesis and connective tissue pathways with a notable lack of any apoptosis or necrosis pathways (**Figure 3.6 D**). While comparing MEIS2A to GFP illuminates the possibility that maintaining cell viability may be more critical for a growth phenotype, although many proliferation pathways are also notably changed (**Figure 3.6 E**). We have identified a list of top candidates for follow-up from the shared 88 DEG's between MEIS2A vs GFP and MEIS1 vs GFP. These genes include the following: CD44, NRP1, SPRY1, TGFB2, ZNF703, and P21.

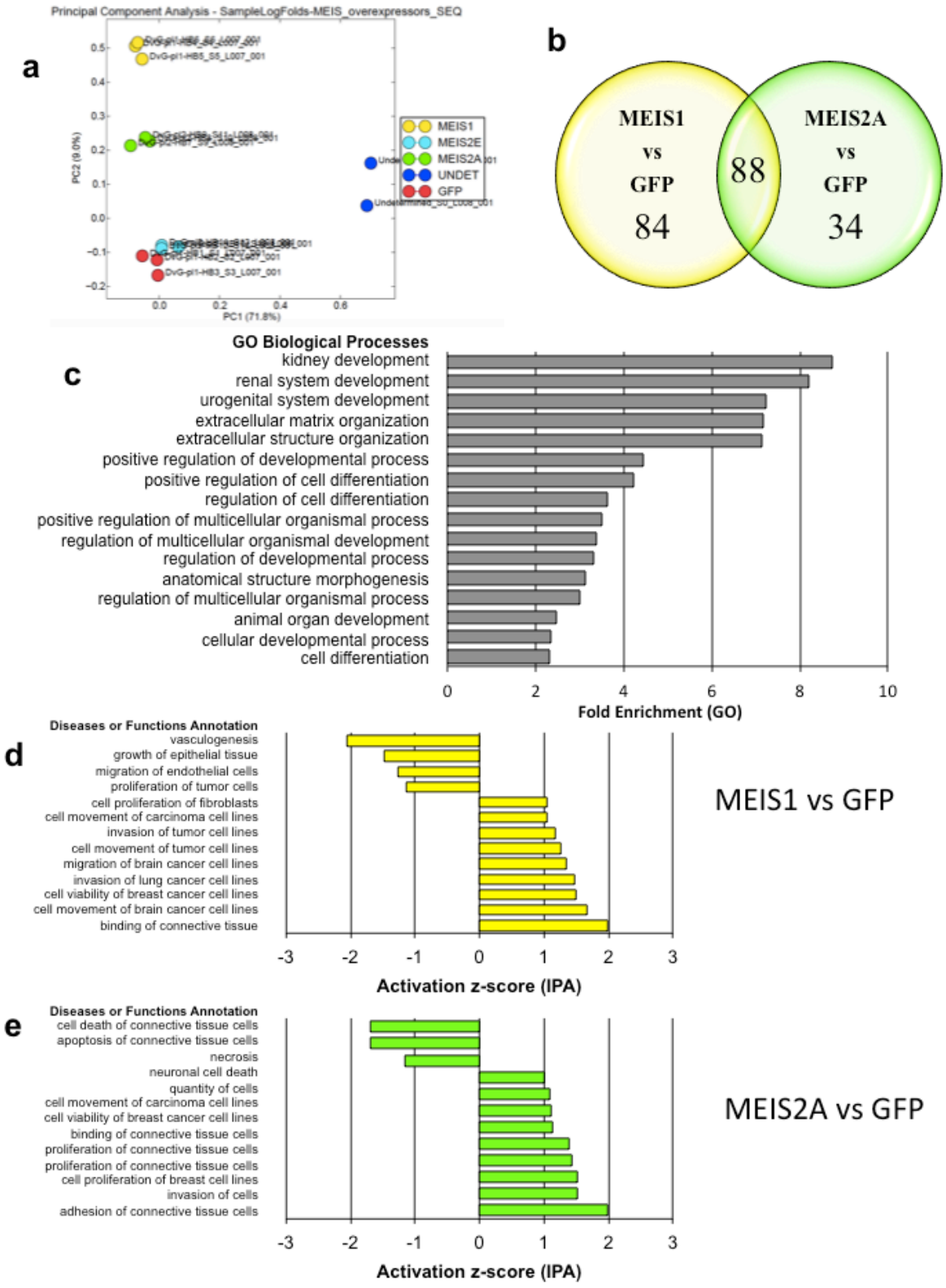

Figure 3.6 Next Generation RNA Sequencing Identifies Pathways of MEIS-Mediated Growth Suppression. Continued on next page.

Figure 3.6 Next Generation RNA Sequencing Identifies Pathways of MEIS-Mediated Growth Suppression. Continued A. PCA of biological triplicates from 50bp single-end RNA-sequencing of MEIS overexpressors as compared to GFP in CWR22Rv1 cell lines. UNDET indicates probes the Kallisto alignment tool was unable to assign to one of the prepared libraries. UNDET does not represent a large portion of the library prep as indicated in Table 3.2, they were 6% or less of each sequencing lane. **B.** Venn Diagram of DEG's. MEIS1 vs GFP yielded 172 DEG's. MEIS2A vs GFP yielded 122. There were 88 overlapping DEG's (Benjamini-Hochberg, FDR $\alpha = 0.05$). **C.** GO Ontology analysis of overrepresented biological processes for the 88 overlapping DEG's identified in (**B**) Fold enrichment shown on horizontal axis. **D and E.** IPA pathway analysis for DEG's from MEIS1 vs GFP (**D**) or MEIS2A vs GFP (**E**). Pathways must have a z-score, must not be biased, must have a z-score above 1 or below -1, and have more than 2 molecules included in the IPA pathway.

Discussion

In this study, we have identified MEIS proteins as prostate cancer tumors suppressors. They are able to slow cell growth by modifying expression of proliferation and cell viability genes in prostate cancer cells. While identified as oncogenes in some other cancer types, leukemias specifically, we show convincing data to support a tumor suppressive role in the prostate. We observed a step-wise progressive loss of MEIS1 and MEIS2 expression from healthy normal stromal cells, to healthy normal epithelial cells, and further to PrCa (**Figure 3.1**). We observed this stepwise progression across multiple data sets and multiple means of detection. We have previously confirmed that this progressive loss is not due to a loss of basal epithelial cells, as loss of basal cells is a common indication of PrCa [20]. Also, MEIS1 and 2 expression is not restricted to basal prostate epithelial cells, but both can be found in prostate stromal and columnar epithelial cells as well [20].

We also found that within PrCa, this stepwise progression of decreased MEIS expression is continued, from benign lesions to local tumors to distant metastases (**Figure 3.2**). This loss of MEIS expression across benign lesions to distant metastases may be connected to their ability to regulate invasion, migration and cell viability as evidenced by our RNA sequencing of MEIS genes in the context of aggressive PrCa cell line models (**Figure 3.6**).

We also rigorously tested the common PrCa model cell lines for expression of various translational isoforms of MEIS, as it has been reported that the homeodomains-less form can have very different functions than the full-length versions [78, 79]. However, we determined that these homeodomainless MEIS-E isoforms are not present in human prostate tissue, nor in our field's commonly used PrCa cell lines (**Figure 3.3**). The knowledge that MEIS2E is not expressed in human tissue is crucial as it eliminates on possible hypothesis for how the MEIS

proteins function as tumor suppressors. If MEIS2E levels had risen in cancer samples as compared to healthy tissue, it is possible that this homeodomainless form could have squelched away Homeobox proteins from their proper healthy genomic binding locations. Other systems have noted this phenomenon in *Xenopus* and *C. elegans*, but understanding that this system is not maintained through mammals helps us narrow our research focus. However, we were still able to use this DNA-binding deficient construct (MEIS2E) in our experiments as a control to determine the role of the DNA binding domain when overexpressing MEIS proteins.

This understanding of the landscape of expression across tissue types will be crucial for future studies regarding the mechanistic role of MEIS proteins in normal prostate development. The stepwise progressive loss of MEIS expression from healthy to cancer to metastases is a critical tool set and jumping off point for future examinations of the role for MEIS in prostate cancer progression. While this is a crucial starting point, a more rigorous landscape of MEIS expression across the natural history of human PrCa is essential for our understanding of how MEIS suppress tumor formation.

We also found that MEIS1 expression may be susceptible to demethylating agents, as many CpGs near the TSS are more highly methylated in tumors than in healthy prostate tissue. While some loci were differentially methylated in the MEIS2 TSS, the most drastic change in MEIS2 expression occurred with treatment of a different class of epigenetic modifying drugs: HDACi's. While we did not see a similar increase in expression of MEIS1 upon treatment with a demethylating agent, our data provide a rationale for future work to be done on how epigenetic modification may enable increased expression of MEIS proteins. It is also still very early in the era of epigenetic drugs, and one day if it is possible to target epigenetic modifications to particular loci, without the dramatic side effects of current hypo-epigenetic modification agents,

we may be able to use this knowledge about the methylation states of *MEIS* genes to our clinical advantage. But until that point, it is unwise to use epigenetic treatments to increase *MEIS* expression in a clinical context.

When we introduced full length MEIS back into PrCa cells, we saw significant reduction in cell number and slowing of the cell cycle, with more cells present in the G1 phase of the cell cycle (**Figure 3.5**). We also saw that when these cells formed tumors in an immunocompromised murine host, the full length MEIS re-expressors showed significantly smaller tumors than controls. Surprisingly, in the *in vivo* context, the MEIS2E DNA binding domainless variant did not phenocopy the *in vitro* results. We hypothesize that there are pressures present in the 3-D context of an *in vivo* model that were not present in the dish that lead to this observation. The RNA sequencing data indicating a key role for MEIS proteins in vasculogenesis, extracellular matrix organization and adhesion of connective tissue may help to explain this 3-D phenotype variation (**Figure 3.6**). This is a logical role for the MEIS' in cancer as one of the earliest identified roles for the MEIS proteins in developmental biology is vasculogenesis, vascular patterning and hematopoiesis [130, 132]. Further examination into MEIS2E is warranted, particularly by determining whether there is a 3-D structural requirement for the growth suppression or whether there is a set of extracellular signaling molecules that may be impacting MEIS2E's effect on growth *in vivo* that is not found in our *in vitro* milieu. However, we did not pursue this line of inquiry in our work presented here as there seems to be limited translational potential for MEIS2E in prostate cancer as it is not expressed at any point in healthy or cancerous human tissue.

While there is much to still learn about MEIS biology in the prostate, and in particular their role in cancer growth, we have demonstrated that the full length MEIS1 and 2 are prostate

cancer tumor suppressors. We are defining tumor suppressors as in the 2017 edition of the Encyclopedia of Cancer for Class II tumor suppressors [165]. Characteristics for a Class II tumor suppressor are based on the revolutionary work done by Ruth Sager in the late nineties where she began the shift in focus of tumor genetics from DNA mutations to alterations in RNA expression levels [166]. Class II tumor suppressors have three major shared characteristics. They negatively regulate cell growth, they are down regulated in cancer by a mechanism other than mutation or genomic deletion, and their down regulation is therefore reversible [165]. Many studies since Dr. Sager's work have revealed many tumor suppressors that follow this pattern including but not limited to: Maspin, Tropomyosin, CAV1, KLK10 and LOX [165].

Four major aspects of tumor suppression support this role of MEIS as PrCa tumor suppressors: First, we observed their ability to inhibit cell proliferation, even in the most aggressive prostate cancer cell line model. Not only do they decrease cell number, but arrest cells in G1, preventing them from efficiently completing the cell cycle. Second, they are able to inhibit tumor formation *in vivo*. The slowed cell number is not a phenomenon limited to the tissue culture dish, but is seen in murine models of prostate tumor initiation, fully fulfilling the first criteria for a Class II tumor suppressor of down regulating tumor growth. Third, cancer cells inactivate MEIS expression as cancer progresses, as seen in the stepwise progressive loss of expression in cell lines and in humans. This down regulation is likely driven by epigenetic modifications decreasing expression. Fourth, and finally, this inactivation by decreased expression can be reversed. We showed that epigenetic modification by drugs is capable of increasing MEIS expression.

We identified developmental growth pathways via RNA-sequencing and pathway analyses that may be responsible for the MEIS-mediated growth suppression seen *in vitro* and *in*

vivo experiments. Growth and proliferation pathways heavily dominate these developmental pathways, in particular. The proliferation regulation genes that were altered by the introduction of full length MEIS into prostate cancer cells tended to be more external growth factors that change whole programs of proliferation across multiple cells. These proliferation regulators included: endothelial growth factors (F3 and NRP-1), heparin growth factors, fibroblast growth factors, and secreted ligands of TGF-β. The growth suppression we see could be the result of MEIS' role in regulating a growth factor program upstream of direct cell cycle regulation.

While we have convincingly shown MEIS to be a tumor suppressor, there are pitfalls to our work. Some of these limitations include a limited scope for human data in this work. We are working on assessing MEIS expression across a larger and clinically annotated dataset to better understand the clinical implications of MEIS expression loss. Further, we recognize that a deeper understanding of how the MEIS proteins are causing slowed cell cycle progression is key to understanding how these proteins function as tumor suppressors. We are validating candidate genes identified from our rigorous RNA sequencing experiment that may shed light on the downstream actors of MEIS-mediated growth suppression. The direct relationship of the MEIS transcription cofactors with these candidates is of high interest, and chromatin immunoprecipitation will be employed to test whether there is direct regulation. Finally, we understand that the drugs used for epigenetic perturbation are not tolerated particularly well clinically, and are general hypo-methylating or –deacetylating agents. Meaning that they are not specifically modifying our target promoters. This may account for the inability of hypomethylating agents to elicit a response in MEIS1 expression. We are interested in interrogating MEIS expression as epigenetic drugs advance. We realize that we are unlikely to treat PrCa patients with epigenetic modifying drugs to increase their MEIS expression. However,

by understanding the biology of novel tumor suppressors we provide future researchers and clinicians the materials to improve early detection of aggressive PrCa and minimize overtreatment of “Men in the Middle” who may not require invasive treatment.

CHAPTER IV

DISCUSSION, CONCLUSIONS AND FUTURE DIRECTIONS

Overall, my contributions as described in this work have provided key insights into the normal development and abnormal hijacking of these developmental processes in prostate cancer. By understanding these fundamental mechanisms of prostate development, we can better understand the etiology of prostate cancer. This knowledge enables researchers and clinicians alike to identify and target weaknesses in prostate cancer cells for improved detection and treatment of prostate cancer. The most effective and pervasive tool we have to treat prostate cancer is androgen signaling intervention, which when functioning normally, is critical for normal prostate development and maintenance [3, 16, 151, 167]. While androgen deprivation is our current main clinical intervention, men with prostate cancer will develop castration resistance if they survive long enough [159, 168]. While PrCa can progress slowly, leaving the patient relatively asymptomatic for years, some patients present with aggressive metastatic PrCa and a subsequently poor prognosis [126, 127]. It can also be difficult to distinguish which men will fall into the indolent or aggressive groups [128], particularly patients with intermediate Gleason scores. There is clinical need for novel therapeutics to treat men with prostate cancer, and it is likely that novel treatment modalities will arise from other developmental pathways that have gone awry in the adult tissue. There is also a clinical need for better tools for clinicians to determine which men will require aggressive treatment courses and which require watchful waiting. Using the paradigms from normal development and applying them to how prostate tumors develop could help us illuminate new treatments and new diagnostic tools.

My research has challenged a paradigm of sexual dimorphism of the CMDM, where previously the role of the Müllerian duct precursor tissue, the CMDM, is solely restricted to female genitourinary development. Our results support a model of prostate development where androgens drive the CMDM to develop into the prostate, and not the periurethral glands (Chapter II). This more nuanced understanding of early prostate development provides support to investigate how factors secreted by the caudal Müllerian duct may be involved in prostate disease prevention and treatment.

We determined the specific time point at which the UGS epithelium gives rise to distinct urethral and prostate epithelial budding at day E16.5. The appearance and maintained expression of NKX3.1 and Hoxb13 in prostate epithelial buds, and distinct lack of expression in urethral glands, suggests that there are key differences in the stromal microenvironment that promote transcription factor expression and prostate lineage specification. Although the MD regresses in males due to anti-Müllerian hormone, a portion of the MD undergoes EMT as it regresses [169-171], potentially leaving a portion of the MDM that expresses AR. Leaving us with the hypothesis that it is this residual portion of the MDM plays a role in prostate differentiation that separates the budding prostate identify from periurethral gland identity.

When either hES cell recombination or adults murine Urothelial cells were combined with CMD stromal cells, glands displaying prostatic cell fate markers were developed in a renal capsule model. As the hES cells did not form HOXB13+ glands, we utilized murine Urothelial cells. As these recombination events did lead to HOXB13+ glands, we concluded that we are missing a key developmental factor to induce HOXB13 in the hES recombination experiment. We realize that there are many steps between hES cells and adult murine Urothelial cells, but

even with this limitation, we were able to illuminate part of the relationship between the CMDM and UGSM in the developing prostate that had never been documented before.

Some limitations of this study include the lack of the identity of the mediator of prostatic cell fate emanating from the microenvironment that drives this branch point in development. We showed the importance of the CMDM in separating cell fate between prostate and periurethral glands, but we do not go on to identify what exactly is causing this identity switch. We also do not fully understand the lack of HOXB13 expression in the recombination experiment with human embryonic stem cells. While the expression of the terminally differentiation marker for luminal epithelial cells is present when we recombine with tissue further along the developmental timeline, we do not understand exactly what is missing from the hES milieu in order to induce HOXB13 expression.

In this study we provide evidence that the caudal Müllerian duct mesenchyme is able to induce prostate epithelia and is likely a key determinant in delineating prostate vs. urethral gland cell fate. This is in contrast to the conventional belief that the prostate is induced solely by the urogenital sinus mesenchyme. Our data is significant for three reasons. First, the ability of MDM to induce prostate formation in the extracellular milieu of androgens helps explain the previously noted observation that vaginal stroma can induce prostate epithelium formation [172]. As well as the observation that high-dose testosterone treatment in post-partum females can result in prostate formation [172]. Second, our data helps to elucidate how a common embryonic structure, the UGS, can be influenced by stroma to form both urethral and prostate epithelium. Third and finally, given the vast disparity in disease incidence between the prostate and urethral gland epithelium, our data provide a rationale for future investigations into whether the caudal MDM could be a potential mediator in prostate neoplasia and cancer initiation; such MDM-

derived paracrine factors have the potential to become novel targets for prostate cancer prevention or therapeutic intervention.

My research has validated that the critical embryonic developmental MEIS genes are prostate cancer tumor suppressors, ripe for further exploration of whether these proteins could be used as biomarkers for distinguishing whether patients will develop aggressive or indolent tumors. While there is much to still learn about MEIS biology in the prostate, and in particular their role in cancer growth, we have demonstrated that the full length MEIS1 and 2 are prostate cancer tumor suppressors. We are defining tumor suppressors as in the 2017 edition of the Encyclopedia of Cancer for Class II tumor suppressors [165]. Characteristics for a Class II tumor suppressor are based on the revolutionary work done by Ruth Sager in the late nineties where she began the shift in focus of tumor genetics from DNA mutations to alterations in RNA expression levels [166]. Class II tumor suppressors have three major shared characteristics. They negatively regulate cell growth, they are down regulated in cancer by a mechanism other than mutation or genomic deletion, and their down regulation is therefore reversible [165]. Many studies since Dr. Sager's work have revealed many tumor suppressors that follow this pattern including but not limited to: Maspin, Tropomyosin, CAV1, KLK10 and LOX [165].

Four major aspects of tumor suppression support this role of MEIS as PrCa tumor suppressors: First, we observed their ability to inhibit cell proliferation, even in the most aggressive prostate cancer cell line model. Not only do they decrease cell number, but arrest cells in G1, preventing them from efficiently completing the cell cycle. Second, they are able to inhibit tumor formation *in vivo*. The slowed cell number is not a phenomenon limited to the tissue culture dish, but is seen in murine models of prostate tumor initiation, fully fulfilling the first criteria for a Class II tumor suppressor of down regulating tumor growth. Third, cancer cells

inactivate MEIS expression as cancer progresses, as seen in the stepwise progressive loss of expression in cell lines and in humans. This down regulation is likely driven by epigenetic modifications decreasing expression. Fourth, and finally, this inactivation by decreased expression can be reversed. We showed that epigenetic modification by drugs is capable of increasing MEIS expression.

Some of the limitations of this work include the need for a deeper understanding of the perturbation of the cell cycle. While we see that re-expression of full length MEIS into cancer cells do not progress to G2 as frequently as their controls, we do not yet understand what molecules are responsible for this cell cycle arrest. We do know that HOXB13 has been identified as responsible for cell cycle changes including regulating G1/S checkpoints [24] and further investigation into the role of HOXB13 and MEIS's interaction affecting the cell cycle is a rich area for future study, in particular the context of their cell cycle regulation. HOXB13 can act as a bivalent regulator of AR chromatin binding and function as either a growth-promoter or growth-suppressor in prostate cancer cells depending on the cellular context [47]. For example, in androgen-sensitive prostate cancer cell lines such as LNCaP, increased HOXB13 activity can decrease levels of Cyclin D1 and lead to growth inhibition through reduction of pRb phosphorylation and stabilization of the pRB-E2F complex [24, 25]. Conversely, in castration-resistant prostate tumors, HOXB13 overexpression can inhibit p21 and thus act as an oncogene through subsequently promoting E2F activation and cell cycle progression [25]. The MEIS status in these contexts has not been investigated, and may shed some light on how HOXB13 is able to have such dynamic control of the cell cycle.

We require a more in-depth analysis of cell cycle alterations, perhaps with a dynamic color-coded imaging vector [173]. We are interested to see if there are similar impacts of cell

cycle control as described in cardiomyocytes, where a loss of *MEIS1* extended the proliferation window in postnatal mice, and overexpression of MEIS1 was sufficient to slow proliferation [69]. Obtaining mice where the *MEIS1* locus could be floxed out under the control of the prostate-specific probasin promoter would be advantageous to investigating the role of MEIS1 *in vivo* regulation of the cell cycle. We also need a more clear understanding of the role of cell death in the growth suppression of MEIS proteins. While we saw no evidence *in vitro* of cell death, our RNA-sequencing IPA pathway analysis indicated some death pathways were altered. We will pursue a deeper investigation of how MEIS proteins may regulate death pathways in the future. Further, the proliferation regulation genes that were altered by the introduction of full length MEIS into prostate cancer cells tended to be more external growth factors that change whole programs of proliferation across multiple cells. These proliferation regulators included: endothelial growth factors (F3 and NRP-1), heparin growth factors, fibroblast growth factors, and secreted ligands of TGF-β. The growth suppression we see could be the result of MEIS' role in regulating a growth factor program upstream of direct cell cycle regulation.

This identification of MEIS-mediated actors of growth suppression will enable further research into the role of Homeobox factors in prostate cancer progression and a platform for better understanding of the mechanism of MESI/HOX biology in hereditary PrCa. We are very interested in pursuing the role of MEIS's favorite binding partner, HOXB13 in our future work, both in terms of how these proteins function together to drive normal prostate organogenesis and how they may be disrupted throughout prostate tumor natural history.

Highlighting the link between cancer and development, we see many genitourinary developmental pathways are perturbed upon re-expression of MEIS into prostate cancer. It is possible that proper MEIS expression directs HOXB13 to the correct locations on the genome,

essentially acting as the rudder for HOXB13. Healthy differentiation into adult prostate may require the increased specificity and affinity provided to HOXB13 by the MEIS rudder. So we have two complementary models for how MEIS and HOXB13 proteins may act in prostate cancer as compared to healthy prostate tissue (**Figure 4.1**). A loss of proper guidance, either through a mutation in the binding domain or a loss of expression of MEIS, would disrupt the healthy differentiation prostate transcription program (**Figure 4.1**). This disrupted healthy prostate transcription program could enable a shift towards cancerous transformation or progression. I would then hypothesize that this shift would go from the more differentiated healthy program to a profile closer to undifferentiated cells.

We expect that the G84E mutation located in the MEIS-binding domain of HOXB13 is sufficient to dislodge transcription cofactors from HOXB13, leading to a rudderless HOX protein that is unable to appropriately find, bind and regulate its adult normal prostate transcriptional program (**Figure 4.1 1**). We require future biochemical studies to fully understand whether the switch from a glycine to a glutamic acid amino acid (G → E) is able to prevent binding between HOXB13 and MEIS. This is an active area of research in our lab. We have also hypothesized that a similar outcome can arise from a different cause. We hypothesize that a similar deregulation in HOXB13 transcriptional program can arise from a dramatic decrease in expression of MEIS. We have shown that there is a stepwise decrease in MEIS expression from normal to cancerous prostates. The stepwise progressive loss of MEIS expression from healthy to cancer to metastases is a critical tool set and jumping off point for future examinations of the role for MEIS in prostate cancer progression. While this is a crucial starting point, a more rigorous landscape of MEIS expression across the natural history of human PrCa is essential for our understanding of how MEIS suppress tumor formation. We also have shown that reintroduction

of MEIS can alter the transcriptional program of aggressive prostate cancer model cell lines to alter cell growth and proliferation (**Chapter III and Figure 4.1 2**). Future work investigating whether the transcriptional profile and phenotype shifts to a more dedifferentiated state is necessary to confirm this idea.

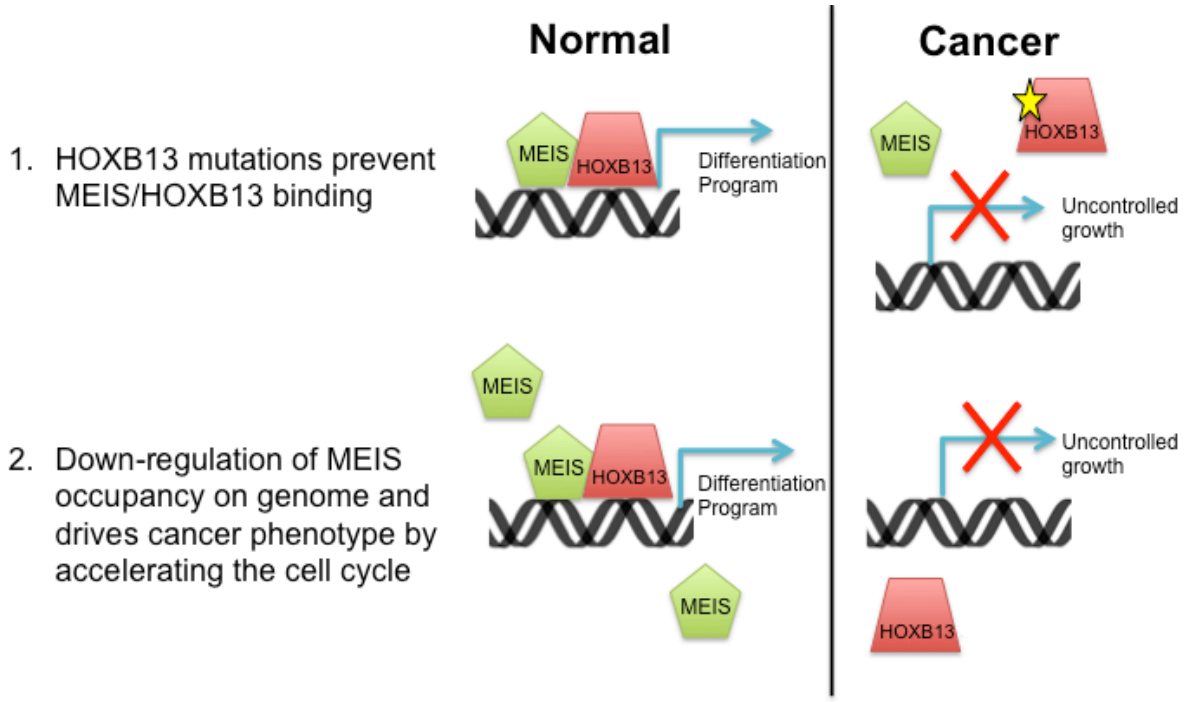

Figure 4.1: MEIS is required to Direct HOXB13 Transcriptional Program in the Prostate. Graphical summary of the two complementary models for how prostate cancer programs may arise from deregulated HOXB13. In (1) the deregulation arises from mutations in HOXB13 (like G84E) that prevent binding of MEIS and HOXB13. The rudderless HOXB13 is unable to commit to the terminal differentiation program required for normal maintenance and function of the healthy prostate. In (2) the deregulation arise from insufficient levels of MEIS to direct the genomic binding and regulation of HOXB13.

An area that limits our results includes the model of a binary regulation system between HOXB13 and MEIS. In reality, there are likely to be multimeric complexes that guide HOXB13 to regulate the appropriate transcriptional program to maintain a healthy prostate. These multimeric complexes may be composed of other HOX proteins, but more likely other TALE proteins [134, 174]. Other TALE proteins could include any of the PREP proteins, but not the PBX family, as they are not able to bind to HOXB13, as it is an Abd-B family member. HOXB13 lacks a typical YPWM motif, which is where Pbx proteins typically interact with HOX proteins [175]. As stated above, the loss of the MEIS/HOXB13 complex may lead to a loss of terminally differentiated identity to a luminal epithelial cell. HOXB13 is known to provide these prostate cell types' identity [23, 28] and we demonstrated that cell differentiation is a key pathway component of MEIS re-expression. This needs to be investigated more deeply, but it is possible that the particular makeup of the MEIS/HOXB13 transcription complex, including other transcriptions cofactors, may enable the identity of terminally differentiation prostatic luminal epithelial cells. Disruption of this complex, by mutation or by a decrease in expression in any of the binding partners, may lead to dedifferentiation or even cancerous transformation.

We saw from Chapter II that the stroma is a driving force of prostate differentiation, particularly the CMDM driving prostate as opposed to periurethral gland formation. The idea of the microenvironment regulating prostate growth and function fits into the paradigm that prostate identity is largely driven by stromal signals, such as androgen signaling[16, 18, 27, 106, 172, 176]. Much of our understanding of how the AR drives prostate caner is based on our knowledge of how it functions in a healthy context. A notable area for future study in regards to MEIS proteins is the high level of expression of these proteins in the prostate stroma. Does the level of expression of stromal cells between healthy prostate glands and cancerous glands change? Or

perhaps does the milieu of MEIS binding proteins in the stroma differ from the partners in the epithelium? The secreted factors as a result of high levels of MEIS compared to low levels of MEIS may help us to understand the longer-range impact of MEIS levels on prostate cancer. From our RNA sequencing, we found that many cell-cell adhesion and secreted growth factor molecules were altered upon introduction of full length MEIS proteins. We need to investigate the role that the MEIS proteins may have on the prostate microenvironment. Understanding how exactly the stroma contributes to normal prostate development could provide researchers a better understanding of what goes wrong in a cancerous context.

Genetic and informatics studies in prostate cancer have clearly implicated a key role for MEIS/HOX signaling in prostate cancer initiation, and have created multiple avenues of potentially fruitful and impactful investigation. Based upon our understanding of MEIS/HOX function in other tumor types and our limited understanding in prostate cancer, several future research questions can be postulated.

First, what properties of prostate development make this tissue so tumor-prone? It is important to elucidate when, during the development and maintenance of the prostate, the HOXB13-G84E mutation manifests itself; that is, to determine whether the prostate of a G84E carrier develops differently or does the G84E mutation impact prostate homeostasis and turnover after puberty and sexual maturity. The idea of a specific cocktail of homeobox transcription cofactors forging prostate luminal epithelial identity may help to understand this large question in the field. It may be that the particular balance of Homeobox cofactors is much more likely to be disrupted. We see that the Homeobox pattern of expression is at least different between the seminal vesicle, periurethral glands and the prostate. Or it could be that the disruption of this specific cocktail of homeobox transcription cofactors forging prostate luminal epithelial identity

is more likely to have serious oncogenic consequences than in adjacent tissues. Comparing the normal development of the prostate to other tissues close in proximity and function, such as the seminal vesicles or periurethral glands, may reveal clues to the preponderance of prostate tumors that plague our health care system. Second, do other *HOXB13* mutations including and beyond G84E impact prostate function similarly or do they have unique etiologies and function? Third, how does the G84E mutation, and other *HOXB13* mutations, functionally modulate MEIS function and MEIS/HOX interactions? Mechanistic studies investigating whether the G84E mutation abrogates or modulates MEIS interaction, and the transcriptional impact of *HOXB13* mutations on *HOXB13* target genes, will illuminate how the G84E mutation leads to prostate tumor initiation. Fourth and finally, how can MEIS/HOX expression, and their gene targets, be exploited for patient benefit? Efforts to screen and genetically counsel individuals with *HOXB13* mutations are clearly warranted; however, mechanistic studies of MEIS/HOX transcriptional function has the high potential to identify targetable pathways for tumor prevention and staging.

Understanding the factors that underpin the identity of the adult prostate is the key to understanding why cancer occurs so frequently in the prostate. Cancer has been commonly described as a disease of developmental biology gone awry, and we need to fully comprehend the healthy development of the prostate to be able to understand far too frequent cancerous transformation of the prostate.

REFERENCES

1. Siegel, R.L., K.D. Miller, and A. Jemal, *Cancer statistics, 2016.* CA Cancer J Clin, 2016. **66**(1): p. 7-30.
2. Huggins, C. and P.J. Clark, *Quantitative Studies of Prostatic Secretion : Ii. The Effect of Castration and of Estrogen Injection on the Normal and on the Hyperplastic Prostate Glands of Dogs.* J Exp Med, 1940. **72**(6): p. 747-62.
3. Huggins, C. and C.V. Hodges, *Studies on prostatic cancer. I. The effect of castration, of estrogen and androgen injection on serum phosphatases in metastatic carcinoma of the prostate.* CA Cancer J Clin, 1972. **22**(4): p. 232-40.
4. Gleason, D.F., *Histologic grading of prostate cancer: a perspective.* Hum Pathol, 1992. **23**(3): p. 273-9.
5. Humphrey, P.A., *Gleason grading and prognostic factors in carcinoma of the prostate.* Mod Pathol, 2004. **17**(3): p. 292-306.
6. Gleason, D.F. and G.T. Mellinger, *Prediction of prognosis for prostatic adenocarcinoma by combined histological grading and clinical staging.* J Urol, 1974. **111**(1): p. 58-64.
7. Mottet, N., et al., *EAU-ESTRO-SIOG Guidelines on Prostate Cancer. Part 1: Screening, Diagnosis, and Local Treatment with Curative Intent.* Eur Urol, 2017. **71**(4): p. 618-629.
8. Cornford, P., et al., *EAU-ESTRO-SIOG Guidelines on Prostate Cancer. Part II: Treatment of Relapsing, Metastatic, and Castration-Resistant Prostate Cancer.* Eur Urol, 2017. **71**(4): p. 630-642.
9. Sountoulides, P. and T. Rountos, *Adverse effects of androgen deprivation therapy for prostate cancer: prevention and management.* ISRN Urol, 2013. **2013**: p. 240108.
10. Lu-Yao, G.L., et al., *Effect of age and surgical approach on complications and short-term mortality after radical prostatectomy--a population-based study.* Urology, 1999. **54**(2): p. 301-7.
11. Alibhai, S.M., et al., *30-day mortality and major complications after radical prostatectomy: influence of age and comorbidity.* J Natl Cancer Inst, 2005. **97**(20): p. 1525-32.
12. Hu, J.C., et al., *Comparative effectiveness of minimally invasive vs open radical prostatectomy.* JAMA, 2009. **302**(14): p. 1557-64.
13. Loeb, S., et al., *Overdiagnosis and overtreatment of prostate cancer.* Eur Urol, 2014. **65**(6): p. 1046-55.
14. Siegel, R.L., K.D. Miller, and A. Jemal, *Cancer Statistics, 2017.* CA Cancer J Clin, 2017. **67**(1): p. 7-30.
15. Podlasek, C.A., D. Duboule, and W. Bushman, *Male accessory sex organ morphogenesis is altered by loss of function of Hoxd-13.* Dev Dyn, 1997. **208**(4): p. 454-65.
16. Hayward, S.W. and G.R. Cunha, *The prostate: development and physiology.* Radiol Clin North Am, 2000. **38**(1): p. 1-14.
17. Economides, K.D., *Hoxb13 is required for normal differentiation and secretory function of the ventral prostate.* Development, 2003. **130**(10): p. 2061-2069.
18. Cunha, G.R., et al., *Hormonal, cellular, and molecular regulation of normal and neoplastic prostatic development.* J Steroid Biochem Mol Biol, 2004. **92**(4): p. 221-36.
19. Cunha, G.R., et al., *Normal and abnormal development of the male urogenital tract. Role of androgens, mesenchymal-epithelial interactions, and growth factors.* J Androl, 1992. **13**(6): p. 465-75.

20. Chen, J.L., et al., *Deregulation of a Hox protein regulatory network spanning prostate cancer initiation and progression.* Clin Cancer Res, 2012. **18**(16): p. 4291-302.
21. Ewing, C.M., et al., *Germline mutations in HOXB13 and prostate-cancer risk.* N Engl J Med, 2012. **366**(2): p. 141-9.
22. Cerda-Esteban, N. and F.M. Spagnoli, *Glimpse into Hox and tale regulation of cell differentiation and reprogramming.* Dev Dyn, 2014. **243**(1): p. 76-87.
23. Huang, L., et al., *Posterior Hox gene expression and differential androgen regulation in the developing and adult rat prostate lobes.* Endocrinology, 2007. **148**(3): p. 1235-45.
24. Hamid, S.M., et al., *HOXB13 contributes to G1/S and G2/M checkpoint controls in prostate.* Mol Cell Endocrinol, 2014. **383**(1-2): p. 38-47.
25. Rezsohazy, R., et al., *Cellular and molecular insights into Hox protein action.* Development, 2015. **142**(7): p. 1212-27.
26. Lappin, T.R., et al., *HOX genes: seductive science, mysterious mechanisms.* Ulster Med J, 2006. **75**(1): p. 23-31.
27. Prins, G.S. and O. Putz, *Molecular signaling pathways that regulate prostate gland development.* Differentiation, 2008. **76**(6): p. 641-59.
28. Takahashi, Y., et al., *Expression profiles of 39 HOX genes in normal human adult organs and anaplastic thyroid cancer cell lines by quantitative real-time RT-PCR system.* Exp Cell Res, 2004. **293**(1): p. 144-53.
29. Favier, B. and P. Dolle, *Developmental functions of mammalian Hox genes.* Mol Hum Reprod, 1997. **3**(2): p. 115-31.
30. Mallo, M., D.M. Wellik, and J. Deschamps, *Hox genes and regional patterning of the vertebrate body plan.* Dev Biol, 2010. **344**(1): p. 7-15.
31. Abate-Shen, C., *Deregulated homeobox gene expression in cancer: cause or consequence?* Nat Rev Cancer, 2002. **2**(10): p. 777-85.
32. Sadler, T.W., *Urogenital System*, in *Langman's Medical Embryology*, T.W. Sadler, Editor. 2012, Lippincott Williams & Wilkins: Baltimore, MD. p. 232-259.
33. Rao, M., and Wilkinson, M.F., *Homeobox Genes and the Male Reproductive System*, in *The Epididymis: From Molecules to Clinical Practice*, B.a.H. Robaire, B.T., Editor. 2002, Springer: United States. p. 269-283.
34. Podlasek, C.A., et al., *Hoxa-10 deficient male mice exhibit abnormal development of the accessory sex organs.* Dev Dyn, 1999. **214**(1): p. 1-12.
35. Podlasek, C.A., J.Q. Clemens, and W. Bushman, *Hoxa-13 gene mutation results in abnormal seminal vesicle and prostate development.* J Urol, 1999. **161**(5): p. 1655-61.
36. Robaire, B., B.T. Hinton, and M.C. Orgebin-Crist, *The epididymis : from molecules to clinical practice : a comprehensive survey of the efferent ducts, the epidiymus, and the vas deferens*. 2002, New York: Kluwer Academic/Plenum Publishers. xiii, 575 p.
37. Wilhelm, D. and P. Koopman, *The makings of maleness: towards an integrated view of male sexual development.* Nat Rev Genet, 2006. **7**(8): p. 620-31.
38. Shaw, G. and M.B. Renfree, *Wolffian duct development.* Sex Dev, 2014. **8**(5): p. 273-80.
39. Bomgardner, D., B.T. Hinton, and T.T. Turner, *5' hox genes and meis 1, a hox-DNA binding cofactor, are expressed in the adult mouse epididymis.* Biol Reprod, 2003. **68**(2): p. 644-50.
40. Snyder, E.M., et al., *Gene expression in the efferent ducts, epididymis, and vas deferens during embryonic development of the mouse.* Dev Dyn, 2010. **239**(9): p. 2479-91.

41. Abate-Shen, C. and M.M. Shen, *Molecular genetics of prostate cancer.* Genes Dev, 2000. **14**(19): p. 2410-34.
42. Warot, X., et al., *Gene dosage-dependent effects of the Hoxa-13 and Hoxd-13 mutations on morphogenesis of the terminal parts of the digestive and urogenital tracts.* Development, 1997. **124**(23): p. 4781-91.
43. Economides, K.D. and M.R. Capecchi, *Hoxb13 is required for normal differentiation and secretory function of the ventral prostate.* Development, 2003. **130**(10): p. 2061-9.
44. Rao, M. and M.F. Wilkinson, *Homeobox Genes and the Male Reproductive System*, in *The Epididymis: From Molecules to Clinical Practice: A Comprehensive Survey of the Efferent Ducts, the Epididymis and the Vas Deferens*, B. Robaire and B.T. Hinton, Editors. 2002, Springer US: Boston, MA. p. 269-283.
45. McMullin, R.P., L.N. Mutton, and C.J. Bieberich, *Hoxb13 regulatory elements mediate transgene expression during prostate organogenesis and carcinogenesis.* Dev Dyn, 2009. **238**(3): p. 664-72.
46. Sreenath, T., et al., *Androgen-independent expression of hoxb-13 in the mouse prostate.* Prostate, 1999. **41**(3): p. 203-7.
47. Norris, J.D., et al., *The homeodomain protein HOXB13 regulates the cellular response to androgens.* Mol Cell, 2009. **36**(3): p. 405-16.
48. Chung, L.W. and G.R. Cunha, *Stromal-epithelial interactions: II. Regulation of prostatic growth by embryonic urogenital sinus mesenchyme.* Prostate, 1983. **4**(5): p. 503-11.
49. McNeal, J.E., *The zonal anatomy of the prostate.* Prostate, 1981. **2**(1): p. 35-49.
50. Timms, B.G., *Prostate development: a historical perspective.* Differentiation, 2008. **76**(6): p. 565-77.
51. Cunha, G.R. and L.W. Chung, *Stromal-epithelial interactions--I. Induction of prostatic phenotype in urothelium of testicular feminized (Tfm/y) mice.* J Steroid Biochem, 1981. **14**(12): p. 1317-24.
52. Mann, R.S., K.M. Lelli, and R. Joshi, *Hox specificity unique roles for cofactors and collaborators.* Curr Top Dev Biol, 2009. **88**: p. 63-101.
53. Longobardi, E., et al., *Biochemistry of the tale transcription factors PREP, MEIS, and PBX in vertebrates.* Dev Dyn, 2014. **243**(1): p. 59-75.
54. Chang, C.P., et al., *Pbx proteins display hexapeptide-dependent cooperative DNA binding with a subset of Hox proteins.* Genes Dev, 1995. **9**(6): p. 663-74.
55. Burglin, T.R., *The PBC domain contains a MEINOX domain: coevolution of Hox and TALE homeobox genes?* Dev Genes Evol, 1998. **208**(2): p. 113-6.
56. Williams, T.M., M.E. Williams, and J.W. Innis, *Range of HOX/TALE superclass associations and protein domain requirements for HOXA13:MEIS interaction.* Dev Biol, 2005. **277**(2): p. 457-71.
57. Gehring, W.J., et al., *Homeodomain-DNA recognition.* Cell, 1994. **78**(2): p. 211-23.
58. Zeltser, L., C. Desplan, and N. Heintz, *Hoxb-13: a new Hox gene in a distant region of the HOXB cluster maintains colinearity.* Development, 1996. **122**(8): p. 2475-84.
59. Moskow, J.J., et al., *Meis1, a PBX1-related homeobox gene involved in myeloid leukemia in BXH-2 mice.* Mol Cell Biol, 1995. **15**(10): p. 5434-43.
60. Moens, C.B. and L. Selleri, *Hox cofactors in vertebrate development.* Dev Biol, 2006. **291**(2): p. 193-206.

61. Mann, R.S. and M. Affolter, *Hox proteins meet more partners.* Curr Opin Genet Dev, 1998. **8**(4): p. 423-9.
62. Mukherjee, K. and T.R. Burglin, *Comprehensive analysis of animal TALE homeobox genes: new conserved motifs and cases of accelerated evolution.* J Mol Evol, 2007. **65**(2): p. 137-53.
63. Ariki, R., et al., *Homeodomain transcription factor Meis1 is a critical regulator of adult bone marrow hematopoiesis.* PLoS One, 2014. **9**(2): p. e87646.
64. Kroon, E., et al., *Hoxa9 transforms primary bone marrow cells through specific collaboration with Meis1a but not Pbx1b.* EMBO J, 1998. **17**(13): p. 3714-25.
65. Kumar, A.R., et al., *A role for MEIS1 in MLL-fusion gene leukemia.* Blood, 2009. **113**(8): p. 1756-8.
66. Wong, P., et al., *Meis1 is an essential and rate-limiting regulator of MLL leukemia stem cell potential.* Genes Dev, 2007. **21**(21): p. 2762-74.
67. Garcia-Cuellar, M.P., et al., *Pbx3 and Meis1 cooperate through multiple mechanisms to support Hox-induced murine leukemia.* Haematologica, 2015. **100**(7): p. 905-13.
68. Calvo, K.R., et al., *Meis1a suppresses differentiation by G-CSF and promotes proliferation by SCF: potential mechanisms of cooperativity with Hoxa9 in myeloid leukemia.* Proc Natl Acad Sci U S A, 2001. **98**(23): p. 13120-5.
69. Mahmoud, A.I., et al., *Meis1 regulates postnatal cardiomyocyte cell cycle arrest.* Nature, 2013. **497**(7448): p. 249-53.
70. Garcia-Borreguero, D. and A.M. Williams, *An update on restless legs syndrome (Willis-Ekbom disease): clinical features, pathogenesis and treatment.* Curr Opin Neurol, 2014. **27**(4): p. 493-501.
71. Jones, T.A., et al., *The homeobox gene MEIS1 is amplified in IMR-32 and highly expressed in other neuroblastoma cell lines.* Eur J Cancer, 2000. **36**(18): p. 2368-74.
72. Geerts, D., et al., *MEIS homeobox genes in neuroblastoma.* Cancer Lett, 2005. **228**(1-2): p. 43-50.
73. Geerts, D., et al., *The role of the MEIS homeobox genes in neuroblastoma.* Cancer Lett, 2003. **197**(1-2): p. 87-92.
74. Zha, Y., et al., *MEIS2 is essential for neuroblastoma cell survival and proliferation by transcriptional control of M-phase progression.* Cell Death Dis, 2014. **5**: p. e1417.
75. Fernandez, P., et al., *Distinctive gene expression of human lung adenocarcinomas carrying LKB1 mutations.* Oncogene, 2004. **23**(29): p. 5084-91.
76. Lasa, A., et al., *MEIS 1 expression is downregulated through promoter hypermethylation in AML1-ETO acute myeloid leukemias.* Leukemia, 2004. **18**(7): p. 1231-7.
77. Li, W., et al., *Meis1 regulates proliferation of non-small-cell lung cancer cells.* J Thorac Dis, 2014. **6**(6): p. 850-5.
78. Sabates-Bellver, J., et al., *Transcriptome profile of human colorectal adenomas.* Mol Cancer Res, 2007. **5**(12): p. 1263-75.
79. Crist, R.C., et al., *A conserved tissue-specific homeodomain-less isoform of MEIS1 is downregulated in colorectal cancer.* PLoS One, 2011. **6**(8): p. e23665.
80. Cui, L., et al., *MEIS1 functions as a potential AR negative regulator.* Exp Cell Res, 2014. **328**(1): p. 58-68.

81. Jung, C., et al., *HOXB13 induces growth suppression of prostate cancer cells as a repressor of hormone-activated androgen receptor signaling.* Cancer Res, 2004. **64**(24): p. 9185-92.
82. Ramberg, H., et al., *PBX3 is a putative biomarker of aggressive prostate cancer.* Int J Cancer, 2016. **139**(8): p. 1810-20.
83. Xu, J., et al., *HOXB13 is a susceptibility gene for prostate cancer: results from the International Consortium for Prostate Cancer Genetics (ICPCG).* Hum Genet, 2013. **132**(1): p. 5-14.
84. Akbari, M.R., et al., *Association between germline HOXB13 G84E mutation and risk of prostate cancer.* J Natl Cancer Inst, 2012. **104**(16): p. 1260-2.
85. Gudmundsson, J., et al., *A study based on whole-genome sequencing yields a rare variant at 8q24 associated with prostate cancer.* Nat Genet, 2012. **44**(12): p. 1326-9.
86. Karlsson, R., et al., *A population-based assessment of germline HOXB13 G84E mutation and prostate cancer risk.* Eur Urol, 2014. **65**(1): p. 169-76.
87. Kluzniak, W., et al., *The G84E mutation in the HOXB13 gene is associated with an increased risk of prostate cancer in Poland.* Prostate, 2013. **73**(5): p. 542-8.
88. Kote-Jarai, Z., et al., *Prevalence of the HOXB13 G84E germline mutation in British men and correlation with prostate cancer risk, tumour characteristics and clinical outcomes.* Ann Oncol, 2015. **26**(4): p. 756-61.
89. Laitinen, V.H., et al., *HOXB13 G84E mutation in Finland: population-based analysis of prostate, breast, and colorectal cancer risk.* Cancer Epidemiol Biomarkers Prev, 2013. **22**(3): p. 452-60.
90. Stott-Miller, M., et al., *HOXB13 mutations in a population-based, case-control study of prostate cancer.* Prostate, 2013. **73**(6): p. 634-41.
91. Storebjerg, T.M., et al., *Prevalence of the HOXB13 G84E mutation in Danish men undergoing radical prostatectomy and its correlations with prostate cancer risk and aggressiveness.* BJU Int, 2016. **118**(4): p. 646-53.
92. Lin, X., et al., *A novel germline mutation in HOXB13 is associated with prostate cancer risk in Chinese men.* Prostate, 2013. **73**(2): p. 169-75.
93. Maia, S., et al., *Identification of Two Novel HOXB13 Germline Mutations in Portuguese Prostate Cancer Patients.* PLoS One, 2015. **10**(7): p. e0132728.
94. Akbari, M.R., et al., *Germline HOXB13 p.Gly84Glu mutation and risk of colorectal cancer.* Cancer Epidemiol, 2013. **37**(4): p. 424-7.
95. Beebe-Dimmer, J.L., et al., *The HOXB13 G84E Mutation Is Associated with an Increased Risk for Prostate Cancer and Other Malignancies.* Cancer Epidemiol Biomarkers Prev, 2015. **24**(9): p. 1366-72.
96. Zhao, Y., T. Yamashita, and M. Ishikawa, *Regulation of tumor invasion by HOXB13 gene overexpressed in human endometrial cancer.* Oncol Rep, 2005. **13**(4): p. 721-6.
97. Miao, J., et al., *HOXB13 promotes ovarian cancer progression.* Proc Natl Acad Sci U S A, 2007. **104**(43): p. 17093-8.
98. Lopez, R., et al., *HOXB homeobox gene expression in cervical carcinoma.* Int J Gynecol Cancer, 2006. **16**(1): p. 329-35.
99. Maeda, K., et al., *Altered expressions of HOX genes in human cutaneous malignant melanoma.* Int J Cancer, 2005. **114**(3): p. 436-41.

100. Ma, X.J., et al., *A two-gene expression ratio predicts clinical outcome in breast cancer patients treated with tamoxifen.* Cancer Cell, 2004. **5**(6): p. 607-16.
101. Kanai, M., et al., *Aberrant expressions of HOX genes in colorectal and hepatocellular carcinomas.* Oncol Rep, 2010. **23**(3): p. 843-51.
102. Cantile, M., et al., *Aberrant expression of posterior HOX genes in well differentiated histotypes of thyroid cancers.* Int J Mol Sci, 2013. **14**(11): p. 21727-40.
103. Marra, L., et al., *Deregulation of HOX B13 expression in urinary bladder cancer progression.* Curr Med Chem, 2013. **20**(6): p. 833-9.
104. Cai, Y., *Participation of caudal mullerian mesenchyma in prostate development.* J Urol, 2008. **180**(5): p. 1898-903.
105. Kurita, T., *Developmental origin of vaginal epithelium.* Differentiation, 2010. **80**(2-3): p. 99-105.
106. Cai, Y., S. Kregel, and D.J. Vander Griend, *Formation of human prostate epithelium using tissue recombination of rodent urogenital sinus mesenchyme and human stem cells.* J Vis Exp, 2013(76).
107. Barbieri, C.E. and J.A. Pietenpol, *p63 and epithelial biology.* Exp Cell Res, 2006. **312**(6): p. 695-706.
108. Grisanzio, C. and S. Signoretti, *p63 in prostate biology and pathology.* J Cell Biochem, 2008. **103**(5): p. 1354-68.
109. Litvinov, I.V., A.M. De Marzo, and J.T. Isaacs, *Is the Achilles' heel for prostate cancer therapy a gain of function in androgen receptor signaling?* J Clin Endocrinol Metab, 2003. **88**(7): p. 2972-82.
110. Yang, Y.A. and J. Yu, *Current perspectives on FOXA1 regulation of androgen receptor signaling and prostate cancer.* Genes Dis, 2015. **2**(2): p. 144-151.
111. Tanaka, M., et al., *Nkx3.1, a murine homolog of Ddrosophila bagpipe, regulates epithelial ductal branching and proliferation of the prostate and palatine glands.* Dev Dyn, 2000. **219**(2): p. 248-60.
112. Abate-Shen, C., M.M. Shen, and E. Gelmann, *Integrating differentiation and cancer: the Nkx3.1 homeobox gene in prostate organogenesis and carcinogenesis.* Differentiation, 2008. **76**(6): p. 717-27.
113. Matusik, R.J., et al., *Prostate epithelial cell fate.* Differentiation, 2008. **76**(6): p. 682-98.
114. Hutmacher, D.W., et al., *Convergence of regenerative medicine and synthetic biology to develop standardized and validated models of human diseases with clinical relevance.* Curr Opin Biotechnol, 2015. **35**: p. 127-32.
115. Thorne, R.M. and T.A. Milne, *Dangerous liaisons: cooperation between Pbx3, Meis1 and Hoxa9 in leukemia.* Haematologica, 2015. **100**(7): p. 850-3.
116. Huang, Q., et al., *A prostate cancer susceptibility allele at 6q22 increases RFX6 expression by modulating HOXB13 chromatin binding.* Nat Genet, 2014. **46**(2): p. 126-35.
117. Wilson, J.D., *The critical role of androgens in prostate development.* Endocrinol Metab Clin North Am, 2011. **40**(3): p. 577-90, ix.
118. Cohen, R.J., et al., *Epithelial differentiation of the lower urinary tract with recognition of the minor prostatic glands.* Hum Pathol, 2002. **33**(9): p. 905-9.
119. Signoretti, S., et al., *p63 is a prostate basal cell marker and is required for prostate development.* Am J Pathol, 2000. **157**(6): p. 1769-75.

120. Signoretti, S., et al., *p63 regulates commitment to the prostate cell lineage.* Proc Natl Acad Sci U S A, 2005. **102**(32): p. 11355-60.
121. Bhatia-Gaur, R., et al., *Roles for Nkx3.1 in prostate development and cancer.* Genes Dev, 1999. **13**(8): p. 966-77.
122. Taylor, R.A., et al., *Formation of human prostate tissue from embryonic stem cells.* Nat Methods, 2006. **3**(3): p. 179-81.
123. Wake, M.H., *Structure and Function of the Male Mullerian Gland in Caecilians, with Comments on Its Evolutionary Significance.* Journal of Herpetology, 1981. **15**(1): p. 17-22.
124. Sever, D.M., *Comparative Anatomy and Phylogeny of the Cloacae of Salamanders (Amphibia: Caudata). I. Evolution at the Family Level.* Herpetologica, 1991. **47**(2): p. 165-193.
125. George, J.M., et al., *Contribution of the secretory material of caecilian (amphibia: Gymnophiona) male Mullerian gland to motility of sperm: a study in Uraeotyphlus narayani.* J Morphol, 2005. **263**(2): p. 227-37.
126. Barlow, L.J. and M.M. Shen, *SnapShot: Prostate cancer.* Cancer Cell, 2013. **24**(3): p. 400 e1.
127. Lin, D.W., M. Porter, and B. Montgomery, *Treatment and survival outcomes in young men diagnosed with prostate cancer: a Population-based Cohort Study.* Cancer, 2009. **115**(13): p. 2863-71.
128. Culig, Z., *Distinguishing indolent from aggressive prostate cancer.* Recent Results Cancer Res, 2014. **202**: p. 141-7.
129. Cui, L., et al., *MEIS1 Functions as a potential AR negative regulator.* Exp Cell Res, 2014.
130. Hisa, T., et al., *Hematopoietic, angiogenic and eye defects in Meis1 mutant animals.* EMBO J, 2004. **23**(2): p. 450-9.
131. Argiropoulos, B. and R.K. Humphries, *Hox genes in hematopoiesis and leukemogenesis.* Oncogene, 2007. **26**(47): p. 6766-76.
132. Azcoitia, V., et al., *The homeodomain protein Meis1 is essential for definitive hematopoiesis and vascular patterning in the mouse embryo.* Dev Biol, 2005. **280**(2): p. 307-20.
133. Graham, A., *Developmental patterning. The Hox code out on a limb.* Curr Biol, 1994. **4**(12): p. 1135-7.
134. Shanmugam, K., et al., *PBX and MEIS as non-DNA-binding partners in trimeric complexes with HOX proteins.* Mol Cell Biol, 1999. **19**(11): p. 7577-88.
135. Choe, S.K., F. Ladam, and C.G. Sagerstrom, *TALE factors poise promoters for activation by Hox proteins.* Dev Cell, 2014. **28**(2): p. 203-11.
136. Shen, W.F., et al., *AbdB-like Hox proteins stabilize DNA binding by the Meis1 homeodomain proteins.* Mol Cell Biol, 1997. **17**(11): p. 6448-58.
137. Merabet, S. and B. Hudry, *Hox transcriptional specificity despite a single class of cofactors: are flexible interaction modes the key? Plasticity in Hox/PBC interaction modes as a common molecular strategy for shaping Hox transcriptional activities.* Bioessays, 2013. **35**(2): p. 88-92.
138. Svingen, T. and K.F. Tonissen, *Hox transcription factors and their elusive mammalian gene targets.* Heredity (Edinb), 2006. **97**(2): p. 88-96.

139. Maeda, R., et al., *Xmeis1, a protooncogene involved in specifying neural crest cell fate in Xenopus embryos.* Oncogene, 2001. **20**(11): p. 1329-42.
140. Yang, Y., et al., *Three-amino acid extension loop homeodomain proteins Meis2 and TGIF differentially regulate transcription.* J Biol Chem, 2000. **275**(27): p. 20734-41.
141. Edwards, S., et al., *Expression analysis onto microarrays of randomly selected cDNA clones highlights HOXB13 as a marker of human prostate cancer.* Br J Cancer, 2005. **92**(2): p. 376-81.
142. Jung, C., et al., *HOXB13 homeodomain protein suppresses the growth of prostate cancer cells by the negative regulation of T-cell factor 4.* Cancer Res, 2004. **64**(9): p. 3046-51.
143. Smith, S.C., et al., *HOXB13 G84E-related familial prostate cancers: a clinical, histologic, and molecular survey.* Am J Surg Pathol, 2014. **38**(5): p. 615-26.
144. Kim, I.J., et al., *HOXB13 regulates the prostate-derived Ets factor: implications for prostate cancer cell invasion.* Int J Oncol, 2014. **45**(2): p. 869-76.
145. Dardaei, L., E. Longobardi, and F. Blasi, *Prep1 and Meis1 competition for Pbx1 binding regulates protein stability and tumorigenesis.* Proc Natl Acad Sci U S A, 2014. **111**(10): p. E896-905.
146. D'Antonio, J.M., et al., *Loss of androgen receptor-dependent growth suppression by prostate cancer cells can occur independently from acquiring oncogenic addiction to androgen receptor signaling.* PLoS One, 2010. **5**(7): p. e11475.
147. Litvinov, I.V., et al., *Low-calcium serum-free defined medium selects for growth of normal prostatic epithelial stem cells.* Cancer Res, 2006. **66**(17): p. 8598-607.
148. Sramkoski, R.M., et al., *A new human prostate carcinoma cell line, 22Rv1.* In Vitro Cell Dev Biol Anim, 1999. **35**(7): p. 403-9.
149. van Bokhoven, A., et al., *Molecular characterization of human prostate carcinoma cell lines.* Prostate, 2003. **57**(3): p. 205-25.
150. Sobel, R.E. and M.D. Sadar, *Cell lines used in prostate cancer research: a compendium of old and new lines--part 1.* J Urol, 2005. **173**(2): p. 342-59.
151. Vander Griend, D.J., et al., *Cell-autonomous intracellular androgen receptor signaling drives the growth of human prostate cancer initiating cells.* Prostate, 2010. **70**(1): p. 90-9.
152. Vander Griend, D.J., et al., *The role of CD133 in normal human prostate stem cells and malignant cancer-initiating cells.* Cancer Res, 2008. **68**(23): p. 9703-11.
153. Gao, J., J.T. Arnold, and J.T. Isaacs, *Conversion from a paracrine to an autocrine mechanism of androgen-stimulated growth during malignant transformation of prostatic epithelial cells.* Cancer Res, 2001. **61**(13): p. 5038-44.
154. Uzgare, A.R., Y. Xu, and J.T. Isaacs, *In vitro culturing and characteristics of transit amplifying epithelial cells from human prostate tissue.* J Cell Biochem, 2004. **91**(1): p. 196-205.
155. Emig, D., et al., *AltAnalyze and DomainGraph: analyzing and visualizing exon expression data.* Nucleic Acids Res, 2010. **38**(Web Server issue): p. W755-62.
156. Salomonis, N., et al., *Alternative splicing regulates mouse embryonic stem cell pluripotency and differentiation.* Proc Natl Acad Sci U S A, 2010. **107**(23): p. 10514-9.
157. Olsson, A., et al., *Single-cell analysis of mixed-lineage states leading to a binary cell fate choice.* Nature, 2016. **537**(7622): p. 698-702.
158. Pflueger, D., et al., *Discovery of non-ETS gene fusions in human prostate cancer using next-generation RNA sequencing.* Genome Res, 2011. **21**(1): p. 56-67.

159. Robinson, D., et al., *Integrative clinical genomics of advanced prostate cancer.* Cell, 2015. **161**(5): p. 1215-28.
160. Price, M.E., et al., *Additional annotation enhances potential for biologically-relevant analysis of the Illumina Infinium HumanMethylation450 BeadChip array.* Epigenetics Chromatin, 2013. **6**(1): p. 4.
161. Diez-Villanueva, A., I. Mallona, and M.A. Peinado, *Wanderer, an interactive viewer to explore DNA methylation and gene expression data in human cancer.* Epigenetics Chromatin, 2015. **8**: p. 22.
162. Geerts, D., et al., *The role of the MEIS homeobox genes in neuroblastoma.* Cancer Letters, 2003. **197**(1-2): p. 87-92.
163. Welsbie, D.S., et al., *Histone deacetylases are required for androgen receptor function in hormone-sensitive and castrate-resistant prostate cancer.* Cancer Res, 2009. **69**(3): p. 958-66.
164. Guo, Y., et al., *Large scale comparison of gene expression levels by microarrays and RNAseq using TCGA data.* PLoS One, 2013. **8**(8): p. e71462.
165. Schwab, M., *Encyclopedia of cancer*. 4th edition. ed. 2017, New York, NY: Springer Berlin Heidelberg. pages cm.
166. Sager, R., *Expression genetics in cancer: shifting the focus from DNA to RNA.* Proc Natl Acad Sci U S A, 1997. **94**(3): p. 952-5.
167. Goodin, S., K.V. Rao, and R.S. DiPaola, *State-of-the-art treatment of metastatic hormone-refractory prostate cancer.* Oncologist, 2002. **7**(4): p. 360-70.
168. Kregel, S., et al., *Acquired resistance to the second-generation androgen receptor antagonist enzalutamide in castration-resistant prostate cancer.* Oncotarget, 2016. **7**(18): p. 26259-74.
169. Allard, S., et al., *Molecular mechanisms of hormone-mediated Mullerian duct regression: involvement of beta-catenin.* Development, 2000. **127**(15): p. 3349-60.
170. Zhan, Y., et al., *Mullerian inhibiting substance regulates its receptor/SMAD signaling and causes mesenchymal transition of the coelomic epithelial cells early in Mullerian duct regression.* Development, 2006. **133**(12): p. 2359-69.
171. Klattig, J., et al., *Wilms' tumor protein Wt1 is an activator of the anti-Mullerian hormone receptor gene Amhr2.* Mol Cell Biol, 2007. **27**(12): p. 4355-64.
172. Cunha, G.R., *Age-dependent loss of sensitivity of female urogenital sinus to androgenic conditions as a function of the epithelia-stromal interaction in mice.* Endocrinology, 1975. **97**(3): p. 665-73.
173. Miwa, S., et al., *Dynamic color-coded fluorescence imaging of the cell-cycle phase, mitosis, and apoptosis demonstrates how caffeine modulates cisplatinum efficacy.* J Cell Biochem, 2013. **114**(11): p. 2454-60.
174. Shen, W.F., et al., *HOXA9 forms triple complexes with PBX2 and MEIS1 in myeloid cells.* Mol Cell Biol, 1999. **19**(4): p. 3051-61.
175. Kim, S.D., et al., *HOXB13 is co-localized with androgen receptor to suppress androgen-stimulated prostate-specific antigen expression.* Anat Cell Biol, 2010. **43**(4): p. 284-93.
176. Podlasek, C.A., et al., *Prostate development requires Sonic hedgehog expressed by the urogenital sinus epithelium.* Dev Biol, 1999. **209**(1): p. 28-39.